Spring 5-5-2018

Mechanisms for the Potassium Sparing Effects of Furosemide in Mice on High Potassium Diets

Bangchen Wang
University of Nebraska Medical Center

MECHANISMS FOR THE POTASSIUM-SPARING EFFECTS OF FUROSEMIDE IN MICE ON HIGH POTASSIUM DIETS

by

Bangchen Wang

A DISSERTATION

Presented to the Faculty of
The University of Nebraska Medical Center
In Partial Fulfillment of the Requirements
For the Degree of Doctor of Philosophy

Cellular & Integrative Physiology Graduate Program

Under the Supervision of Professor Steven C. Sansom

University of Nebraska Medical Center
Omaha, Nebraska

May 2018

Supervisory Committee:

Pamela K. Carmines, Ph.D.	Babu Padanilam, Ph.D.
Troy Plumb, M.D.	Irving H. Zucker, Ph.D.

ACKNOWLEDGEMENT

I am very grateful to all the people who helped me during the four years of my Ph.D. training that lead to this dissertation. I would like to express my sincere thanks and appreciation to:

My graduate advisor and mentor, Dr. Steven Sansom, who has always provided me guidance, support, advice, and encouragement throughout my Ph.D. training.

My supervisory committee members, Dr. Pamela Carmines, Dr. Babu Padanilam, Dr. Plumb, and Dr. Zucker, for their helpful advice both during and outside committee meetings.

All the current and past members of Sansom lab: Jun Wang-France, Huaqing Li, Donghai Wen, Ryan Cornelius, Yang Yuan, Paige Warner, and Dianelys Rivero-Hernandez, for their help inside and outside the lab. Special thanks to Huaqing Li for performing the patch clamp experiments shown in Chapter 1.

All the current and past graduate students in the Department of Cellular & Integrative Physiology for all their help and constructive feedback.

The department office staff, Cindy Norton, Kimberly Kavan, Pearl Sorensen, and Debra Davis, for their help with all the administrative work such as travel, fellowship, and event planning.

And most of all, my wife, Xiaoyi Shi, my children, Franklin, Caroline, and William, my parents and parents in law for their unconditional support and the endless joy and comfort they bring at home.

ABSTRACT

MECHANISMS FOR THE POTASSIUM-SPARING EFFECTS OF FUROSEMIDE IN MICE ON HIGH POTASSIUM DIETS

Bangchen Wang, Ph.D.

University of Nebraska Medical Center, 2018

Supervisor: Steven C. Sansom, Ph.D.

Because of its cardio-protective benefits, diets that are low in Na^+ and high in K^+ are often warranted in conjunction with use of diuretics such as furosemide for treating hypertension. It is critical to understand how such diets influence the diuretic actions on renal K^+ handling in order to choose the best drug for patients.

Furosemide is a commonly used K-wasting diuretic. It increases urinary K^+ excretion by increasing distal Na^+ delivery that stimulates K^+ secretion. However, in wild-type mice (WT) adapted to an alkaline low Na^+ high K^+ diet (LNaHK), both 12-hour IP furosemide injection and 7-day furosemide water treatment decreased renal K^+ clearance. We hypothesized that there is furosemide-sensitive net K^+ secretion in WT adapted to LNaHK. Free-flow micropuncture experiments showed that furosemide increased $[K^+]$ in the early distal tubule (EDT $[K^+]$) in WT on a regular diet (RD) but decreased EDT $[K^+]$ in WT on LNaHK. Furosemide did not affect EDT $[K^+]$ in ROMK knockout mice (ROMK KO) on LNaHK or WT on an alkaline normal Na^+ high K^+ diet (HK). Furosemide-sensitive Na^+ excretion was significantly greater in mice on LNaHK than those on RD or HK. Patch clamp analysis of split-open thick ascending limbs (TAL) revealed that the 70-pS ROMK channel exhibited a higher open probability (Po) but similar density in WT on LNaHK, compared to WT on RD. These results indicate that mice adapted to

LNaHK exhibit furosemide-sensitive net K^+ secretion in the TAL that is dependent on increased NKCC2 activity and mediated by ROMK channels.

Furosemide acidifies the urine by increasing acid secretion via the Na^+-H^+ exchanger 3 (NHE3) in TAL and vacuolar H^+-ATPase (V-ATPase) in the distal nephron. Because alkaline urine is required for BK-αβ4-mediated K^+ secretion, we hypothesized that furosemide reduces BK-αβ4-mediated K^+ secretion by acidifying the urine. Furosemide water treatment for 11 days led to decreased urine pH in both WT and BK-β4 knockout mice (BK-β4 KO) with increased V-ATPase expression and elevated plasma aldosterone levels. However, furosemide water decreased renal K^+ clearance and elevated plasma [K^+] in WT but not BK-β4 KO. Addition of acetazolamide in furosemide water restored urine pH along with renal K^+ clearance and plasma [K^+] to similar levels as control group. Additionally, western blotting and immunofluorescence staining showed that furosemide decreased cortical expression of BK-β4 and reduced apical localization of BK-α in connecting tubules (CNT); they were restored by adding acetazolamide to furosemide water. These results indicate that in mice adapted to HK, furosemide reduces BK-αβ4-mediated K^+ secretion by acidifying the urine.

In conclusion, by inhibiting net K^+ secretion in the TAL and BK-αβ4-mediated K^+ secretion in CNT, furosemide acts as a K-sparing diuretic in mice adapted to LNaHK and HK.

TABLE OF CONTENTS

LIST OF FIGURES

LIST OF TABLES

LIST OF ABBREVIATIONS

AC	adenylyl cyclase
Actz	acetazolamide
Ang II	angiotensin II
ASDN	aldosterone-sensitive distal nephron
AVP	arginine vasopressin
BK	large conductance potassium channel
CaSR	Ca^{2+}-sensing receptor
CCD	cortical collecting duct
CD	collecting duct
CNT	connecting tubule
cTAL	cortical thick ascending limb
DASH	dietary approaches to stop hypertension
DCT	distal convoluted tubule
EDT	early distal tubule
ENaC	epithelial Na channel
ERK	extracellular signal regulated kinase
FIKS	flow-induced K^+ secretion
Furo	furosemide
GFR	glomerular filtration rate

GPR4	G-protein coupled receptor 4
Hct	hematocrit
HK	(alkaline) high K diet
HKCl	high KCl diet
HPLC	high performance liquid chromatography
IP	intra-peritoneal
IV	intravenous
KCC4	K^+-Cl^- cotransporter 4
KCNJ	potassium inwardly-rectifying channel, subfamily J
Kir	inwardly-rectifying K channels
KO	knockout mice
LNaHK	(alkaline) low Na high K diet
LNaHKCl	low Na high KCl diet
MAP	mean arterial pressure
MAPK	mitogen-activated protein kinases
MCD	medullary collecting duct
mTAL	medullary thick ascending limb
NCC	Na^+-Cl^- cotransporter
NCX1	Na^+-Ca^{2+} exchanger 1
NHANES	National Health and Nutrition Examination Survey

NHE3	Na^+-H^+ exchanger 3
NKA	Na^+-K^+-ATPase
NKCC1	Na^+-K^+-$2Cl^-$ cotransporter 1
NKCC2	Na^+-K^+-$2Cl^-$ cotransporter 2
PGE_2	prostaglandin E_2
PKA	protein kinase A
Po	open probability
PT	proximal tubule
RAAS	renin-angiotensin-aldosterone system
RCK	regulators of K^+ conductance
RD	regular diet
ROMK	renal outer medullary K channel
TAL	thick ascending limb
THP	Tamm-Horsfall protein
TRPV4	transient receptor potential vanilloid 4
TRPV5	transient receptor potential vanilloid 5
U Osm	urine osmolality
$U_K\dot{V}$	urinary K^+ excretion
$U_{Na}\dot{V}$	urinary Na^+ excretion
$\dot{V}$	urine flow

V-ATPase	vacuolar-H^+ ATPase
Vp	pipette potential
WNK4	with-no-lysine 4
WT	wild-type mice

INTRODUCTION

Health benefits of high potassium diets

For tens of thousands of years, humans have been hunter-gatherers and consumed an ancient diet that is rich in fruits and vegetables with low sodium (Na) and high potassium (K). In the past 200 years since the industrial evolution, modern humans, especially in the western culture, have switched to the modern western diet, which contains abundant processed food but few fruits and vegetables with high Na^+ and low K (1). The high Na^+ low K^+ modern diet has long been known for its association with cardiovascular diseases including hypertension and stroke (2, 3). The FDA-recommended daily intake in adults is less than 2300 mg/day for Na^+ and at least 4700 mg/day for K. Unfortunately, according to data from the National Health and Nutrition Examination Survey (NHANES), most US adults exceed the recommended Na^+ intake with an average of 3600 mg/day and only 2800 mg/day K^+ intake (4, 5).

The most extensively studied of dietary impacts on cardiovascular diseases are the DASH (Dietary Approaches to Stop Hypertension) diet studies. In one study, 412 subjects, with an average blood pressure of 135/86 mmHg and without antihypertensive treatments, were given either the control diet or the DASH diet that is rich in fruits, vegetables, and low-fat dairy products with three different levels of Na^+ intake: low at 50 mmol/day (2.2 g/day), intermediate at 100 mmol/day (4.3 g/day), and high at 150 mmol/day (6.5 g/day). The K^+ intake was approximately 40 mmol/day (1 g/day) for control group and 80 mmol/day (2 g/day) for DASH group. When compared to those on the control diet, subjects on DASH diet had lower blood pressure at each Na^+ intake level, with the lowest blood pressure in the low Na^+ DASH group (6).

Other widely promoted healthy diets include Mediterranean, Paleolithic, and vegetarian diets. They all emphasize the consumption of fruits and vegetables and contain higher K^+ and lower Na^+ contents than the western diet. They have been associated with lower risks for

cardiovascular diseases, cancer and overall mortality (7-12). The Paleolithic diet best mimics the diet consumed by ancient humans for tens of thousands of years as hunter-gatherers. From studies of over 50 hunter-gatherer societies, Eaton SB *et. al.* (13) estimated the daily Na^+ and K^+ intake of ancient humans. **Table 1** clearly demonstrates the large difference in Na^+ and K^+ contents between the Paleolithic hunter-gatherer and modern western diets. Furthermore, the study on the Yanomami tribe (14) showed an even more strikingly high K/Na^+ intake ratio with an average blood pressure of 100/60 mmHg.

Another important aspect of the high K^+ diets is the alkalinity. Many high K^+ foods including fruits, vegetables and legumes are naturally alkaline. The large difference between urinary K^+ and Cl^- excretion in the Yanomami people suggests the highly alkaline nature of their diet (**Table 1**). In stroke-prone spontaneously hypertensive rat, supplemental $KHCO_3$ or K^+ citrate attenuated hypertension compared to control; while supplemental KCl exacerbated hypertension and increased stroke risk (1, 15, 16). The studies of supplemental $KHCO_3$/citrate vs KCl in humans, however, did not show an effect on blood pressure (17-19).

Nonetheless, the benefits of high K^+ diets as well as K^+ supplements have been strongly supported by numerous studies. Therefore, it is critical to understand how the body maintains K^+ homeostasis with the excess K^+ intake.

Table 1. Daily urinary Na^+ and K^+ excretion of different diets.

Diet	Na^+ **(mmol/day)**	**K (mmol/day)**	**K**/Na^+ **ratio**	**Cl (mmol/day)**
FDA Guideline	100	120	1.2	N/A
Modern (5)	157	72	0.5	N/A
DASH (low Na) (6)	65	82	1.3	N/A
Paleolithic (13)	30	282	9.3	N/A
Yanomami (14)	1	152	152	13.7

N/A, not available

Normal K^+ homeostasis in the body

The plasma [K^+] has to be tightly controlled within the range of 3.5 – 5.0 mM. Both hypokalemia and hyperkalemia may lead to dysfunctions in muscles, kidneys and especially the heart. In a healthy person, the entire daily intake of K^+ is excreted, 90% in urine and 10% in stools. Compared to the 100 mmol daily K^+ intake and 65 mmol extracellular K^+, 3300 mmol K^+ is stored in the intracellular compartment, mainly in muscle cells (**Figure 1**). In addition to renal excretion, this large pool of intracellular K^+ plays a critical role in quickly adjusting plasma [K^+] to prevent hyperkalemia during an acute K^+ intake. K^+ is shifted into the cells by the Na^+-K^+-ATPase (NKA) that pumps 2 K^+ in and 3 Na^+ out of the cell.

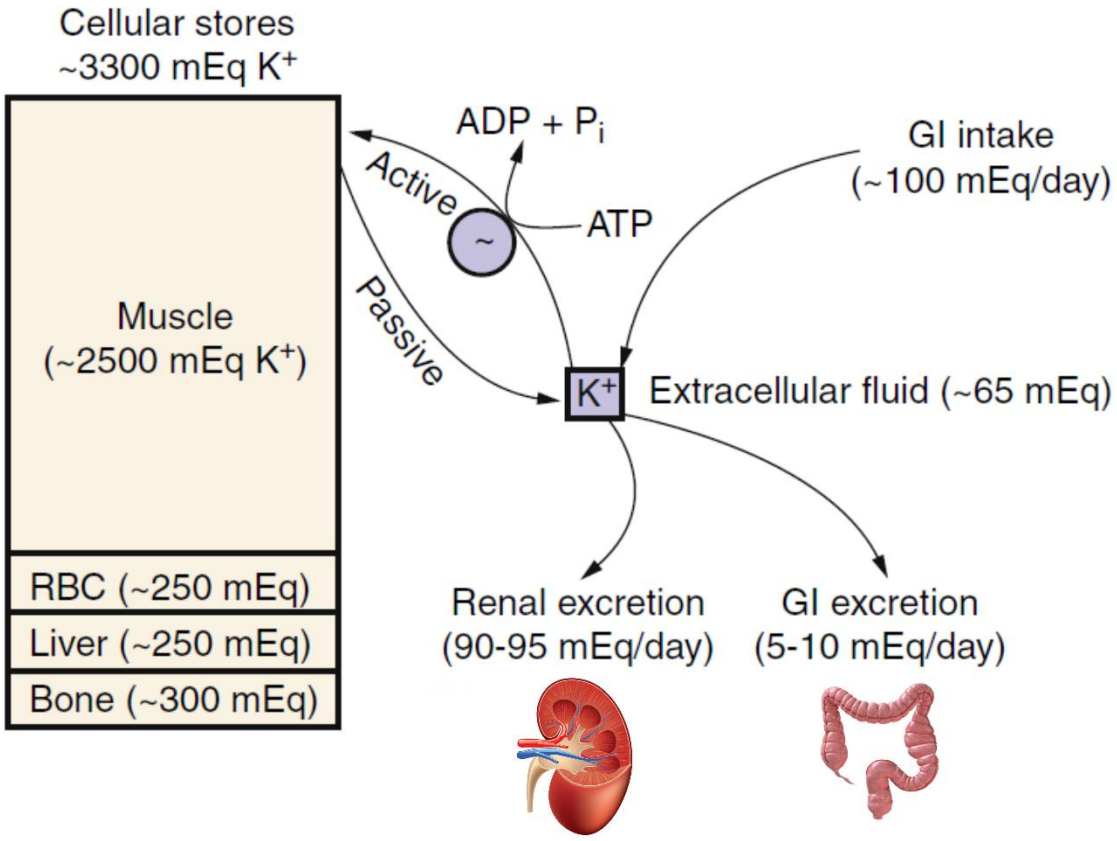

Figure 1. Normal K^+ balance in the body (modified from Wingo CS, *et. al.* 2000) (20).

K^+ in the body is balanced between the small extracellular pool (~65 mEq) and the large intracellular pool (~3300 mEq). K^+ is actively pumped into the cells by NKA. In equilibrium, the daily K^+ intake (~100 mEq/day) is completely excreted by the kidneys (90 – 95 mEq/day) and the colon (5 – 10 mEq/day).

Kidneys play the essential role to maintain K^+ balance in the long term. Under normal conditions, K^+ in blood is freely filtered into the glomerulus. Most of filtered K^+ is reabsorbed by the proximal tubule (PT) and the thick ascending limb (TAL) of the loop of Henle, following Na^+ reabsorption. In the aldosterone-sensitive distal nephron (ASDN), which consists of distal convoluted tubule 2 (DCT2), connecting tubule (CNT), and cortical collecting duct (CCD), K^+ is secreted into the tubular lumen (**Figure 2**) (21). This distal K^+ secretion is driven by the negative lumen potential generated by Na^+ reabsorption via epithelial Na^+ channel (ENaC) and is mediated by two K^+ channels, renal outer medullary K^+ (ROMK) channels in principal cells and large conductance Ca^{2+}-activated K^+ (BK) channels in both principal cells and intercalated cells. The ROMK channel is considered constitutively active and mediates K^+ secretion under basal conditions, *i. e.* regular diets (regular rodent chow) (22, 23). The BK channel, however, has a minimal role under regular diets. It is activated by high urinary flows under high K^+ dietary conditions (24). Given the high K^+ nature of the ancient diets, the BK channel is considered to be the ancient K^+ channel (25). Deletion of either channel is compensated by the overexpression of the other (26, 27). The two K^+ channels are regulated differently and work together to safeguard against the life-threatening hyperkalemia (25).

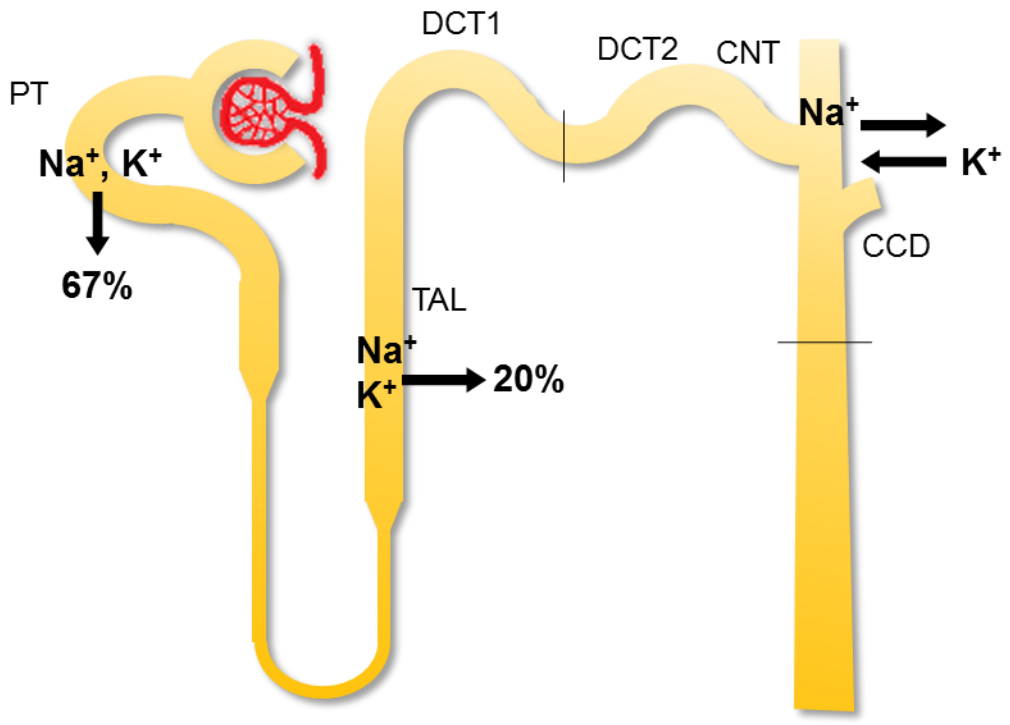

Figure 2. K^+ transport in the nephron.

K^+ is freely filtered into the glomerulus. Approximately 2/3 of filtered K^+ is reabsorbed in the PT following Na^+ and water reabsorption. Approximately 20% is reabsorbed in the TAL by Na^+-K^+-$2Cl^-$ cotransporter 2 (NKCC2). K^+ is secreted into the lumen of the ASDN (consisting of DCT2, CNT, and CCD), driven by the negative lumen potential generated by Na^+ reabsorption via ENaC.

Structure, localization and function of ROMK channels in the kidney

ROMK (a.k.a. Kir1.1 or KCNJ1) is a member of the *KCNJ* family (potassium inwardly-rectifying channel, subfamily J) that is characterized by a larger inward current than outward current (22). They have two transmembrane domains, a K^+ selectivity filter, and cytoplasmic N- and C- terminal domains (**Figure 3**). Kir channels (inwardly-rectifying K^+ channels) are constructed by four homomeric or heteromeric subunits, forming a pore in the center (28). In the kidney, ROMK channels are localized in the apical membrane of the TAL as well as the principal cells of ASDN. Differing from other members in the family, ROMK channels are only weakly inwardly-rectifying with a high basal open probability and mediates K^+ secretion into the tubular lumen (22).

Patch clamp studies have found an apical 30-pS Kir channel in the CCD and both a 30-pS and a 70-pS Kir channel in the TAL (29-32). Several lines of evidence indicate that these secretory K^+ channels were ROMK channels. First, immunostaining found ROMK expressed in these nephron segments (33-35). Secondly, expression of ROMK in *Xenopus* oocytes exhibited indistinguishable biophysical and pharmacological properties compared to the secretory 30-pS Kir channel (22, 23, 36). Finally, the 30-pS and 70-pS Kir channels were not found in the TAL and CCD of ROMK knockout mice (37).

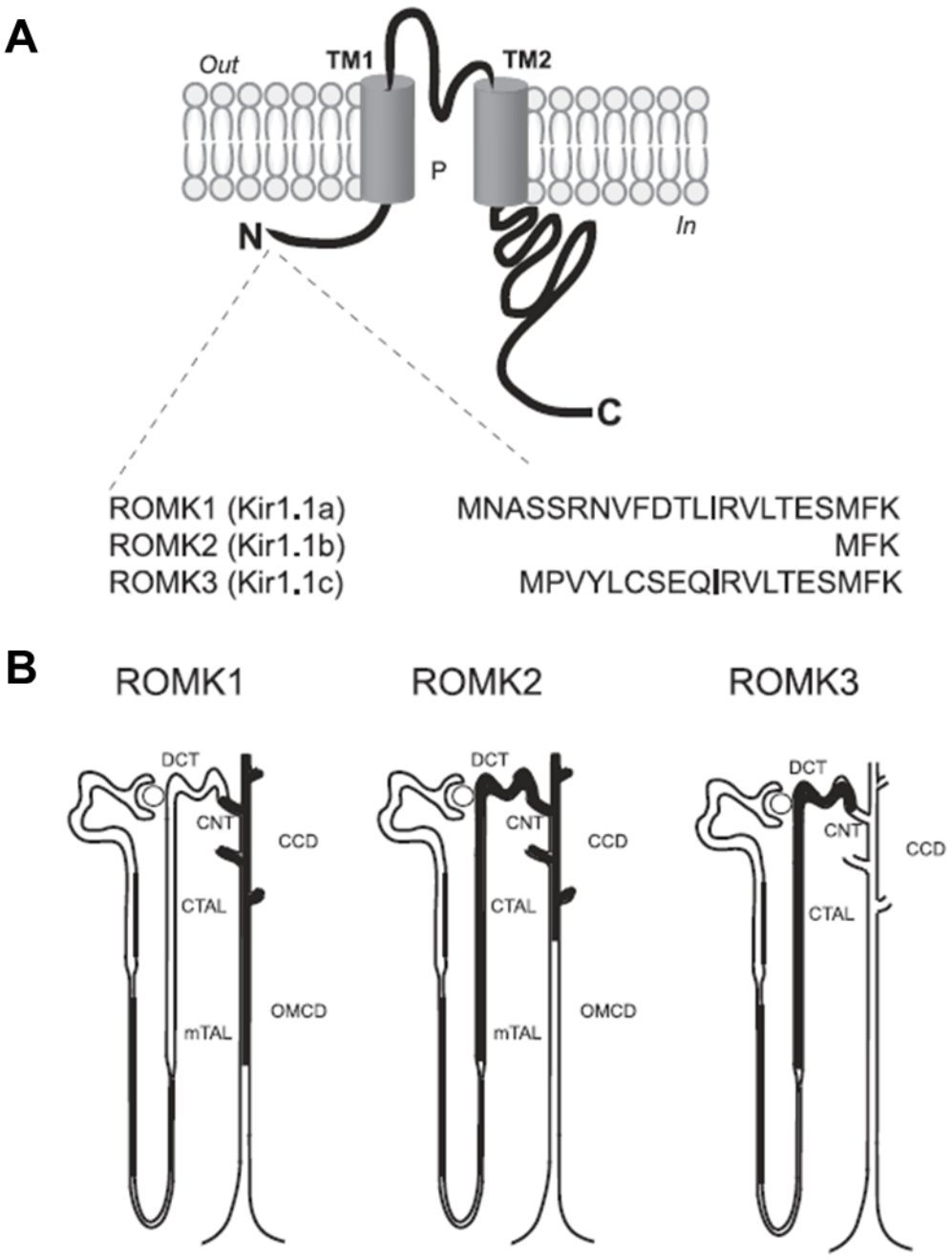

Figure 3. ROMK structure and isoform expression along the nephron (modified from Welling and Ho, 2009) (28).

A. ROMK consists of two transmembrane domains, a K^+ selectivity filter, and cytoplasmic N- and C-terminal domains. **B.** ROMK has three different splicing variants. ROMK1 is expressed in the CNT and CD. ROMK2 is expressed in the TAL, DCT, CNT, and CCD. ROMK3 is expressed in the TAL and DCT.

ROMK channels play different roles in the TAL vs ASDN (**Figure 4**). In the TAL, ROMK is required for recycling K^+ back into the lumen in order to maintain NaCl reabsorption via Na^+-K^+-$2Cl^-$ cotransporter 2 (NKCC2). Mutations in ROMK cause the type 2 Bartter Syndrome, which presents with maternal polyhydramnios, premature delivery, polyuria, polydipsia, volume depletion, transient hyperkalemic acidosis and later hypokalemia (38, 39). Consistently, ROMK knockout mice also exhibit a similar phenotype with high neonatal mortality and severe volume depletion with impaired NaCl reabsorption in TAL (40). In the ASDN, however, ROMK channels mainly serve to secrete K^+ in a well-regulated fashion to maintain K^+ balance in the body (41, 42). The different roles of ROMK channels in different nephron segments may have to do with the differential expressions of ROMK isoforms (**Figure 3**) (28). ROMK2 and ROMK3 are expressed in the TAL; while ROMK1 and ROMK2 are expressed in the ASDN. A recent study showed that ROMK1 deletion impaired ROMK regulation by high K^+ diets in the ASDN without affecting NaCl reabsorption in the TAL (43).

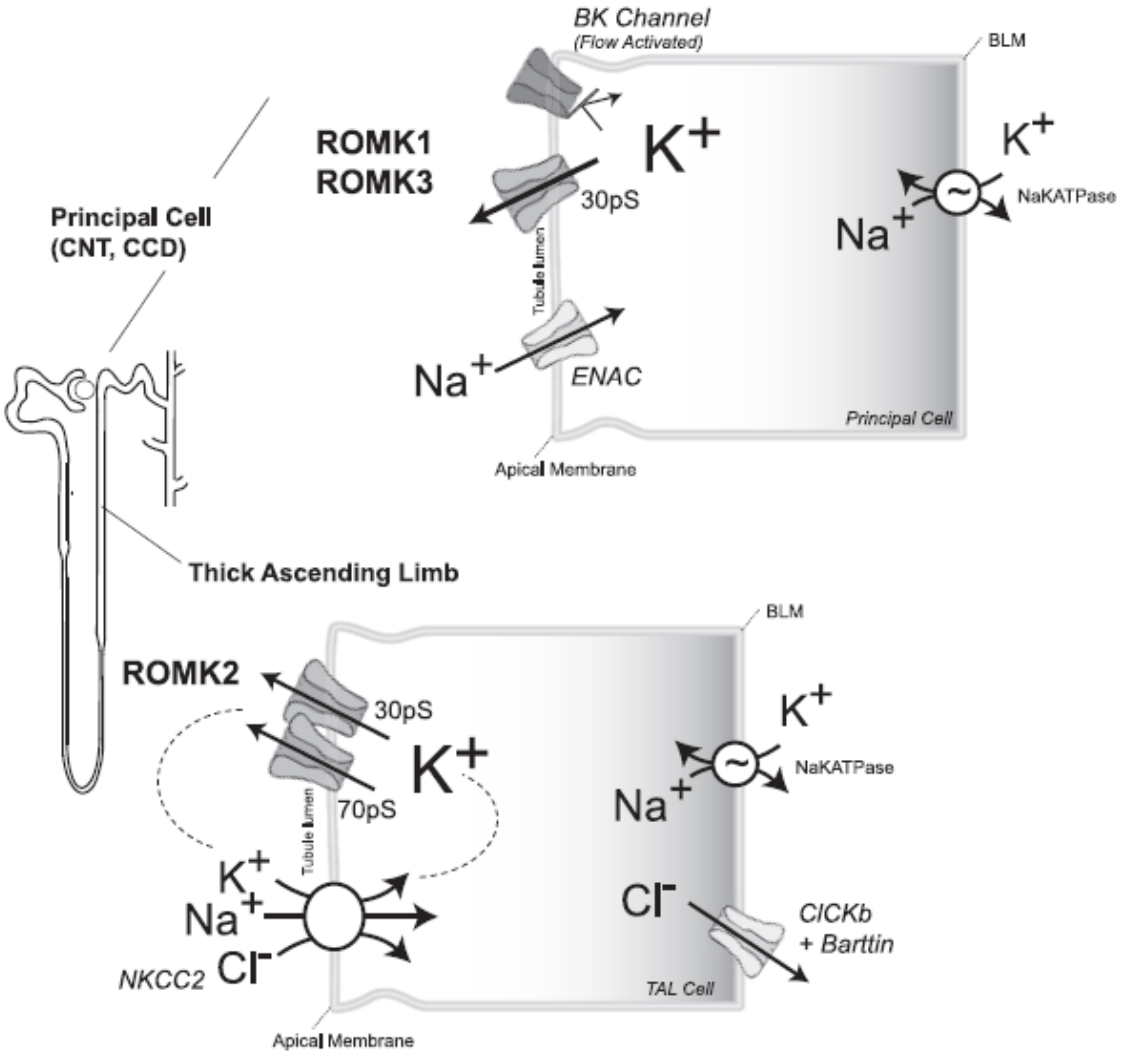

Figure 4. Role of ROMK in the TAL and ASDN (modified from Welling and Ho, 2009) (28)**.**

ROMK channels play different roles in the TAL and ASDN. In the TAL, ROMK encodes for the 30-pS and 70-pS K^+ secretory channels in the apical membrane, which are required for the recycling of K^+ reabsorbed by NKCC2 to maintain NaCl reabsorption. The NKCC2 transport is powered by NKA in the basolateral membrane. In the ASDN, ROMK encodes for the 30-pS K^+ secretory channel in the apical membrane. The K^+ secretion is driven by the negative lumen potential generated by Na^+ reabsorption via ENaC. They are also powered by NKA in the basolateral membrane.

Structure, localization and function of BK channels in the kidney

BK channels (also called Maxi-K, KCa1.1 or SLO1) are large conductance (150 – 250 pS), voltage-gated, Ca^{2+}-activated K^+ channels. The BK channel consists of four pore-forming α subunits, encoded by the *Kcnma1* gene, and one of the four different accessory β subunits (β1 – β4), encoded by the *Kcnmb1-4* genes. The α-subunit consists of seven transmembrane domains and a large cytosolic C-terminal domain (**Figure 5**) (44-46). As a unique part of the BK channel, the S0 segment is required for the modulation by β subunits (47, 48). The S1-S4 segments form the voltage sensor; S5 and S6 segments form the pore and selectivity filter (49). The C-terminal domain of BK-α contains two regulators of K^+ conductance (RCK) domains. The RCK1 contains a Ca^{2+} and a Mg^{2+} binding site, while the RCK2 contains another Ca^{2+} binding site in a region termed as the Ca^{2+} bowl. These sites are responsible for BK channel activation by Ca^{2+} and Mg^{2+} [50, 51]. Each β subunit of BK has two transmembrane domains connected by a large extracellular loop (**Figure 5**). The four β subunits exert different and complex effects on the BK channel, including modulations of voltage and Ca^{2+} sensitivities, pharmacokinetics, and protein trafficking (52-58). Recently, four γ subunits of BK were discovered, and they seem to regulate BK channels in a similar manner as the β subunits (45, 59-61). BK channels are expressed in a wide variety of tissues and play important roles in various physiological processes including smooth muscle contractility, neuronal excitability, and hair cell tuning (62-68). The diverse functions of BK channels may be explained by the alternative splicing of the α subunit and modulations by tissue-specific β subunits (45, 69-71).

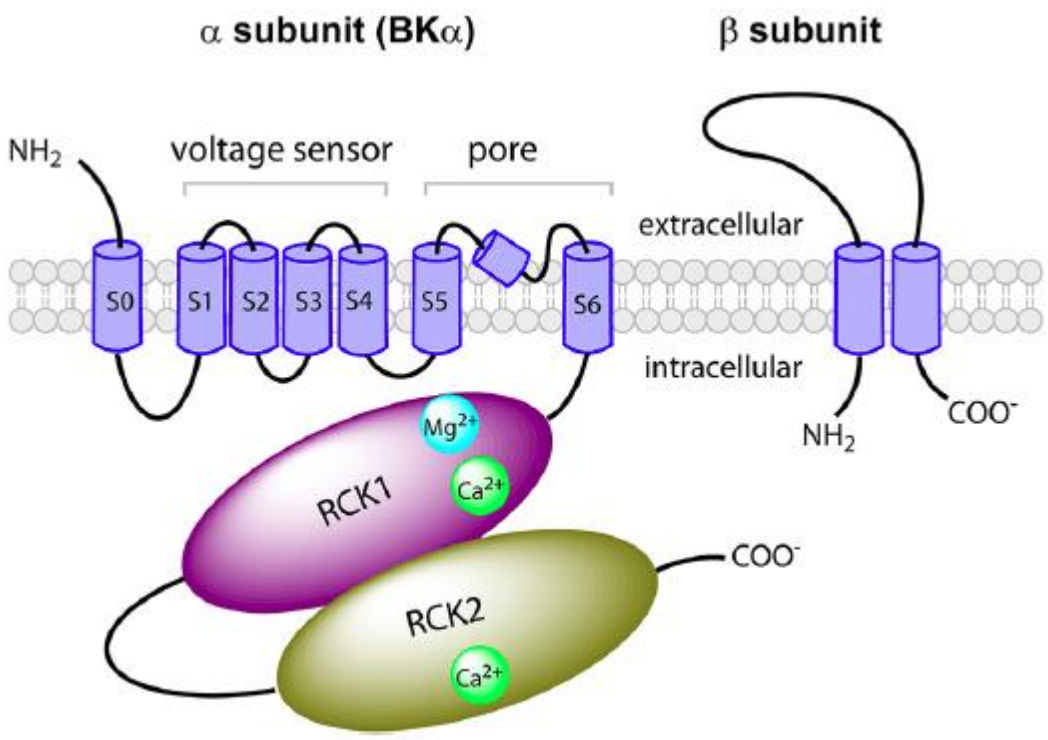

Figure 5. Structure of the α and β subunits of BK (modified from Zhang J. *et. al.* 2014) (45).

BK-α subunit consists of seven transmembrane domains and a large cytosolic C-terminal domain. The BK-β subunit consists of two transmembrane domains and a large extracellular loop.

In the kidney, BK channels are also expressed in a variety of cell types, including renal vascular smooth muscle cells, podocytes, mesangial cells, and tubular epithelial cells. In the afferent arterioles, BK channels had modest tonic dilator effects (72). In podocytes and mesangial cells, BK channels regulate mesangial contractility and glomerular filtration rate (GFR) (73, 74). In renal tubules, BK channels have been found in the TAL (75, 76), DCT (77), CNT (78-80), and CD (24, 81-83). High luminal fluid flow has been long known to stimulate distal K^+ secretion. Traditionally, high flow was thought to stimulate K^+ secretion by rapidly flushing tubular fluid downstream to maintain the chemical gradient for K^+ secretion (84). However, studies by Woda *et. al.* (24, 80) were the first to identify the BK channel as the main player in the flow-induced K^+ secretion (FIKS) in the CNT and CCD. This was further confirmed by genetic deletion of BK-α, where vasopressin blockade caused no change in K^+ excretion in BK-α knockout mice despite a profound increase in urinary flow (27).

Among the four BK-β subunits, BK-β1, β2, and β4 are expressed in mouse kidneys (85). BK-β1 is expressed in principal cells of mouse CNT (79, 85) and rabbit CNT and CCD (79, 86). BK-β1 knockout mice had attenuated kaliuretic response to volume expansion (79, 87). On high K^+ diets (HK), BK-β1 knockout exhibited elevated plasma [K^+], reduced K^+ clearance and exacerbated hypertension due to elevated aldosterone (88). BK-β4 is expressed in the TAL, DCT and intercalated cells of CNT and CD (85). BK-β4 was found to protect BK-α from lysosomal degradation (58). On HK, BK-β4 knockout mice presented with elevated plasma [K^+] and reduced K^+ clearance, which may be due to decreased apical localization of BK-α or attenuated intercalated cell size reduction in response to HK diets (58, 89, 90). Most recently, the study by Larsen *et. al.* (91) found that BK-β2 knockout mice displayed normal plasma [K^+] and urinary K^+ excretion with elevated plasma aldosterone on both regular diets (RD) and HK diets. This indicates that BK-αβ1 and BK-αβ4 channels are the major players in BK-mediated K^+ secretion.

The exact mechanism of how flow activates BK channels remains an area of great interest. High tubular fluid flow causes increases in intracellular [Ca^{2+}], which can activate BK channels (92). However, the Ca^{2+} current is only transient and cannot sustain BK activation. Recent studies have discovered that paracrine and autocrine factors such as ATP and prostaglandin E_2 (PGE_2) may stimulate signaling pathways to sustain BK activity (93-95). Furthermore, the primary cilium of principal cells may serve as the mechanosensor for tubular fluid flow (96). According to the model shown in **Figure 6** (97), high luminal fluid flow bends the primary cilium on principal cells, driving Ca^{2+} entry through the transient receptor potential vanilloid 4 (TRPV4) channels (98), stimulating Ca^{2+} release from intracellular Ca^{2+} stores, activating BK-αβ1 channels in principal cells (92). The sustained activation of BK-αβ1 in principal cells and BK-αβ4 in intercalated cells may be achieved via paracrine and autocrine signaling of PGE_2 and ATP (93-95).

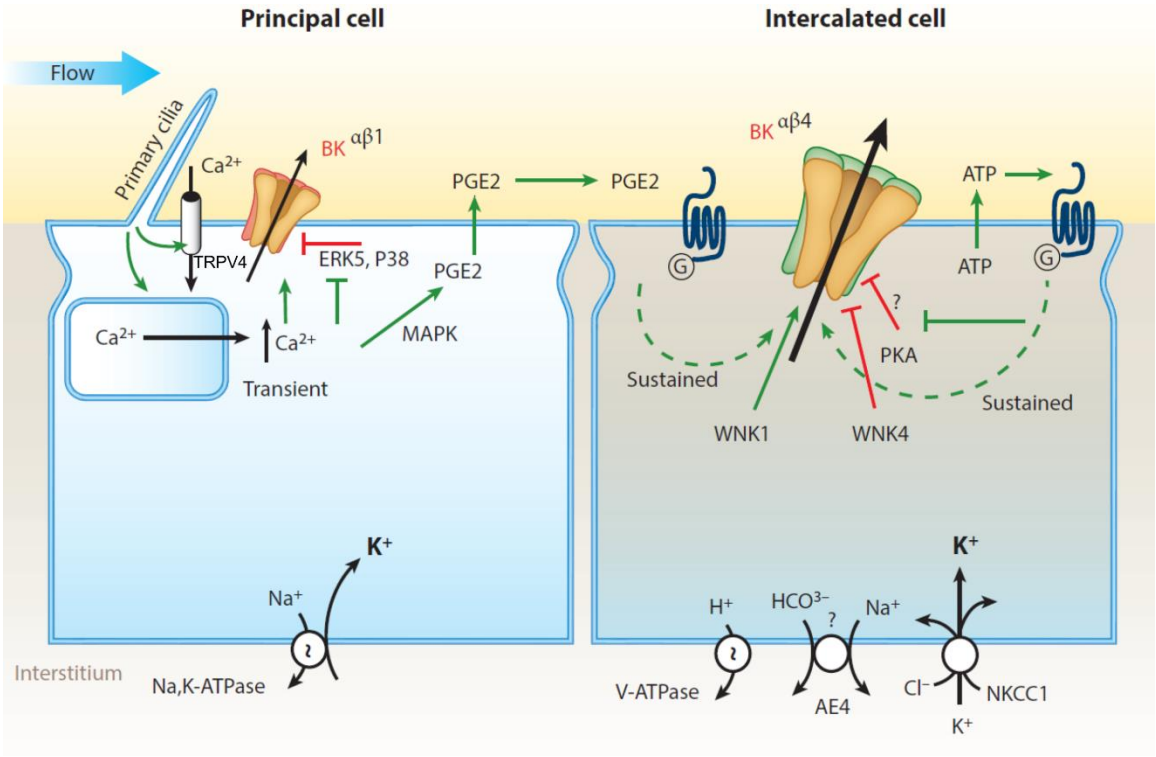

Figure 6. Flow-dependent activation of BK channels (modified from Welling, 2016) (97).

High flow bends the primary cilium on principal cells, driving Ca^{2+} entry via the TRPV4 channel, stimulating Ca^{2+} release from intracellular storage, activating BK-αβ1 channels in principal cells. The sustained activation of BK-αβ1 channels in principal cells and BK-αβ4 channels in intercalated cells occur indirectly through paracrine signaling of PGE_2 and autocrine signaling of ATP. Abbreviations: MAPK, mitogen-activated protein kinases; ERK, extracellular signal regulated kinase; PGE_2, prostaglandin E_2; PKA, protein kinase A; V-ATPase, vacuolar-H^+ ATPase; AE4, Anion Exchanger 4.

Renal K^+ handling on high K^+ diets

Kidneys can quickly adapt to excrete high K^+ intake by increasing K^+ secretion through ROMK and BK channels in the ASDN. As indicated by the name of the nephron segment, aldosterone is a major regulator of K^+ excretion in the aldosterone-sensitive distal nephron (ASDN). In mice fed on a high K^+ diet, plasma aldosterone levels reaches to approximately 750 pg/mL from 240 pg/mL on a regular diet (99). Aldosterone has various actions in the ASDN to stimulate urinary K^+ excretion. In the principal cells, aldosterone upregulates ENaC expression and activity to increase Na^+ reabsorption (100, 101), increasing the driving force for K^+ secretion via both ROMK and BK channels. It also upregulates the activity of the NKA in the basolateral membrane to facilitate Na^+ reabsorption and K^+ secretion (102). Additionally, aldosterone can increase the forward trafficking of ROMK channels to increase channel expressions in the apical membrane (42, 103). Furthermore, aldosterone upregulates BK-α expression in the intercalated cells (58) and TRPV4 expression in both principal cells and intercalated cells (104) to facilitate BK channel activation and K^+ secretion. Interestingly, under the condition of LNaHK, plasma aldosterone is elevated to approximately 3600 pg/mL, 15 times higher than the basal level. It seems that this elevation is necessary to generate a high rate of BK-α/β4-mediated K^+ secretion, creating an osmotic diuresis to maintain K^+ homeostasis (99).

Besides aldosterone, other factors also contribute to maintain K^+ balance under HK and LNaHK conditions. Recent studies showed that elevated plasma [K^+] itself could increase kaliuresis by inhibiting Kir4.1/5.1 channels in the basolateral membrane of DCT1, depolarizing the cell membrane and blocking Cl^- exit (105). The increased intracellular [Cl^-] inhibits the With-no-lysine 4 (WNK4) kinase and reduces the phosphorylation and activity of the Na^+-Cl^- cotransporter (NCC) in DCT (105). The inhibition of NCC causes increased Na^+ delivery and increased tubular fluid flow to the distal nephron, increasing distal K^+ secretion through both ROMK and BK channels.

Recent studies indicate that the alkalinity of HK diets plays a critical role in renal K^+ handling. Mice fed an alkaline HK or LNaHK diet maintain their plasma [K^+] below 5.0 mM (58, 90, 99). However, mice fed high KCl (HKCl) or low Na^+ high KCl diets (LNaHKCl) have substantial hyperkalemia with plasma [K^+] above 6.5 mM (58, 90, 99). The intolerance of HKCl results from the lack of BK-αβ4-mediated K^+ secretion which is only active under alkaline conditions (90). Therefore, BK-αβ4 channels are required for increasing urinary K^+ excretion and maintaining plasma [K^+] on alkaline HK and LNaHK diets (58, 90). For simplicity, in the rest of this dissertation, HK and LNaHK will refer to the alkaline diets unless otherwise noted.

Dietary influences on the actions of diuretics

Diuretic drugs are very commonly used for treating many diseases such as hypertension, heart failure, and edema. The CDC estimates that more than 20% of all people over the age of 65 are taking diuretics (106). The effects of diuretics have been extensively studied and well understood. In general, diuretics act on different segments of the nephron to inhibit Na^+ reabsorption to induce diuresis (**Figure 7**). Diuretics that act on nephron segments proximal to ASDN, such as loop and thiazide diuretics, are K-wasting because they increase Na^+ delivery to the ASDN and thus lead to increased distal K^+ secretion. On the other hand, diuretics that act on ASDN such as amiloride and spironolactone are K-sparing because they inhibit Na^+ reabsorption via ENaC and thus inhibit K^+ secretion in the ASDN.

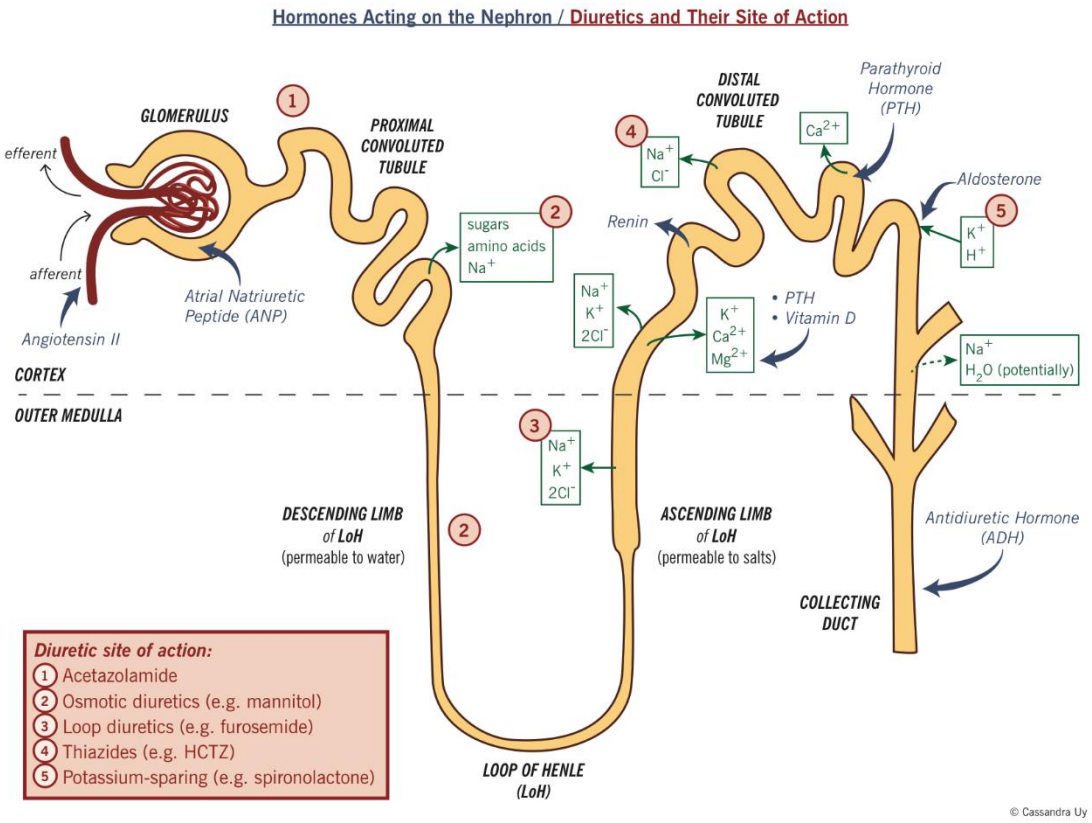

Figure 7. Diuretic sites of actions in the nephron (modified from Chaudhry S.) (107).

However, the actions of diuretics have been only studied in subjects eating modern diets. Little is known about how dietary K^+ contents influence the effects of diuretics in humans. Animal studies provide useful insights into the effects of diuretics under high dietary K^+ conditions. In mice adapted to HK diet, NCC activity is inhibited to shift Na^+ reabsorption to ENaC in the ASDN in exchange for K^+ secretion (105). As a result, on both HK and LNaHK diets, the effects of thiazide diuretics are greatly attenuated (108, 109); while the effects of K-sparing diuretics such as amiloride and spironolactone are much enhanced (99, 109). In fact, mice on HK diet treated with amiloride or spironolactone exhibit profound hyperkalemia (109).

Furosemide, commonly known as Lasix® or "water pill", is one of the most commonly used diuretics. It is secreted by the proximal tubule into the lumen. From the luminal side, it blocks the Cl^- binding site of NKCC2 in the TAL (110). This leads to a series of consequences. Furosemide inhibits NaCl reabsorption in the TAL, which usually reabsorbs 20% of filtered Na^+, leading to profound natriuresis. The increased Na^+ delivery to the ASDN creates a more negative lumen potential due to Na^+ reabsorption by ENaC, causing increased K^+ secretion and thus kaliuresis. Additionally, furosemide obliterates the medullary interstitial gradient, which is established by NaCl reabsorption in the TAL, reducing the urinary concentrating ability. Furthermore, furosemide inhibits the tubuloglomerular feedback by disrupting the Cl^--sensing mechanism of the macula densa, which is mediated by NKCC2 (111-115). However, the furosemide-induced volume depletion can still activate the renin-angiotensin-aldosterone system (RAAS) probably by activation of sympathetic nervous system (116-118).

The cardiovascular benefits of HK diets are at least partially attributed to their diuretic effects (17, 119, 120). Traditionally, this was thought to be due to the inhibition of NKCC2 in the TAL. Micropuncture experiments in Munich-Wistar rats that have exposed renal papilla showed that the medullary interstitial $[K^+]$ at vasa recta reached 46 mM due to medullary K^+ recycling (121). The *in vitro* microperfusion experiments by Stokes *et. al.* (122) showed that, compared to 5

mM [K^+], bath solutions with 25 mM [K^+] inhibited the basolateral K^+ channels in isolated medullary TAL. The consequent depolarization of the cell membrane blocked Cl- exit, thereby inhibiting the NKCC2-mediated NaCl reabsorption. However, there are a few flaws with this mechanism. Chronic K^+ loading increased the interstitial [K^+] from 32 mM to 46 mM in the vasa recta at the bend of the loop with an osmolality of 900 mOsm (121). This 44% increase was not well represented in the *in vitro* experiments, which compared the effects of 5 mM to 25 mM [K^+] bath solutions. Additionally, the Munich-Wistar rats have renal developmental abnormalities, which allow for the loop measurement but may also differ from normally developed animals. Furthermore, the inhibition of fluid reabsorption in PT (123) as well as the recent discovery of plasma [K^+] regulation of NCC in DCT (119) provides another explanation for the diuretic effect of HK diet. Overall, the effect of HK or LNaHK diet on the action of furosemide remains unclear.

The studies in this dissertation seek to investigate how LNaHK and HK diet influence the effect of furosemide on renal K^+ handling.

CHAPTER 1: NET K^+ SECRETION IN THE THICK ASCENDING LIMB OF MICE ON AN ALKALINE LOW NA HIGH K^+ DIET *

Introduction

In contrast to the modern Western diet that has high Na^+ and low K^+ contents, the "ancient" diets, such as the Paleolithic and Mediterranean diets, comprise a preponderance of fruits and vegetables and are low in Na^+ and high in K. The ancient diets are well known for their health benefits in cardiovascular diseases, diabetes, obesity, and multiple cancers (7, 10, 124-126). Our understanding of such diets has, in large part, derived from studies of the South American Yanomami, an isolated culture known for consuming a high K^+ alkaline diet with nearly zero Na (14). Our lab has developed and studied the renal K^+ handling of mice on LNaHK diet as an exaggeration of the ancient diet consumed by the Yanomami (90, 99, 127). Our understanding of the mechanism for handling LNaHK intake is crucial to choosing effective diuretics and preventing the drastic consequences of hypokalemia or hyperkalemia for patients on such diets (108).

Potassium ions are freely filtered in the nephron and reabsorbed by the proximal tubule and the TAL. Potassium is secreted into the lumen in the ASDN by the ROMK and BK channels (25, 128). Potassium secretion is driven by the negative lumen potential generated by Na^+ reabsorption through ENaC channel (42, 109). On HK diet, the medullary interstitial $[K^+]$ can reach 39-53 mM by medullary K^+ recycling (121). The *ex vivo* microperfusion experiments by Stokes *et. al.* (122) showed that high medullary interstitial $[K^+]$ may inhibit NaCl reabsorption via NKCC2 and increase distal flow and Na^+ delivery to stimulate K^+ secretion in the distal nephron. This is a recognized cause for the diuretic effect of high K^+ diets (42, 129). On the other hand,

* The materials presented in this chapter was previously published: Wang, B., Wen, D., Li, H., Wang-France, J. & Sansom, S. C. Net K(+) secretion in the thick ascending limb of mice on a low-Na, high-K diet. Kidney Int 92, 864-875, 2017.

studies showed that NKCC2 activity is increased in mice on a low Na^+ diet (130, 131). The dietary effect of both low Na^+ and high K^+ on the ion transport in the TAL remains uncertain.

Ex vivo microperfusion studies showed that K^+ was reabsorbed in the isolated perfused medullary TAL but secreted in the cortical TAL (132, 133). However, net K^+ secretion in the TAL has not been shown *in vivo*, and the physiological conditions and implications of net K^+ secretion in the TAL remain unclear. In the current study, we found that after mice were adapted to LNaHK diet, furosemide, an inhibitor of NKCC2, enhanced urinary Na^+ and decreased urinary K^+ excretion. Given the high interstitial [K^+] generated by medullary K^+ recycling, we hypothesized that, in mice fed a LNaHK diet, NKCC2 is still active with net K^+ secretion in the TAL which can be inhibited by furosemide.

Methods

Animals

All animals were maintained in accordance with the Institutional Animal Care and Use Committee of the University of Nebraska Medical Center. Wild-type mice on C57BL/6 background (Charles River Laboratories, Wilmington, MA), ROMK wild-type and knockout littermates on 129/SvJ background (generously provided by Dr. Tong Wang, Yale University School of Medicine) were housed in the UNMC animal facility and maintained on a 12-hour day-night cycle, with free access to water and food.

Metabolic cage

Wild-type mice, at 10–12 weeks of age, were given either regular mouse chow (RD; 0.3% Na, 0.6% K), a high K^+ diet (HK diet; 0.3% Na, 5% K with equimolar carbonate/citrate/Cl as anions; TD.07278; Envigo, Indianapolis, IN) or a low Na, high K^+ diet (LNaHK diet; 0.01% Na, 5% K with equimolar carbonate/citrate/Cl as anions; TD.07278; Envigo, Indianapolis, IN) for 4–7 days. Before experiments, mice were placed in metabolic cages for 1 day for acclimation. For acute diuretic treatments, mice were given intraperitoneal injections of vehicle (100 µL poly (ethylene glycol); PEG) or furosemide (15 mg/kg) and returned to metabolic cages for 12 hours to collect urine and measure food and water consumption. For chronic furosemide treatments, mice were provided either furosemide water (0.1 mg/mL, pH 8.4 with 0.7 mM K^+) or control water (0.7 mM $KHCO_3$, pH 8.4). Urine was collected in metabolic cages for 24 hours the day before treatment and on day 1, day 4, and day 7 after treatments. The mice were then anesthetized, sacrificed by exsanguination from the carotid artery, and blood and kidneys were collected. Urine and plasma osmolality were measured with an osmometer (Model 3250, Advanced Instruments, Norwood, MA). Urine and plasma Na^+ and K^+ concentrations were determined by a flame photometer (PFP7, Jenway, Burlington, NJ).

Micropuncture

A mixture of male and female wild-type and ROMK knockout mice at 10–12 weeks of age were given RD, LNaHK diet, or HK diet for 4–7 days. Micropuncture procedures were previously described (134). Briefly, mice were anesthetized with ketamine/xylazine cocktail and the left kidney was immobilized in a Lucite kidney cup (Vestavia Scientific, Atlanta, GA). Modified saline solution with FITC-inulin (140 mM NaCl, 5 mM $KHCO_3$, 2% Mannitol, 500 µg/mL FITC-inulin) was infused via left jugular vein at a rate of 0.5 mL/hr. Urine was collected under mineral oil through a bladder catheter. Blood pressure was monitored with a pressure transducer (Model 427488, Harvard Apparatus, Holliston, MA) via right common carotid artery. Distal tubules were identified by injecting proximal tubules with 0.5% Fast Green FCF (Sigma, St Louis, MO). Microelectrodes were made as previously described (134). A K^+-selective microelectrode and a reference microelectrode were placed in the lumen of an early distal tubule (EDT). The voltage readings were recorded using a high impedance electrometer (Model FD223, World Precision Instruments, Hamden, CT) before and after an intravenous administration of furosemide (5 mg/kg in normal saline) via a separate catheter in left jugular vein. K^+ concentrations were determined from calibration curves generated by standard solutions that minimize Na^+ interference on measurements (55 mM NaCl with 2.5, 5, 10, or 20 mM KCl). Furosemide-sensitive $U_{Na}\dot{V}$ was calculated by subtracting $U_{Na}\dot{V}$ before furosemide treatment from $U_{Na}\dot{V}$ after furosemide treatment.

GFR measurement

Glomerular filtration rate was measured using FITC-inulin (Sigma, St Louis, MO) during the micropuncture experiments as previously described (87). The mice were allowed to equilibrate for 1 hour after IV catheter placement. Urine was collected under mineral oil for 30 minutes before and 20 minutes after furosemide administration. Approximately 20 µL blood was collected from carotid catheter at the midpoint of each clearance period. Urine flow was

determined gravimetrically, and the inulin concentration in urine and plasma were measured using a fluorescence microplate reader at 480 nm excitation and 520 nm emission. GFR was calculated for the periods before and after furosemide administration.

Patch clamp

Wild-type and ROMK knockout mice were provided either RD or LNaHK diet for 7 days. The mice were anesthetized and sacrificed, and the kidneys were removed and cut in coronal sections. TALs were isolated and placed onto a 5 x 5 mm cover glass coated with Poly-L-lysine (Sigma, St Louis, MO) in the bath solution (in mM: 140 NaCl, 5 KCl, 1.8 $MgCl_2$, 1.8 $CaCl_2$, and 10 HEPES and pH 7.4). The cover glass was transferred to a plexiglass chamber on the stage of an inverted microscope (IX73, Olympus Corporation, Center Valley, PA). The tubules were split open by a sharpened micropipette to access the apical surface of TAL. Single-channel patch clamping was performed as described previously (135, 136). Briefly, glass pipettes were pulled using a micropipette puller (P-97, Sutter Instruments, Novato, CA), polished and filled with the pipette solution (in mM: 140 KCl and 10 HEPES with pH 7.4 adjusted with KOH). Single-channel currents were amplified by the Axopatch 200B Amplifier (AutoMate Scientific, Berkeley, CA) and low-pass filtered at 200 Hz by the Low-pass Bessel (LPF-8, Warner Instruments, Hamden, CT). Signals were digitized at a sampling rate of 10 kHz by the Digidata 1440A digitizer (Axon Instruments, Foster City, CA) and recorded and analyzed with pCLAMP 10 software (Molecular Devices, Sunnyvale, CA).

Immunofluorescence staining

Kidneys from sacrificed mice were placed in HistochoiceMB tissue fixative (Bioworld, Dublin, OH) for 24 hours, embedded in paraffin, and sectioned onto slides. Procedures for immunofluorescence staining were previously described (89). In short, slides were rinsed for 10 min in xylene twice, and 2 min in 100%, 95%, 75%, 50%, 35% ethanol, and distilled water. Antigen retrieval was performed by microwaving slides in 0.01 M Na^+ citrate solution at pH 6.0

for 15 min. Slides were then cooled to room temperature and rinsed in 0.1% PBS-Tween for 2 min (3 times), blocked with 1% BSA in PBS for 30 min, and incubated with primary antibody overnight at 4 °C. The next day, slides were rinsed in PBS-T for 2 min (3 times) and incubated with secondary antibodies for 1 hour at room temperature. Slides were again rinsed in PBS-T for 2 min (3 times) and mounted with EMS Shield Mount with DABCO (Electron Microscopy Sciences, Hatfield, PA). The following primary antibodies were used: ROMK (rabbit, diluted 1:200, generous gift from Dr. Paul Welling, University of Maryland, Baltimore, MD), and THP (goat, diluted 1:200, Santa Cruz). The following secondary antibodies were applied for 1 hour: donkey anti-rabbit IgG conjugated Alexa Fluor 488 and donkey anti-goat IgG conjugated Alexa Fluor 594, diluted 1:200 (Invitrogen, Carlsbad, CA).

Results

K^+ secretion in the TAL with LNaHK diet

In traditional understanding, a high K^+ diet inhibits NKCC2 in the TAL, causing its diuretic effect (122). We first examined the effect of furosemide in mice on either RD or LNaHK diet. On both regular diet (RD) and LNaHK diet, wild-type mice (WT) receiving IP furosemide exhibited significantly higher urinary Na^+ clearance and lower urine osmolality than those treated with vehicle **(Figure 8A, Table 2).** Thus, Na^+ is still actively reabsorbed via NKCC2 in mice on LNaHK diet.

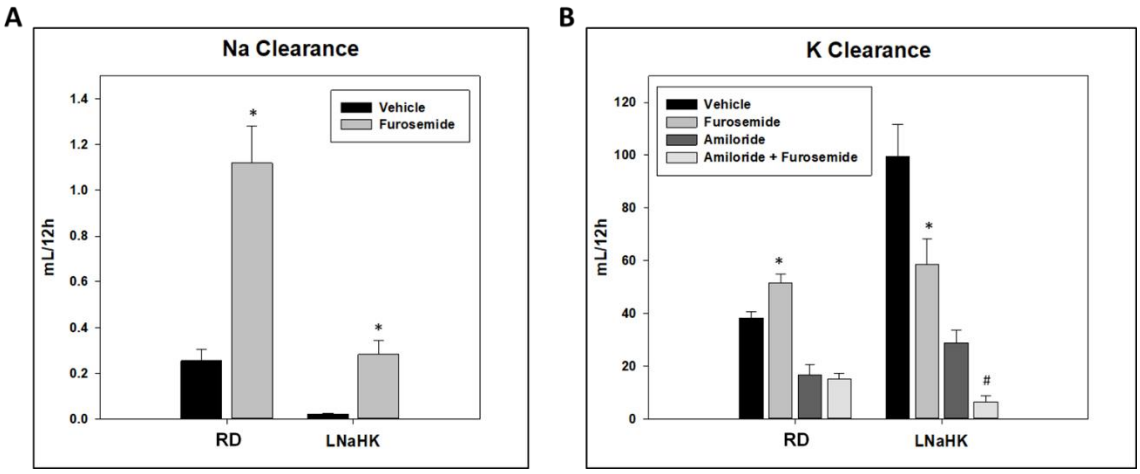

Figure 8. Effect of furosemide on urinary Na^+ and K^+ clearances in mice on RD and LNaHK diet.

A. Twelve-hour renal Na^+ clearance of mice on RD or LNaHK diet treated with IP injections of vehicle or furosemide. **B.** Twelve-hour renal K^+ clearance of mice on RD or LNaHK diet treated with IP injections of vehicle, furosemide, amiloride, or amiloride + furosemide. N = 4 – 14 per group. *$p < 0.05$ vs vehicle; $^{\#}p < 0.05$ vs amiloride analyzed using two-way ANOVA with a post-hoc Tukey test.

Table 2. Metabolic cage measurements for 12 hours, effects of diuretics.

	RD + vehicle (5)	RD + furosemide (8)	LNaHK + vehicle (12)	LNaHK + furosemide (7)
Body weight (g)	21.9 ± 0.3	22.0 ± 0.1	22.8 ± 0.3	19.8 ± 0.3$^{\#}$
Kidney weight (g)	0.27 ± 0.01	0.27 ± 0.01	0.28 ± 0.01	0.27 ± 0.01
Food intake (g/day)	0.2 ± 0.1	0.7 ± 0.3	0.6 ± 0.1	0.2 ± 0.1$^{\#}$
Water intake (mL/day)	0.4 ± 0.1	1.3 ± 0.4	2.1 ± 0.3$^{\$}$	1.9 ± 0.6
Urine flow (mL/day)	1.3 ± 0.2	2.6 ± 0.5	2.1 ± 0.2	3.4 ± 0.6$^{\#}$
Urine osmolality (mOsm)	2276 ± 332	1521 ± 308	1878 ± 186	786 ± 123$^{\#}$
$U_{Na}\dot{V}$ (µmol/day)	142 ± 63	315 ± 47*	6.2 ± 0.6$^{\$}$	72.6 ± 15.7$^{\#}$
$U_{K}\dot{V}$ (µmol/day)	339 ± 17	390 ± 48	1132 ± 148$^{\$}$	609 ± 113$^{\#}$
Hematocrit (%)	41.2 ± 1.2	48.2 ± 1.4*	40.4 ± 1.0	42.4 ± 2.5
Plasma osmolality (mOsm)	296.7 ± 3.3	295.0 ± 2.7	288.2 ± 4.0	293.3 ± 6.1
Plasma [Na^+] (mM)	155 ± 3	140 ± 3*	151 ± 2	141 ± 1$^{\#}$
Plasma [K^+] (mM)	4.2 ± 0.2	4.1 ± 0.2	6.0 ± 0.3$^{\$}$	5.8 ± 0.2
Urine pH	6.4 ± 0.2	5.8 ± 0.1*	6.9 ± 0.1$^{\$}$	6.0 ± 0.2$^{\#}$

Parentheses indicate the number of animals. Data are shown as mean ± SEM. *$p < 0.05$ compared to RD + vehicle; $^{\#}p < 0.05$ compared to LNaHK + vehicle; $^{\$}p < 0.05$ compared to RD + vehicle analyzed by two-way ANOVA with a post-hoc Tukey test.

On RD, the mice treated with furosemide exhibited a higher renal K^+ clearance than the vehicle group. This is expected since furosemide is a K-wasting diuretic by stimulating K^+ secretion in the distal nephron (137, 138). However, on LNaHK diet, furosemide-treated mice had a lower renal K^+ clearance than the vehicle group **(Figure 8B)**. To exclude the complicating effects of K^+ secretion in the distal nephron, mice were treated with furosemide + amiloride and amiloride alone, which inhibits the Na^+ reabsorbing driving force required for both ROMK- and BK-mediated K^+ secretion (108, 109). Compared to the amiloride-treated group, the furosemide + amiloride group had lower renal K^+ clearance on LNaHK diet, but not on RD **(Figure 8B)**. These results indicate that the furosemide effect on K^+ clearance is independent of the distal K^+ secretion in mice on LNaHK diet.

To assess the chronic effect of furosemide, WT were kept on LNaHK diet for 7 days and then treated them with either furosemide water or control water for 7 days. The results are shown in **Figure 9** and **Table 3**. For mice on control water, urinary K^+ excretion ($U_K\dot{V}$) was unchanged after 7 days. For mice on furosemide water, however, $U_K\dot{V}$ was reduced on the first day of furosemide treatment **(Figure 9A)**. After 7 days, plasma [K^+] was significantly higher and K^+ clearance significantly lower in mice on furosemide water compared to control water **(Figure 9B, C)**. These results indicate that furosemide is a K-sparing diuretic and can raise plasma [K^+] in mice on LNaHK diet.

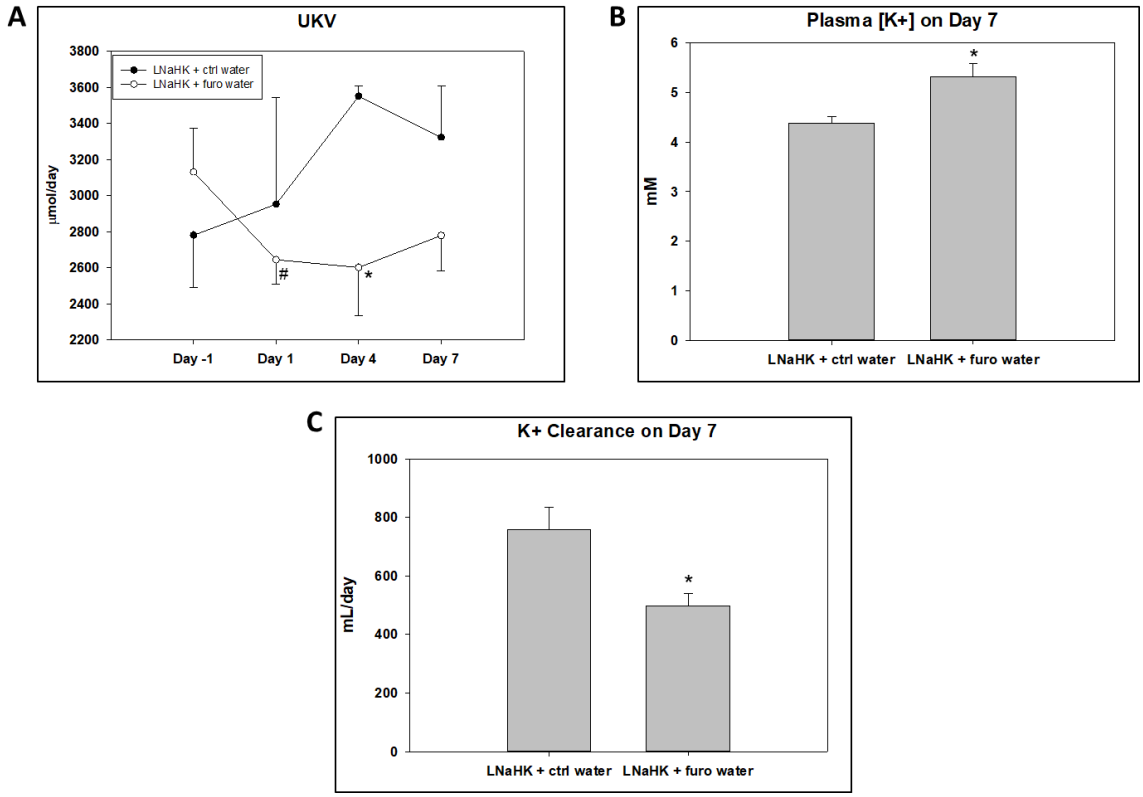

Figure 9. Chronic effect of furosemide on renal K^+ handling in mice on LNaHK diet.

A. Urinary K^+ excretion ($U_K\dot{V}$) on the day before treatment (day -1), day 1, day 4, and day 7 after treatment with control (Ctrl) or furosemide (Furo) water in WT on LNaHK diet. * $p < 0.05$ compared to LNaHK + Ctrl water; # $p < 0.05$ compared to Day -1 analyzed with two-way repeated measures ANOVA with post-hoc Holm-Sidak test. **B.** Plasma [K^+] after 7 days of treatment with Ctrl or Furo water in WT on LNaHK diet. **C.** Urinary K^+ clearance after 7 days of treatment with Ctrl or Furo water in WT on LNaHK diet. * $p < 0.05$ compared to LNaHK + Ctrl water analyzed with one-way ANOVA.

Table 3. Metabolic cage measurements for chronic effect of furosemide.

	LNaHK + Ctrl water (4)	LNaHK + Furo water (4)
Body weight (g)	22.1 ± 0.8	20.9 ± 0.7
Food intake (g/day)	3.1 ± 0.2	3.4 ± 0.3
Water intake (mL/day)	8.4 ± 0.8	15.4 ± 1.6*
Urine flow (mL/day)	4.0 ± 0.2	6.0 ± 0.2*
Urine osmolality (mOsm)	1872 ± 105	1002 ± 77*
$U_{Na}\dot{V}$ (µmol/day)	35.7 ± 7.5	43.6 ± 2.8
$U_{K}\dot{V}$ (µmol/day)	3323 ± 283	2620 ± 152
Hematocrit (%)	41.4 ± 1.2	42.3 ± 1.7
Plasma osmolality (mOsm)	295 ± 2.6	295 ± 2.6
Plasma [Na^+] (mM)	139.5 ± 1.1	137.1 ± 1.3
Plasma [K^+] (mM)	4.4 ± 0.1	5.3 ± 0.3*
K Clearance (mL/day)	758 ± 76	498 ± 42*
Urine pH	9.2 ± 0.1	8.6 ± 0.1*

Parentheses indicate the number of animals. Data are shown as mean ± SEM. *$p < 0.05$ compared to LNaHK + Ctrl water analyzed by one-way ANOVA.

One possible explanation for the effect of furosemide in mice on LNaHK diet is that net K^+ secretion in the TAL is inhibited. To test this hypothesis more directly, micropuncture techniques were used to measure the K^+ concentration in the EDT (EDT [K^+]) before and after intravenous (IV) administration of vehicle or furosemide in mice on RD or LNaHK diet. As shown in **Figure 10**, vehicle administration did not affect the EDT [K^+] in mice on either diet. Before furosemide treatment, the EDT [K^+] was significantly higher in mice on LNaHK diet than RD. Furosemide infusion increased the EDT [K^+] in mice on RD but decreased EDT [K^+] in mice on LNaHK diet without affecting MAP or GFR during the collection period **(Table 4).** These results indicate furosemide-sensitive net K^+ reabsorption in the TAL of mice on RD and net K^+ secretion in mice on LNaHK diet.

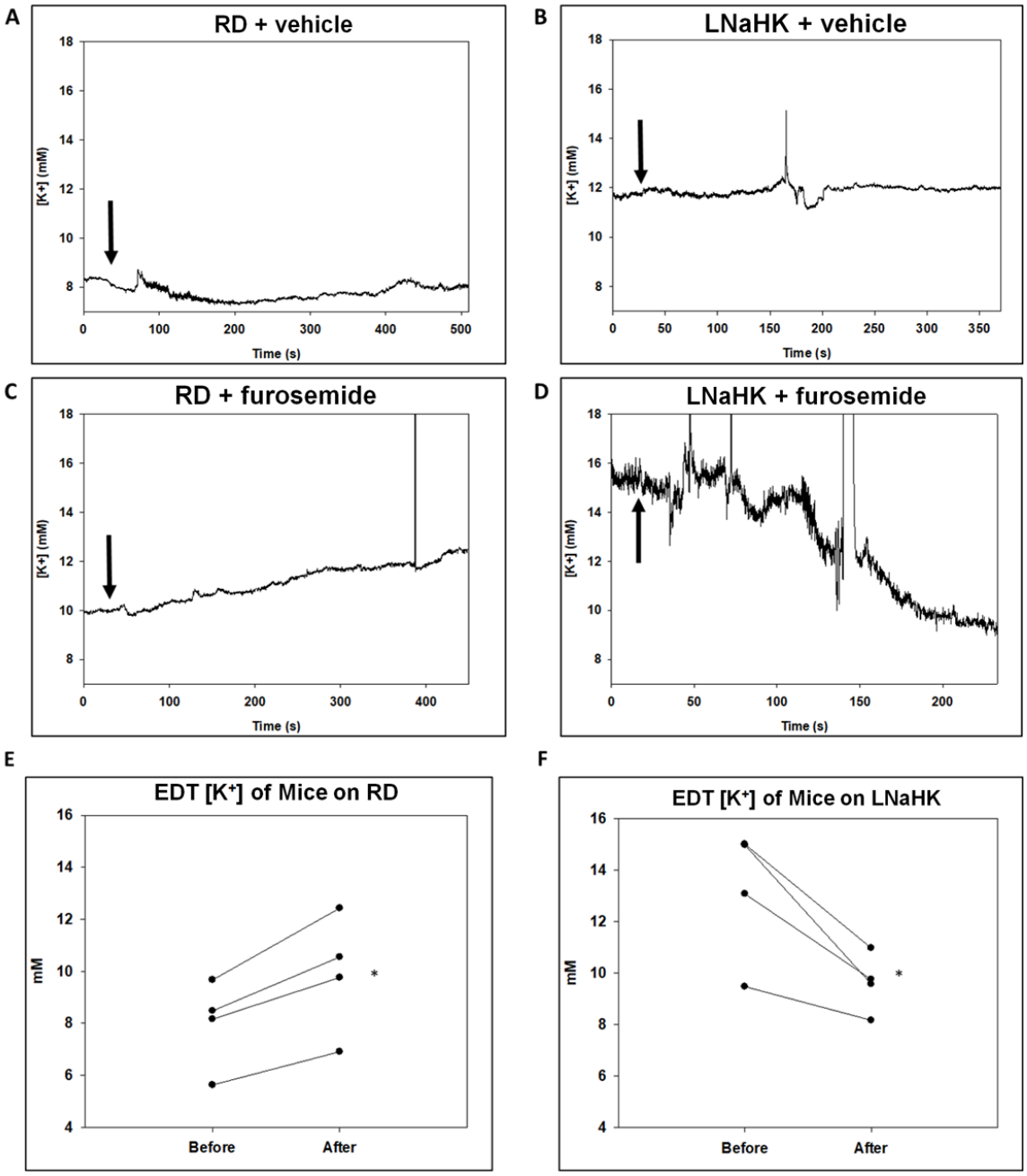

Figure 10. Effect of furosemide on EDT [K^+] in mice on RD or LNaHK diet.

A-D. Representative recordings of K-selective microelectrodes in the lumen of EDT before and after IV injections of vehicle or furosemide in WT on RD or LNaHK diet. Arrows indicate the time of injections. **E and F.** EDT [K^+] of mice on RD **(E)** or LNaHK diet **(F)** before and after IV furosemide injections. N = 4 per group. *$p < 0.05$ vs before furosemide analyzed using a paired t-test.

Table 4. Hemodynamic measurements in micropuncture experiments.

		WT RD (4)	WT LNaHK (5)	WT HK (4)	ROMK KO LNaHK (4)
MAP (mmHg)	**Before Furo**	108.7 ± 6.6	102.7 ± 3.0	100.0 ± 8.6	96.4 ± 8.4
	After Furo	107.7 ± 7.4	103.4 ± 3.6	100.0 ± 10.0	96.0 ± 9.2
GFR (µL/min/g)	**Before Furo**	9.3 ± 1.7	9.3 ± 1.1	7.1 ± 0.6	4.8 ± 0.6*
	After Furo	9.4 ± 0.5	8.4 ± 1.1	6.0 ± 1.1	5.5 ± 0.3*

Numbers in parentheses indicate the number of animals. Data are shown as mean ± SEM. *$p < 0.05$ compared to WT LNaHK analyzed by two-way ANOVA with a post-hoc Tukey test.

Normal Na, high K^+ diet

The net K^+ secretion in the TAL may be partly due to the high interstitial K^+ concentration generated by medullary K^+ recycling in mice on HK diet (122, 139). We examined whether there was net K^+ secretion in the TAL of mice on HK diet. As revealed by the results of micropuncture experiments in **Figure 11**, furosemide did not affect the EDT [K^+] of WT on HK diet despite decreased urine osmolality as an indication of its effectiveness **(Figure 11A and B)**. There was no significant difference in MAP and GFR before and after furosemide treatment **(Table 4).**

These results suggest that the low Na^+ content of LNaHK diet is essential for net K^+ secretion in the TAL. Studies have shown that HK diet can reduce NKCC2 activity, probably by inhibiting Cl^- exit from the TAL(122). In agreement with this notion, compared to vehicle, the furosemide-treated mice exhibited higher $U_{Na}\dot{V}$ than vehicle group in WT on RD, but not in WT on HK diet **(Figure 12A)**. In contrast to WT on HK diet, the furosemide group exhibited higher $U_{Na}\dot{V}$ than vehicle in mice on LNaHK diet **(Figure 8A)**. Because of the difference in dietary Na^+ content, we were unable to compare the furosemide-sensitive $U_{Na}\dot{V}$ between mice on RD and LNaHK diet using metabolic cage experiments. Thus, the furosemide-sensitive $U_{Na}\dot{V}$ was evaluated during micropuncture experiments, in which all mice received the same IV infusion for the same time period. The mice on LNaHK diet exhibited significantly greater furosemide-sensitive $U_{Na}\dot{V}$ than those on RD or HK diet. There was no significant difference in furosemide-sensitive $U_{Na}\dot{V}$ between mice on RD and HK diet **(Figure 12B)**.

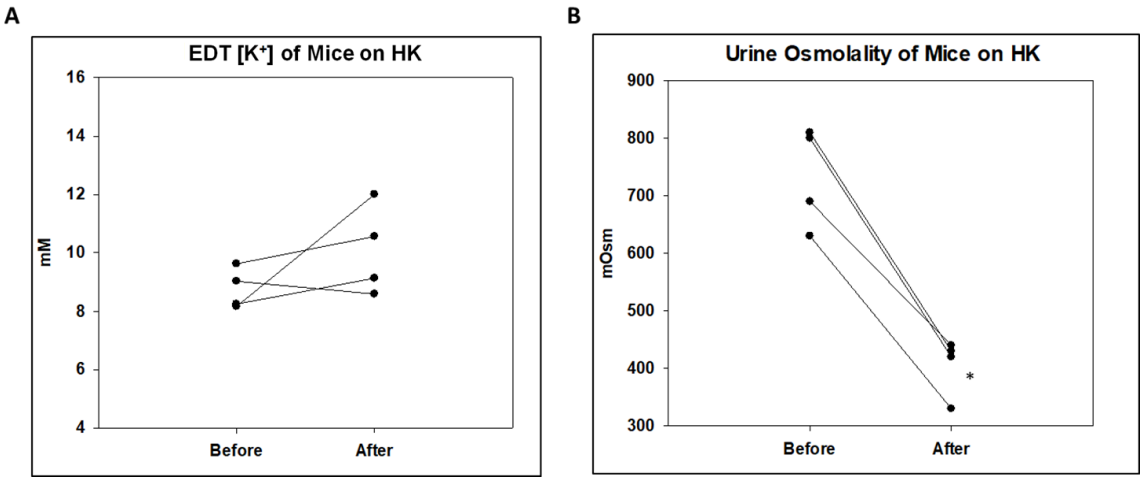

Figure 11. Effect of furosemide on EDT [K^+] and urine osmolality of mice on HK diet.

A. EDT [K^+] of mice on HK diet before and after IV furosemide injection. **B.** Urine osmolality of mice on HK diet before and after furosemide. N = 4 per group. *$p < 0.05$ vs before furosemide analyzed using a paired t-test.

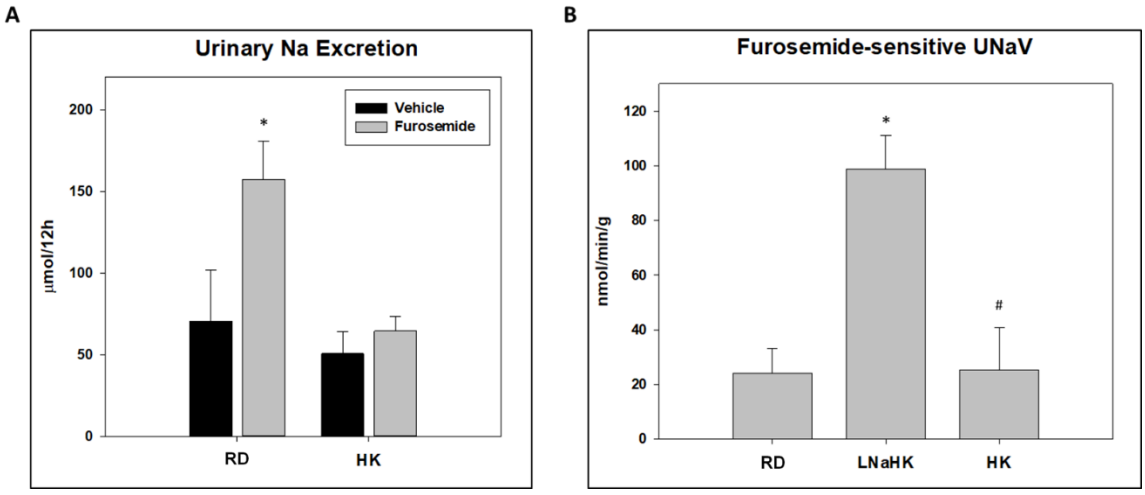

Figure 12. Effect of furosemide on urinary Na^+ excretion in mice on RD or HK diet.

A. Twelve-hour $U_{Na}\dot{V}$ of mice on RD or HK diet treated with IP injections of vehicle or furosemide. N = 8 per group. *$p < 0.05$ vs vehicle analyzed using two-way ANOVA with a post-hoc Tukey test. **B.** Furosemide sensitive $U_{Na}\dot{V}$ normalized to body weight of mice on RD, LNaHK diet, or HK diet. N = 4 – 9 per group. *$p < 0.001$ vs RD; $^{\#}p < 0.05$ vs LNaHK diet analyzed by one-way ANOVA.

Role of ROMK in net K^+ secretion

Both 30 pS and 70 pS inward rectifying K^+ channels (Kir) have been reported to represent ROMK in the apical membrane of TAL(37, 140). To investigate which K^+ channel mediates net K^+ secretion, Dr. Huaqing Li in our lab performed single-channel patch clamp experiments on split-open TALs from WT and ROMK knockouts (ROMK KO) on RD or LNaHK diet. Whereas the 70 pS Kir appeared as one or two channels in a patch, we often found the 30 pS Kir as multiple channels (2-5) in a patch. **Figure 13A** shows recordings of a single 30 pS Kir (top; -Vp = -60 mV) and multiple 30 pS Kir (middle and bottom; -Vp = -40 mV) in cell-attached patches from TALs of WT and ROMK KO. No difference was found in Po of the 30 pS Kir from mice on LNaHK diet compared with RD **(Figure 13C)**. However, as shown by the recordings of **Figure 13B** and the summary plot of **Figure 13C**, the Po of the 70 pS Kir (-Vp = -40 mV) was greater in mice on LNaHK diet compared with RD.

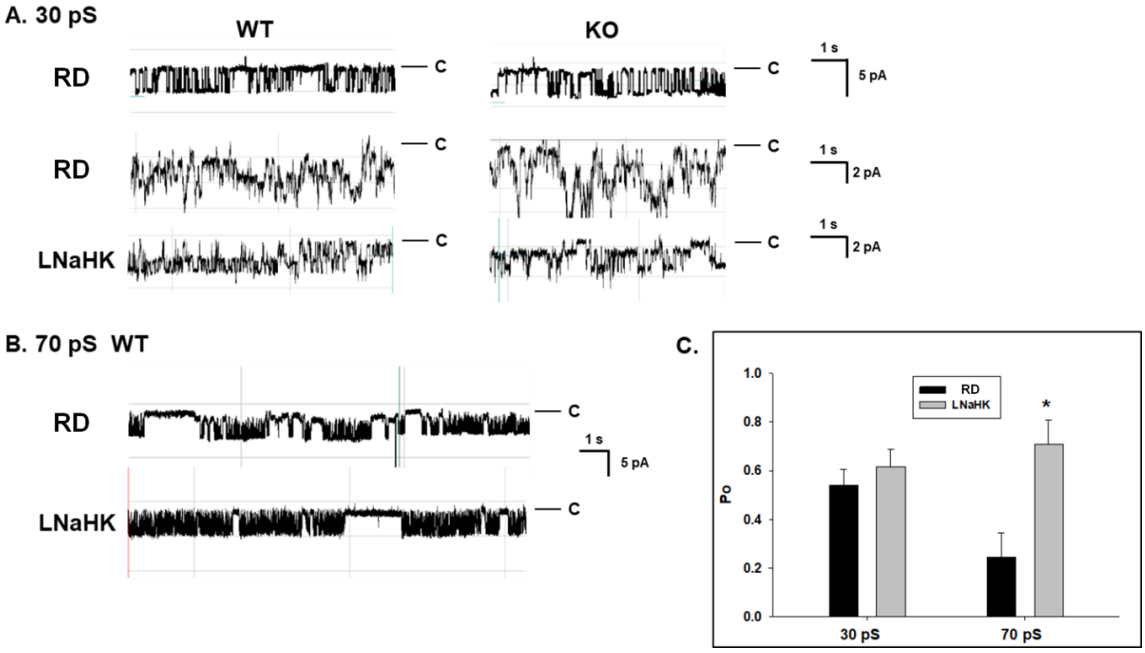

Figure 13. Patch clamp recordings of apical K^+ channels in the TAL of mice on RD and LNaHK diet (performed by Dr. Huaqing Li).

A. Recordings of single (top; RD, -Vp = -60 mV) and multiple (-Vp = -40 mV) 30 pS (inward currents) K^+ channels from cell-attached patches of split-open TAL of WT and ROMK KO mice on RD or LNaHK diet. Pipette solution contained 140 mM KCl. Red lines denote closed states. **B.** Recordings of 70 pS Kir channels in apical membrane of WT mice. The recordings indicate 2 closed states (long and short) with an increased duration in long closed state in channels of mice on RD. **C.** Summary of Po at –Vp = -40 mV of the 30 pS and 70 pS Kir in the TAL from WT on RD and LNaHK diet. *$p < 0.05$ vs RD analyzed by one-way ANOVA.

Table 5 shows the number and conductance of apical K^+ channels in the TALs from WT and ROMK KO on RD or LNaHK diet. The single channel conductance of the "30 pS" Kir varied with a range of 25 to 38 pS (inward currents) in cell-attached patches and was not significantly different among the four groups. Likewise, the single channel conductance of the 70 pS Kir and the BK channel was not different in WT on LNaHK diet compared with RD. The same density (channels per patch) of 30 pS Kir was found in all four groups. The densities of the 70-pS Kir and BK in WT were also not significantly different between the two diets. However, unlike the 30 pS Kir, no 70 pS Kir was found in the TAL from ROMK KO on RD nor LNaHK diet. Overall, these results show that only the 70 pS Kir is ROMK in the TAL and the 70 pS ROMK channel was more active in the apical membranes in mice on LNaHK diet, compared to RD.

Consistent with the patch clamp results, immunofluorescence staining showed similar labeling of ROMK in the apical membrane of TAL for WT on both diets **(Figure 14A-F)**. The antibody specificity was validated by ROMK KO as a negative control **(Figure 14G-I)**.

To further determine the role of ROMK in the TAL net K^+ secretion *in vivo*, micropuncture was used to measure the EDT $[K^+]$ before and after IV furosemide in ROMK WT and ROMK KO on LNaHK diet. As shown in **Figure 15A**, WT on LNaHK diet exhibited furosemide-sensitive net K^+ secretion in the TAL. However, as shown in **Figure 15B**, ROMK KO on LNaHK diet did not exhibit furosemide-sensitive net K^+ secretion. These results indicate that ROMK is required for the net K^+ secretion in the TAL of mice on LNaHK diet.

Table 5. Number and conductance of apical K^+ channels in the TAL.

	Diet	N of mice	N of patches	30 pS Kir			70 pS Kir			BK		
				P#	C#	G (pS)	P#	C#	G (pS)	P#	C#	G (pS)
WT	**RD**	8	17	7	13	31.4 ± 1.4	7	11	70.7 ± 2.2	2	5	165.0 ± 5.0
WT	**LNaHK**	7	27	4	5	34.7 ± 0.5	5	6	69.8 ± 0.9	4	6	185.2 ± 24.3
KO	**RD**	5	20	6	12	35.5 ± 0.6	0*	0		1	1	225.8
KO	**LNaHK**	4	17	6	9	34.2 ± 1.7	0	0		0	0	

Experiment performed by Dr. Huaqing Li. "P#" denotes the number of patches that contain one or more respective channel. "C#" denotes the total number of respective channels. "G" denotes single channel conductance (mean ± SEM). *$p < 0.05$ compared to WT analyzed by a chi-squared test.

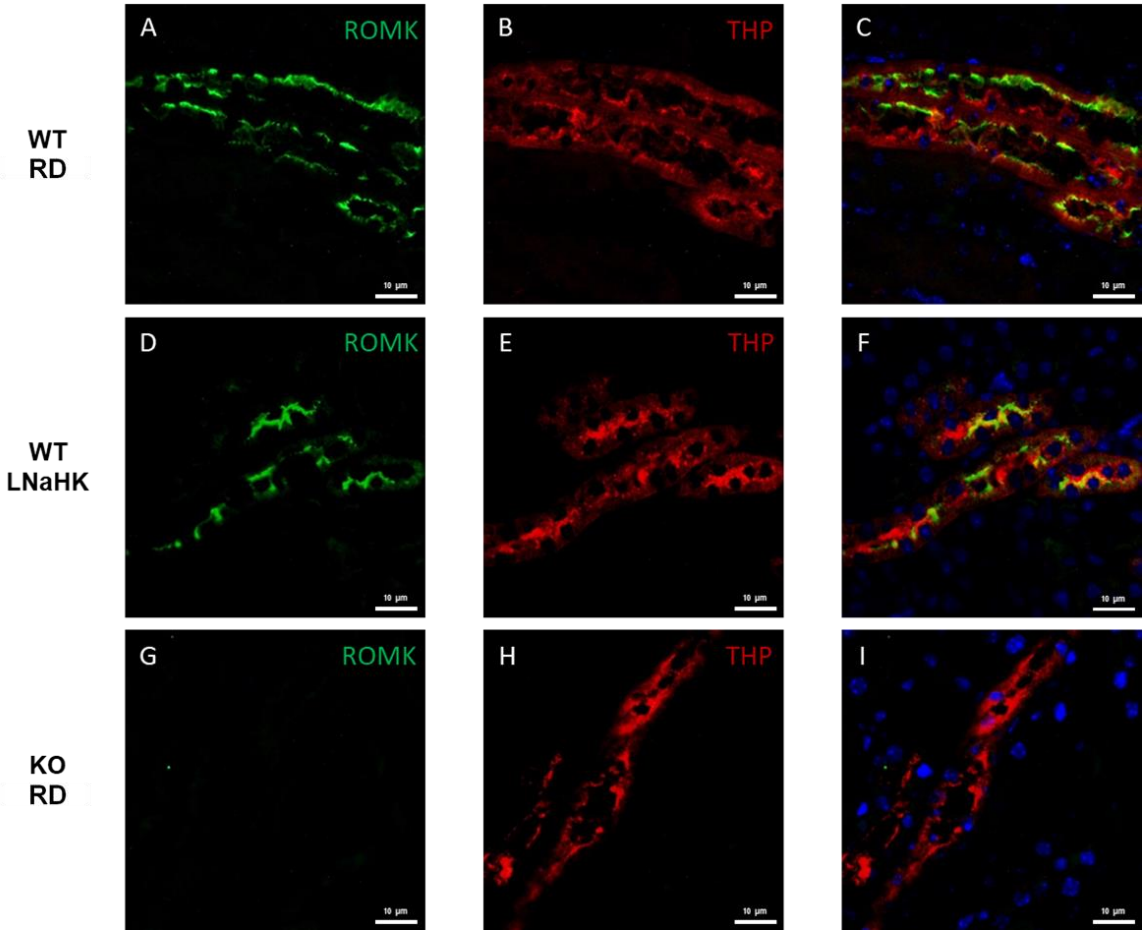

Figure 14. ROMK localization in the TAL of mice on RD and LNaHK diet.

A-C. Immunostaining of ROMK (green), Tamm-Horsfall Protein (THP; marker of TAL; red), and both in the outer medulla of WT on RD. **D-F.** Immunostaining of ROMK (green), THP (red), and both in the outer medulla of WT on LNaHK diet. **G-I.** Immunostaining of ROMK (green), THP (red), and both in the outer medulla of ROMK KO on RD. All images were taken at 400X magnification. All scale bars are 10 µm.

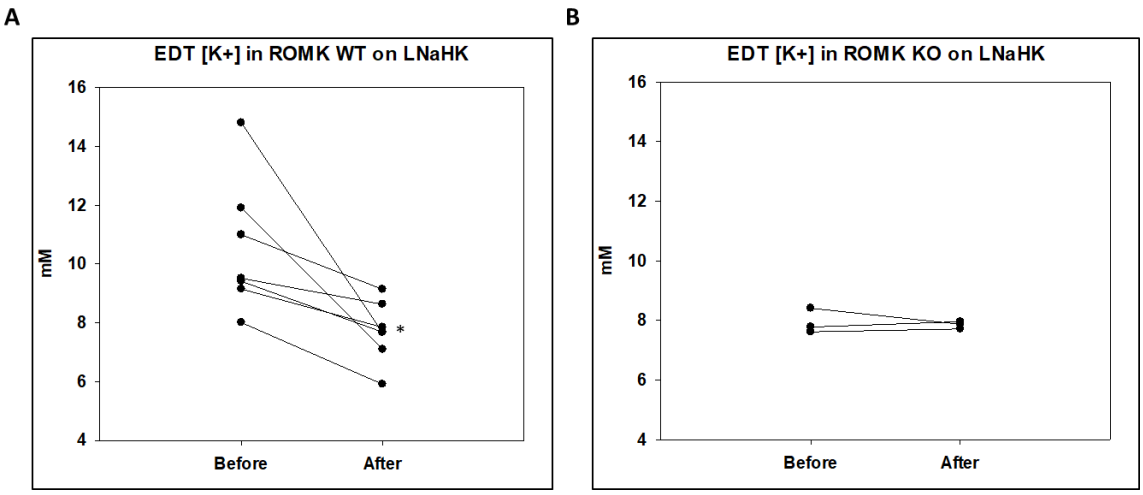

Figure 15. Effect of furosemide on EDT [K^+] in ROMK WT and KO on LNaHK diet.

A and B. EDT [K^+] of ROMK WT **(A)** and KO **(B)** on LNaHK diet before and after IV furosemide injection. N = 7 for WT; N = 3 for ROMK KO. *$p < 0.05$ vs before furosemide, analyzed by a paired t-test.

Discussion

The TAL reabsorbs about 25% of filtered K^+ via the apical NKCC2 and basolateral K-selective channels. However, much of the K^+ transported by the NKCC2 is recycled back to the lumen through the apical ROMK in order to maintain a continual supply of K^+ for NaCl reabsorption (28, 40). In the *ex vivo* microperfusion experiments with isolated hamster TAL, Tsuruoka *et. al.* (132) found net K^+ reabsorption in the medullary TAL but net K^+ secretion in the cortical TAL. Bailly *et. al.* (133) also found a net K^+ secretion in isolated perfused mouse cortical TALs. However, two other groups failed to observe net K^+ secretion with isolated perfused TALs (141, 142). The discrepancies are probably due to differences in experimental conditions. Nonetheless, net K^+ secretion in the TAL has never been described *in vivo*, and its physiological conditions and implications remain unclear. The present study demonstrates *in vivo* net K^+ secretion in the TAL of mice that are adapted to LNaHK diet, but not to a high K^+ diet with normal Na. The 70 pS ROMK channel is the likely avenue for K^+ secretion in mice on LNaHK diet.

Net K^+ secretion in TAL with LNaHK diet

Furosemide is a widely used diuretic for the treatment of hypertension, edema, congestive heart failure, hepatic failure, and chronic kidney disease (143, 144). Empiric potassium is a recommended supplement for furosemide due to its K-wasting effect (145). Furosemide inhibits NKCC2 in the TAL and increases distal Na^+ delivery and flow, thus promoting distal K^+ secretion in the ASDN (138). Consistent with this understanding, in mice on RD, furosemide increased renal K^+ clearance. In mice on LNaHK diet, however, furosemide showed the opposite effect of reducing renal K^+ clearance. The fact that furosemide reduced K^+ clearance both in the presence and absence of amiloride strongly suggests furosemide-sensitive net K^+ secretion in the TAL. Notably, 12 hours after IP furosemide injection, renal K^+ clearance was decreased, but plasma

$[K^+]$ was unaffected. This may be due to extrarenal K^+ handlings including transcellular shift into muscle cells and excretion in the colon (146). Chronic treatment with furosemide for 7 days decreased K^+ clearance and elevated plasma $[K^+]$, demonstrating that furosemide changes from a K-wasting to a K-sparing diuretic when the mice are kept on LNaHK diet.

Additionally, in mice on LNaHK diet, elevated aldosterone along with other factors upregulate ENaC, ROMK, and BK expressions and activities to promote K^+ secretion in the ASDN (42, 99, 101, 109). As shown in **Table 2**, furosemide still increased urine flow and decreased urine osmolality but did not increase $U_{Na}\dot{V}$ after 7 days. This indicates that the increased distal Na^+ delivery by furosemide is completely reabsorbed by ENaC, provided that NCC in the DCT is completely inhibited by the LNaHK diet (108). Along with increased distal flow, furosemide should further stimulate K^+ secretion through ROMK and BK in the ASDN. However, the overall effect of furosemide in mice on LNaHK diet is a decrease in $U_K\dot{V}$, suggesting that the inhibition of TAL net K^+ secretion must exceed the stimulation of distal K^+ secretion.

Our micropuncture studies provided more direct evidence for net K^+ secretion. Furosemide had strikingly opposite effects on EDT $[K^+]$ in mice on RD and LNaHK diet without altering MAP or GFR within the periods of measurements. Because of the high interstitial $[K^+]$, the paracellular pathway could mediate net K^+ secretion. However, the EDT $[K^+]$, which was initially different in the two diets before treatment, reached similar concentrations a few minutes after furosemide injections. This result makes the paracellular pathway unlikely because furosemide would not block K^+ secreted by the paracellular route. Moreover, for paracellular K^+ secretion, the EDT $[K^+]$ after furosemide should still be greater in mice on LNaHK diet than on RD.

In vivo micropuncture of the mouse distal nephron has the limitation of the absence of flow measurements before and after systemic injections of furosemide. Intravenous injections of

furosemide will diminish the medullary interstitial gradient and change the flow in the EDT. However, with the inhibition of NKCC2 by furosemide, we expect that the tubular fluid in EDT is similar to the fluid in late proximal tubule. For mice on LNaHK diet, the EDT [K^+] before furosemide was higher than after furosemide, suggesting that the [K^+] in the EDT was greater than [K^+] in the late proximal tubule. Along with the opposite effect in mice on RD, we provide strong evidence for net K^+ secretion in the TAL. Additionally, furosemide may inhibit carbonic anhydrase (147), causing more K^+ following Na^+ delivery to the EDT, which would increase the EDT [K^+]. Therefore, if furosemide inhibits carbonic anhydrase, the actual amount of furosemide-sensitive K^+ secretion in the TAL of LNaHK diet mice would be greater than that observed.

Role of NKCC2 in net K^+ secretion

The diuretic effect of HK diet was thought to be due to inhibition of NKCC2 (42, 122). On LNaHK diet, however, NKCC2 activity is enhanced, indicating that the diuretic effect of LNaHK diet is not by the same mechanism as in HK diet. In fact, a recent study by Cornelius *et. al.* (99) showed that in mice on LNaHK diet, the BK-αβ4-mediated K^+ secretion in the distal nephron may contribute to the diuretic effect.

Another important finding in our study is that the net K^+ secretion in TAL seems to be unique for mice on LNaHK diet but not HK diet, probably because of upregulated NKCC2 activity. This is consistent with a previous *ex vivo* study showing that NKCC2 was inhibited by the high interstitial [K^+] in mice on HK diet (122). Without an active NKCC2, the NKA cannot supply enough intracellular K^+ for secretion. This provides further evidence for transcellular K^+ secretion. The exact mechanism for increased NKCC2 activity in mice on LNaHK diet needs investigation.

The low Na^+ content of LNaHK diet may result in volume depletion leading to the activation of the renin-angiotensin-aldosterone system (RAAS) and elevated plasma vasopressin (AVP). Both AVP and angiotensin II (Ang II) are regulators of NKCC2. AVP increases NKCC2 expression via V2 receptor-mediated pathways (148). However, studies showed that plasma and urinary AVP levels were either unchanged or decreased in animals fed a low Na^+ diet (149-151). The effect of LNaHK diet on plasma AVP remains unclear. Another possible candidate is Ang II. Studies showed that a low Na^+ diet increased NKCC2 phosphorylation and caused a shift from the low-affinity NKCC2A to the high-affinity NKCC2B isoform, partly mediated by the actions of Ang II on AT1 receptors (130, 152). Ang II level is greatly increased in mice on LNaHK diet, but not on HK diet (99, 127, 153). These findings suggest that elevated Ang II may be responsible for the upregulated NKCC2 activity in mice on LNaHK diet.

Role of ROMK in net K^+ secretion

Other K^+ channels, including BK channels, have been observed by our laboratory and others (76) in the TAL. However, ROMK has been identified as the K^+ channel involved in recycling the K^+ that is reabsorbed by NKCC2 (37, 40, 140). ROMK KO exhibit type 2 Bartter's with extreme natriuretic diuresis (40). Consistent with the previous study (140), our patch clamp experiments identified the 70 pS K^+ channel as ROMK in the apical membrane of TAL. In contrast to the study by Lu *et. al.* (37), we found the same density and Po of a 30 pS K^+ channel in ROMK KO. It is possible that ROMK KO exhibited no furosemide-sensitive net K^+ secretion in the TAL because of decreased NKCC2 activity. However, the increased activity of the ROMK channel, but not the 30 pS channel, in WT on LNaHK diet indicates that ROMK mediates the observed net K^+ secretion.

Unlike ROMK in the ASDN, the mechanism for regulating ROMK in the TAL is not well understood. In the ASDN, ROMK activity is upregulated in response to high dietary K^+ by

increasing channel density rather than Po (154). Aldosterone-dependent signaling pathways, including SGK1 and PKA, promote the forward trafficking of ROMK channels to the apical membrane of ASDN by phosphorylating ROMK (42, 103, 155). Interestingly, our patch clamp experiments showed that TAL from mice on LNaHK diet exhibited increased Po rather than channel density of ROMK. The immunofluorescence staining also indicates that LNaHK diet did not affect ROMK trafficking. The recent study by Dong *et. al.* (43) demonstrated that ROMK1 isoform, which is expressed in the CCD, but not TAL, was required for ROMK trafficking in response to high K^+ intake. This study suggests that the ROMK2 isoform in the TAL is regulated by different signaling pathways than the ROMK1 in the ASDN. Mice on LNaHK diet have highly elevated aldosterone and Ang II compared to RD (99, 127, 153). Since the TAL is absent of 11-β-hydroxysteroid dehydrogenase 2 (156), aldosterone is unlikely to regulate ROMK in TAL. WNK1, WNK3, and WNK4 all regulate ROMK by affecting clathrin-dependent endocytosis in the ASDN (97). Thus, the WNKs are unlikely to regulate the Po of ROMK in the TAL. The patch clamp study by Lu *et. al.* (157) also showed that Ang II regulates the activity of the 70 pS ROMK in the TAL. Thus, Ang II may play a role to increase ROMK activity in the TAL of mice on LNaHK diet.

Intracellular pH is another important regulator of ROMK activity. Like other Kir channels, the Po of ROMK is highly sensitive to intracellular pH (30). The urine pH was higher in mice on LNaHK diet than on RD due to the alkaline dietary content. However, the dietary effect on the intracellular pH of TAL cells remains unclear.

In summary, we have provided *in vivo* evidence of furosemide-sensitive net K^+ secretion in the TAL of mice on LNaHK diet. Net K^+ secretion is dependent on increased NKCC2 activity and may be mediated by ROMK. With net K^+ secretion in the TAL, furosemide becomes a K-sparing diuretic and may lead to hyperkalemia. As summarized in **Figure 16**, furosemide inhibits the net K^+ reabsorption in the TAL of mice on RD, increasing distal Na^+ delivery and flow,

thereby promoting K^+ secretion through ROMK and BK channels in ASDN. In mice on LNaHK diet, upregulated ROMK and NKCC2 activity results in net K^+ secretion in the TAL via ROMK channels. Elevated plasma aldosterone on LNaHK diet upregulates ENaC, ROMK, and BK in ASDN to promote distal K^+ secretion. Furosemide not only inhibits the net K^+ secretion in the TAL but also increases distal flow and Na^+ delivery that further stimulate distal K^+ secretion. The net result of these two opposing effects is a decrease in K^+ excretion. Our finding is especially important when considering diuretic treatments for patients consuming a healthy low Na^+ high K^+ diet, which changes furosemide from a K-wasting to a K-sparing diuretic.

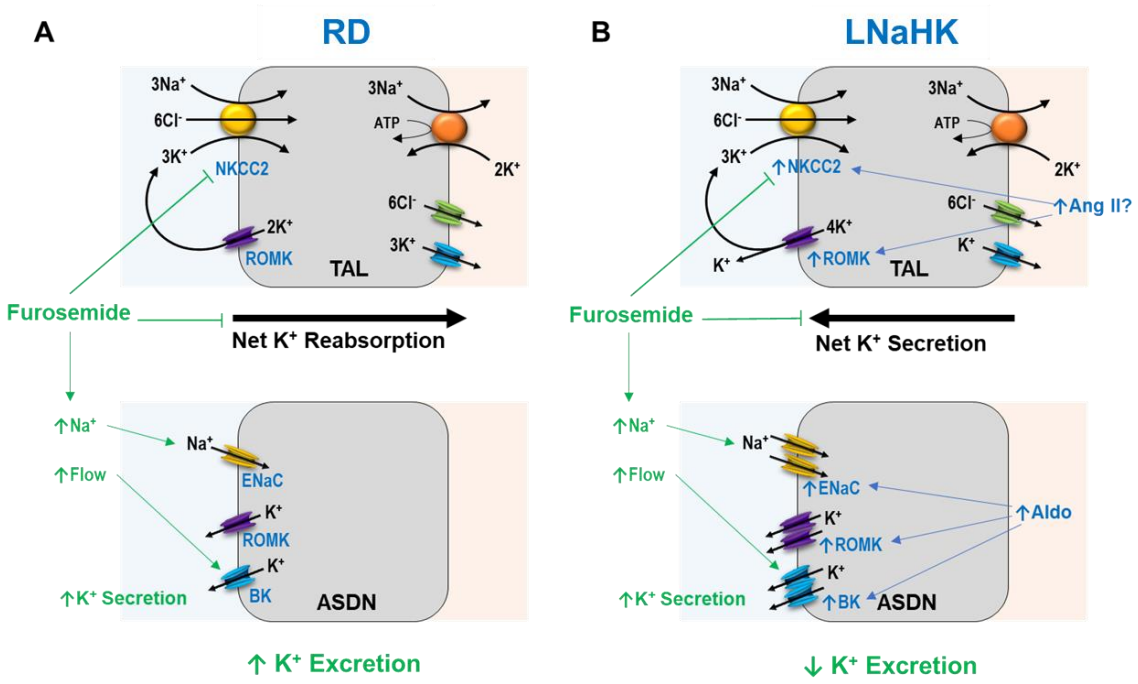

Figure 16. Summary figure of dietary effects on furosemide actions on urinary K^+ excretion.

A. On RD diet, furosemide blocks NKCC2, inhibiting net K^+ reabsorption in the TAL while increasing distal Na^+ delivery and flow, which stimulates K^+ secretion through ROMK and BK in ASDN. The net effect of furosemide is an increase in urinary K^+ excretion. **B.** On LNaHK diet, up-regulated NKCC2 and ROMK, possibly by Ang II, results in net K^+ secretion in the TAL. Elevated aldosterone (Aldo) from LNaHK diet upregulates ENaC, ROMK, and BK in the ASDN to promote distal K^+ secretion. Furosemide blocks NKCC2, inhibiting net K^+ secretion in the TAL. Although furosemide increases distal Na^+ delivery and flow that stimulate K^+ secretion in ASDN, the net result is a decrease in urinary K^+ excretion. Transporters in the basolateral membrane and cell types of ASDN have been omitted for simplicity.

CHAPTER 2: FUROSEMIDE REDUCES BKαβ4-MEDIATED K^+ SECRETION IN MICE ON A NORMAL NA HIGH K^+ DIET

Introduction

K^+ is freely filtered into the glomerulus, reabsorbed in the proximal tubule and TAL, and secreted into the lumen in the distal nephron via ROMK and BK channels. ROMK channels are considered constitutively active and secrete K^+ at the basal conditions (22, 23). By contrast, BK channels are activated by high urinary flow and secrete K^+ under high dietary K^+ conditions (24, 25). In particular, the BK-αβ4 channel located in the intercalated cells of distal nephron (85) is required to maintain K^+ homeostasis in mice on an alkaline high K^+ diet (127). The BK-β4 subunit of the BK-αβ4 channel is an accessory subunit that protects the pore-forming BK-α subunit from lysosomal degradation (58). BK-β4 is regulated by the acidity/alkalinity of the diet (90). Compared to those on a high KCl diet (HKCl), mice on an alkaline HK diet exhibited increased BK-β4 expression and increased apical membrane localization of BK-α (90). However, it is unclear whether BK-β4 is regulated by tubular fluid pH or plasma pH.

Diuretics are among the most commonly used medications in the US. More than 20% of the population over the age of 65 are taking diuretics in the US (106). Numerous studies have shown the influences of high dietary K^+ intake on the actions and effectiveness of diuretics. Compared to those on a regular diet, mice on HK diet exhibit diminished thiazide-sensitive natriuresis due to decreased NCC activity (105, 158) but enhanced amiloride-sensitive natriuresis due to upregulated ENaC activity (108, 109). Furosemide has a reduced natriuretic effects on HK diet (122, 159), but increased efficacy on LNaHK diets (159).

Additionally, furosemide is well known for its effect to acidify the urine. Classically, this was thought to be due to increased Na^+ delivery to distal nephron, generating a more favorable negative lumen potential for H^+ secretion from the vacuolar H^+-ATPase (V-ATPase) (160, 161).

Chronic furosemide treatment increases V-ATPase expression (162). More recently, the study by de Bruijn *et. al.* (163) showed that furosemide acidifies the urine by increasing H^+ secretion via the Na^+-H^+ exchanger 3 (NHE3) in the TAL. Taking these together with the notion that BK-β4 is regulated by pH, we hypothesize that in mice on HK diet, furosemide reduces BK-αβ4-mediated K^+ secretion by acidifying the urine.

Methods

Animals

All animals were maintained in accordance with the Institutional Animal Care and Use Committee of the University of Nebraska Medical Center. Wild-type mice with C57BL/6 background (Charles River Laboratories, Wilmington, MA) and BK-β4 knockout mice with C57BL/6 background (generously provided by R. Brenner, Stanford University, CA) were housed in the UNMC animal facility and maintained on a 12-hour day-night cycle, with free access to water and food.

Metabolic cage

Wild-type (WT) and BK-β4 knockout mice (β4-KO), both male and female, at 12–16 weeks of age, were kept on either a regular diet (RD; 0.3% Na, 0.6% K), an alkaline high K^+ diet (HK diet; 5.0% K^+ with 5% of equal carbonate/citrate/Cl and 0.32% Na^+; TD.07278; Envigo, Indianapolis, IN), and regular drinking water for 7 days. They were then given either control water (0.8 mM $KHCO_3$ in drinking water) or furosemide water (0.1 g/L furosemide + 0.8 mM KOH for HK diet; 0.4 g/L furosemide + 0.8 mM KOH for RD) for 11 days. Another group of WT mice were kept on HK diet for 7 days and then given furosemide + acetazolamide water (0.1 g/L furosemide + 0.4 g/L acetazolamide + 2.0 mM KOH) for 7 days. All mice were acclimated to metabolic cages for one day each time, for a total of three times before experiments. Urine was collected for 24 hours in metabolic cages on the day before treatment water and 1, 4, 7, and 11 days after treatment. The mice were then anesthetized, sacrificed by exsanguination from the carotid artery, and blood and kidneys were collected. Urine pH was measured with a pH meter (Model 215, Denver Instruments, Bohemia, NY). Arterial blood gas values and hematocrit were determined by the MN 300 i-STAT system with EC8+ cartridges (Abbott Point of Care, Princeton, NJ). Urine and plasma osmolality were measured with an osmometer (Model 3250,

Advanced Instruments, Norwood, MA). Urine and plasma Na^+ and K^+ concentrations were determined by a flame photometer (PFP7, Jenway, Burlington, NJ).

Perfusion-fixation and immunofluorescence staining

Kidneys were fixed with 2% paraformaldehyde as previously described (164). Mice were anesthetized with ketamine/xylazine cocktail, and chest cavity was opened. PBS containing 2% paraformaldehyde was perfused via the left ventricle for 5 minutes. The kidneys were then removed and cut into slices, which were fixed in 2% paraformaldehyde at 4 °C overnight. Specimen were then embedded in paraffin and cut into serial sections on slides. Procedures for immunofluorescence staining were previously described (89). The following primary antibodies were used: anti-BK-α (mouse, diluted 1:100, UC Davis/NIH NeuroMab, Davis, CA), anti-V-ATPase B1 (rabbit, diluted 1:100, Santa Cruz), and anti-calbindin-D28K (mouse, diluted 1:100, Sigma, St. Louis, MO). The following secondary antibodies were applied for 1 hour at room temperature: donkey anti-mouse IgG conjugated Alexa Fluor 488 and donkey anti-rabbit IgG conjugated Alexa Fluor 594 (diluted 1:200, Invitrogen, Carlsbad, CA). The stained sections were mounted using EMS Shield Mount with DABCO (Electron Microscopy Sciences, Hatfield, PA).

Western blotting

Kidneys were collected from sacrificed mice, and kidney cortex was separated from medulla tissue and used for Western blotting as previously described (99, 134). Kidney samples were placed in cold lysis buffer containing RIPA buffer + protease/phosphatase inhibitor (Sigma, St Louis, MO) + 0.1% Triton X-100 (Sigma, St Louis, MO) + 1mM PMSF (Sigma, St Louis, MO). Samples were cut into small pieces, sonicated, and kept on ice for 30 min before centrifuged at 12500 g for 30 min at 4 °C. Supernatant was collected, to which 4X Laemmli sample buffer (Bio-Rad, Hercules, CA) containing 10% β-mercaptoethanol (Sigma, St Louis, MO) was added. Samples were boiled for 5 min and loaded into 4 – 20% gradient gel (Bio-Rad) and run at 100 V for 1.5 hrs. The gel was then transferred onto Amersham Hybond-P membrane

(GE Healthcare Life Sciences, Pittsburgh, PA) at 100 V for 1 hr. The membrane was then blocked with 3% BSA 3% non-fat milk in TBS-T for 1 hr at room temperature. It was then incubated with primary antibodies in blocking buffer overnight at 4 °C. The next day, the blot was washed in TBS-T for 5 min 3 times and incubated with secondary antibodies for 1 hr at room temperature. The blot was then washed and developed with Femto reagent (Thermo Fisher Scientific) and imaged. Primary antibodies included anti-BK-β4 (rabbit polyclonal, diluted 1:500, Alomone Laboratories, Jerusalem, Israel), anti-NHE3 (mouse monoclonal, diluted 1:200, Invitrogen, Carlsbad, CA), and anti-V-ATPase B1 (rabbit polyclonal, diluted 1:200, GeneTex, Irvine, CA). Secondary antibodies included goat anti-mouse IgG HRP-conjugated (diluted 1:15,000, Santa Cruz Biotechnology, Santa Cruz, CA), goat anti-rabbit IgG HRP-conjugated (diluted 1:15,000, Santa Cruz Biotechnology, Santa Cruz, CA), and anti-β-actin HRP-conjugated (diluted 1:15,000, Thermo Fisher Scientific, Waltham, MA). Densitometry analysis was performed using imageJ software.

Aldosterone Measurement

Plasma aldosterone levels were measured using the aldosterone ELISA kit EIA-5298 (DRG Diagnostics, Marburg, Germany) following manufacturer's protocol.

HPLC measurement of furosemide concentration

The concentrations of furosemide in urine were determined with high-performance liquid chromatography (HPLC) as previously described (165). The instrument (Agilent LC 1200; Santa Clara, CA) was connected to a G1321A Agilent fluorescent detector and the chromatograms were recorded using Agilent ChemStation software. A C18 column (Waters Spherisorb 10.0 µm) was used as the stationary phase. The mobile phase consisted of cetonitrile – 0.125 M SDS – 0.01 M perchloric acid (234.6:35:665, w/w) pumped at a constant flow-rate of 0.6 ml/min. The retention time of furosemide was 3.7 min and was separated from the rest of the compounds present in urine and plasma in chromatographs obtained with excitation at 360 nm and emission at 413 nm.

A standard curve was constructed using the areas under the furosemide peak of plasma samples containing 0, 10, 20, 50, 100, 200, 500, 1000, 2000, and 5000 μM furosemide. The furosemide concentrations of urine samples were then calculated using the standard curve.

Results

Furosemide effect on urine pH

Consistent with the urine acidification effect of furosemide (138, 163, 166, 167), our results showed that over the course of treatment, furosemide water (Furo) reduced urine pH in both WT and β4-KO on HK diet (**Figure 17**). However, blood pH was not different between the HK + Ctrl and HK + Furo group (**Table 6**). Notably, urine pH kept decreasing until day 7. This gradual reduction could be due to increased V-ATPase expression in the distal nephron (162). Indeed, compared to HK + Ctrl group, the HK + Furo group had higher V-ATPase expression (**Figure 18A**). The NHE3 expression remained unchanged in the whole kidney and the medulla (**Figure 18**). Since V-ATPase expression is regulated by aldosterone, we measured the plasma aldosterone levels. HK + Furo group had significantly higher plasma aldosterone levels compared to HK + Ctrl group (**Table 6**).

Table 6. Blood measurements after 11 days (or 7 days for HK + Furo Actz) of treatment

Genotype	**WT**					**KO**	
Treatment	**HK + Ctrl**	**HK + Furo**	**HK + Furo Actz**	**RD + Ctrl**	**RD + Furo**	**HK + Ctrl**	**HK + Furo**
Number of Mice	12	14	3	4	4	8	7
Plasma Na^+ (mM)	137.6 ± 1.1	140.9 ± 1.0*	143.5 ± 8.2	138.3 ± 0.7	138.0 ± 1.3	139.8 ± 1.2	140.1 ± 1.0
Hct (%)	36.5 ± 0.3	39.8 ± 0.5*	38.3 ± 1.5	37.0 ± 0.6	40.5 ± 0.6*	35.4 ± 0.3	38.0 ± 1.2*
Blood pH	7.46 ± 0.02	7.45 ± 0.03	7.44 ± 0.03	7.46 ± 0.02	7.46 ± 0.03		7.45 ± 0.03
P Aldo (pg/mL)	862 ± 165	1489 ± 179*					

*$p < 0.05$ vs Ctrl group; #$p < 0.05$ vs Furo group analyzed with two-way ANOVA with a post-hoc Tukey test.

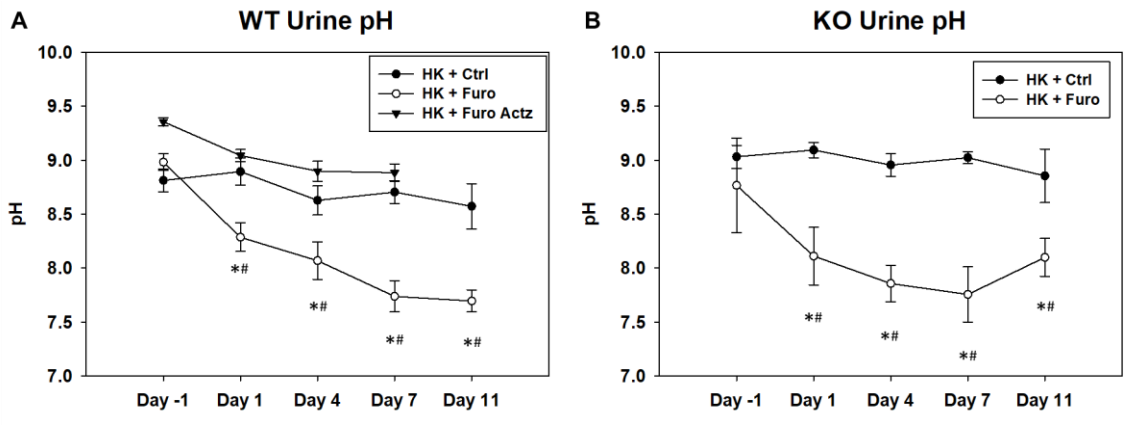

Figure 17. Furosemide effect on urine pH.

Urine pH of WT **(A)** and β4-KO **(B)** on day -1, 1, 4, 7, and 11 of Ctrl and Furo treatments, or day -1, 1, 4, and 7 of Furo + Actz treatment. *p < 0.05 vs. HK + Ctrl water; #p < 0.05 vs. Day -1, analyzed with two-way repeated measures ANOVA with a post-hoc Holm-Sidak test (p < 0.001 for both treatment and days with interaction p < 0.01). N = 4 – 14 animals per group.

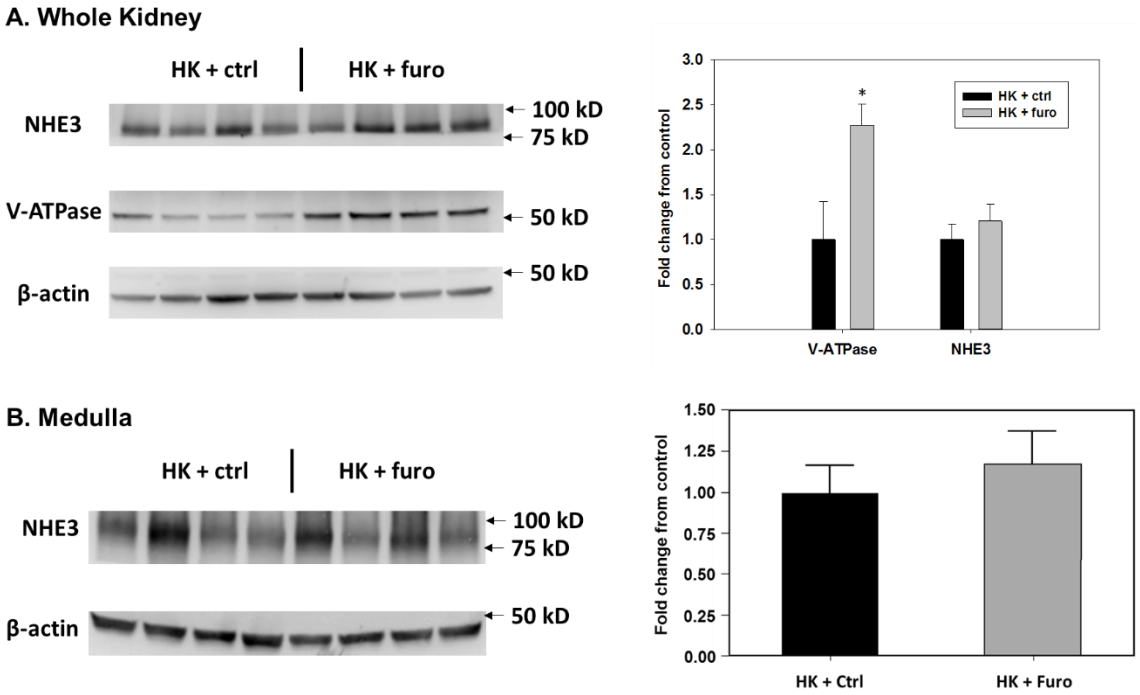

Figure 18. Western blot and quantification of NHE3 and V-ATPase expressions normalized to β-actin in mice treated with HK + ctrl and HK + furo.

*p < 0.05 vs. HK + Ctrl analyzed with a student's t-test. N = 4 animals per group.

Furosemide effect on renal K^+ handling

As a well-known K-wasting diuretic, in mice on RD, Furo water group had a significantly lower plasma [K^+] and a higher trend of K^+ clearance compared to the Ctrl water group (**Figure 19**). However, in WT on HK, Furo treatment reduced $U_K\dot{V}$ on day 1 (**Figure 20**). After 11 days of treatment, the HK + Furo group had a lower K^+ clearance and higher plasma [K^+] than the HK + Ctrl group (**Figure 21**). This indicates that furosemide becomes a K-sparing diuretic in mice on HK. Interestingly, this effect seems to be dependent on BK-β4 since furosemide did not affect K^+ clearance or plasma [K^+] in β4-KO on HK (**Figure 21**).

To test whether the furosemide effect on K^+ excretion is due to urine acidification, another group of mice on HK were treated with furosemide water with acetazolamide added to alkalinize the urine (HK + Furo Actz). Because of volume depletion in HK + Furo Actz mice, the treatment was 7 days instead of 11 days. The addition of Actz successfully kept the urine alkaline without affecting the blood pH (**Figure 17**, **Table 7**). Unlike HK + Furo, HK + Furo Actz group showed similar $U_K\dot{V}$, plasma [K^+], and renal K^+ clearance as HK + Ctrl group (**Figure 20**, **Figure 21**). Interestingly, the combination of furosemide and acetazolamide produced a much more profound diuresis than furosemide alone (**Table 7**), consistent with the recognized synergistic effect of these two diuretics (168, 169).

Tubular fluid pH is well known to be positively correlated with K^+ secretion in the distal nephron (170, 171). To illustrate this relationship, we plotted renal K^+ clearance vs urine pH and included data from WT and β4-KO kept on HKCl diet. Consistent with this notion, in WT on HK, renal K^+ clearance was positively correlated with urine pH. However, such a correlation was not significant for β4-KO on HK (**Figure 22**). This indicates that the correlation between urine pH and K^+ clearance was dependent on BK-β4 expression.

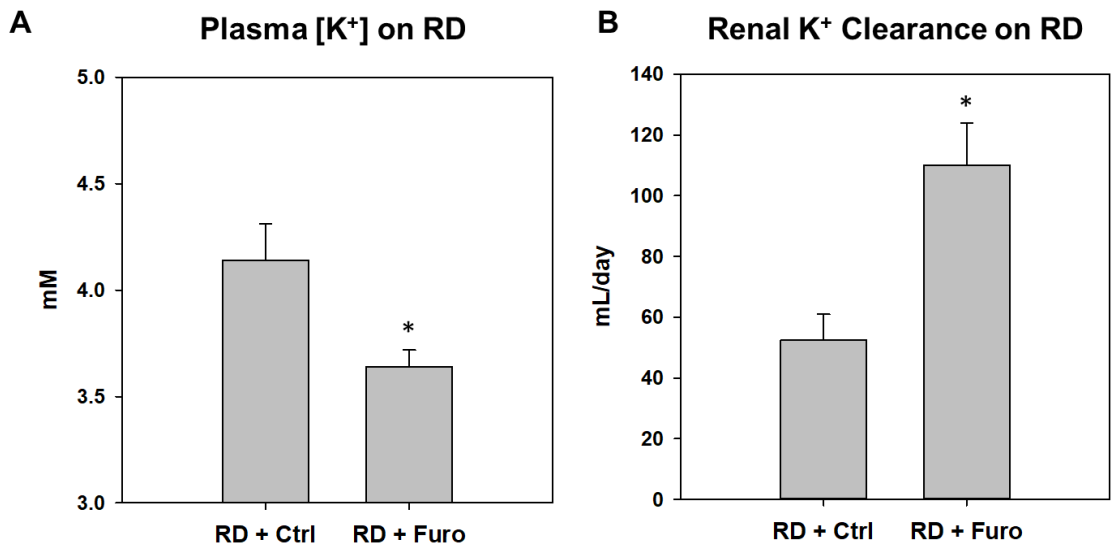

Figure 19. Furosemide effect on plasma [K^+] and renal K^+ clearance in mice on RD.

Plasma [K^+] **(A)** and renal K^+ clearance **(B)** of WT on RD on day 11 of Ctrl or Furo treatments. *$p < 0.05$ vs. RD + Ctrl analyzed with a student's t-test. N = 4 animals per group.

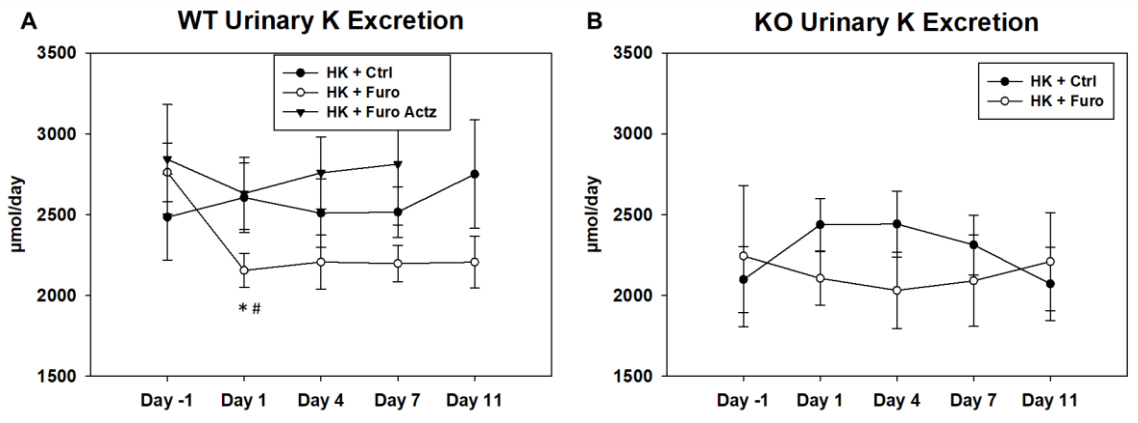

Figure 20. Furosemide effect on urinary K^+ excretion ($U_K\dot{V}$) in mice on HK.

$U_K\dot{V}$ of WT **(A)** and β4-KO **(B)** on day -1, 1, 4, 7, and 11 of Ctrl and Furo treatment, or day -1, 1, 4, and 7 of Furo + Actz treatment. *$p < 0.05$ vs. HK + Ctrl, #$p < 0.05$ vs. Day -1, analyzed with two-way repeated measures ANOVA ($p < 0.05$ for drug treatment in WT) with a post-hoc Holm-Sidak test. N = 4 – 17 per group.

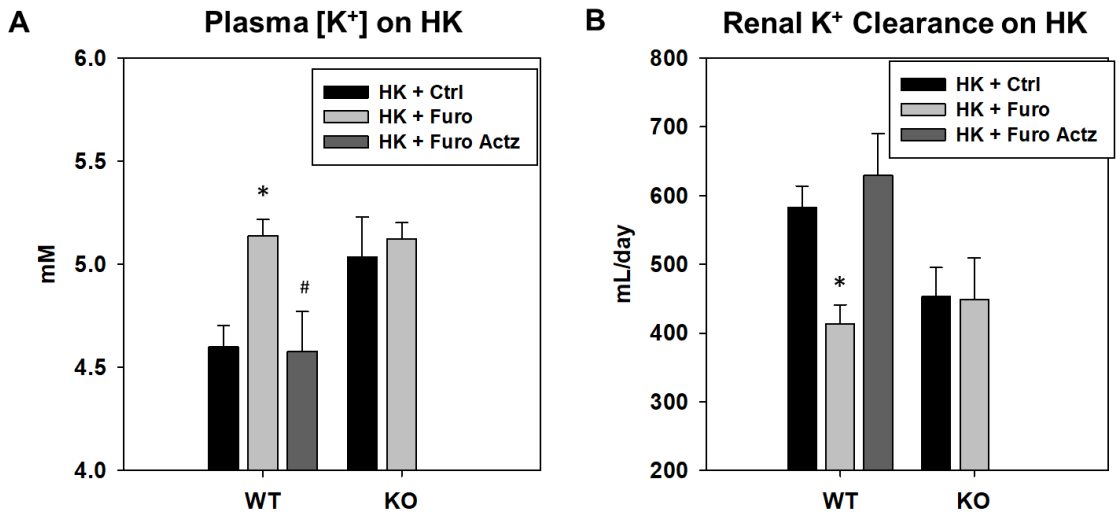

Figure 21. Furosemide effect on plasma [K^+] and renal K^+ clearance in mice on HK.

Plasma [K^+] **(A)** and renal K^+ clearance **(B)** of WT and β4-KO on day 11 of Ctrl and Furo treatment, or day 7 of Furo + Actz treatment. *$p < 0.05$ vs. HK + Ctrl; #$p < 0.05$ vs. HK + Furo, analyzed with two-way ANOVA with a post-hoc Tukey test ($p < 0.001$ for treatment in plasma [K^+]; $p < 0.01$ for treatment in renal K^+ clearance). N = 4 – 17 animals per group.

Table 7. Metabolic cage measurements after 11 days (or 7 days for HK + Furo Actz) of treatment

Genotype	WT					KO	
Treatment	**HK + Ctrl**	**HK + Furo**	**HK + Furo Actz**	**RD + Ctrl**	**RD + Furo**	**HK + Ctrl**	**HK + Furo**
Number of Mice	12	14	6	4	6	8	7
Body Weight (g)	22.4 ± 0.4	21.4 ± 0.5	20.5 ± 0.8	18.9 ± 1.4	19.2 ± 2.1	21.0 ± 0.6	19.1 ± 0.7
Food Intake (g/day)	2.55 ± 0.18	2.20 ± 0.13	2.00 ± 0.62	0.09 ± 0.04	0.21 ± 0.07	2.65 ± 0.23	2.23 ± 0.48
Water Intake (mL/day)	14.8 ± 1.1	12.7 ± 1.1	16.0 ± 2.2	1.1 ± 0.4	5.5 ± 1.6*	10.5 ± 1.1	12.8 ± 1.0
$\dot{V}$ (mL/day)	7.2 ± 0.7	7.1 ± 0.6	10.3 ± 1.5#	0.7 ± 0.2	2.6 ± 0.8	5.4 ± 0.6	6.8 ± 0.7
U Osm (mOsm)	1020 ± 73	809 ± 47*	720 ± 39*	2725 ± 452	1367 ± 451*	1173 ± 42	908 ± 81*
$U_{Na}\dot{V}$ (µmol/day)	277 ± 18	281 ± 11	336 ± 47	142 ± 19	129 ± 26	284 ± 25	302 ± 45

*p < 0.05 vs Ctrl group; #p < 0.05 vs Furo group analyzed with two-way ANOVA with a post-hoc Tukey test.

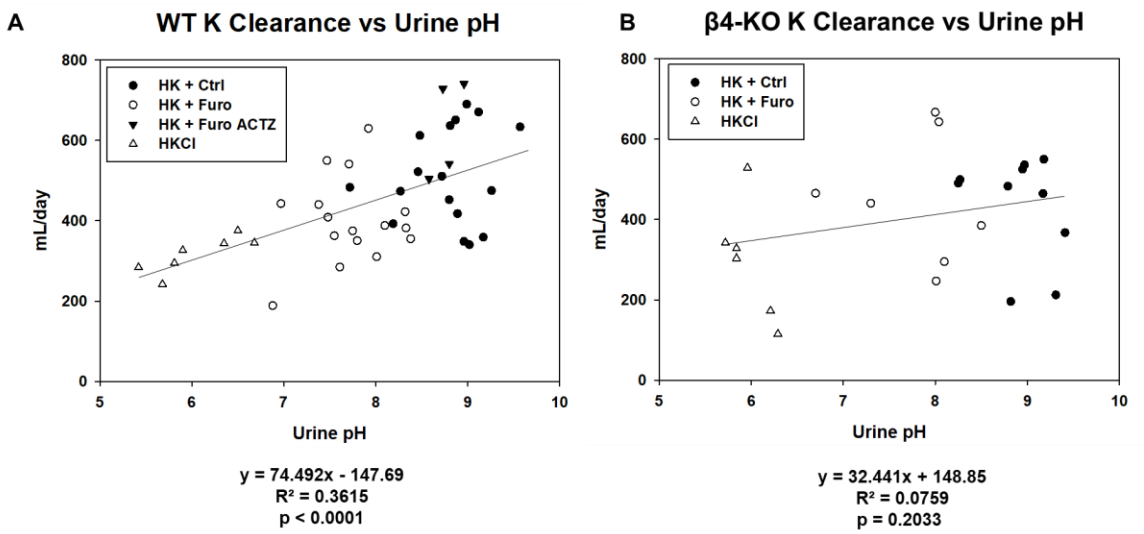

Figure 22. Correlation between renal K^+ clearance and urine pH in WT (A) and β4-KO (B) on HK.

Solid circles denote HK + Ctrl group; empty circles denote HK + Furo group; solid triangles denote HK + Furo Actz group; empty triangles denote HKCl group.

Furosemide effect on BK-αβ4 expression

Previous studies showed that the alkalinity/acidity of diets regulates the BK-αβ4-mediated K^+ secretion by altering BK-β4 expression, which is required for maintaining the apical localization of BK-α(58, 90). We hypothesized that furosemide would have similar effects by acidifying the urine. Shown by the western blot in **Figure 23** and the immunofluorescent staining in **Figure 24**, compared to HK + Ctrl group, HK + Furo group but not HK + Furo Actz group had significantly reduced BK-β4 expression and decreased apical localization of BK-α in the kidney cortex. Interestingly, in HK + Ctrl group, BK-α was only located in the apical membrane of intercalated cells of CNT but not CCD or MCD, as evidenced by co-staining with V-ATPase (IC marker) and calbindin (DCT/CNT marker). Consistent with this differential regulation of BK-α in different nephron segments, the BK-β4 expression in the whole kidney remained unaffected by Furo treatment (**Figure 23C)**.

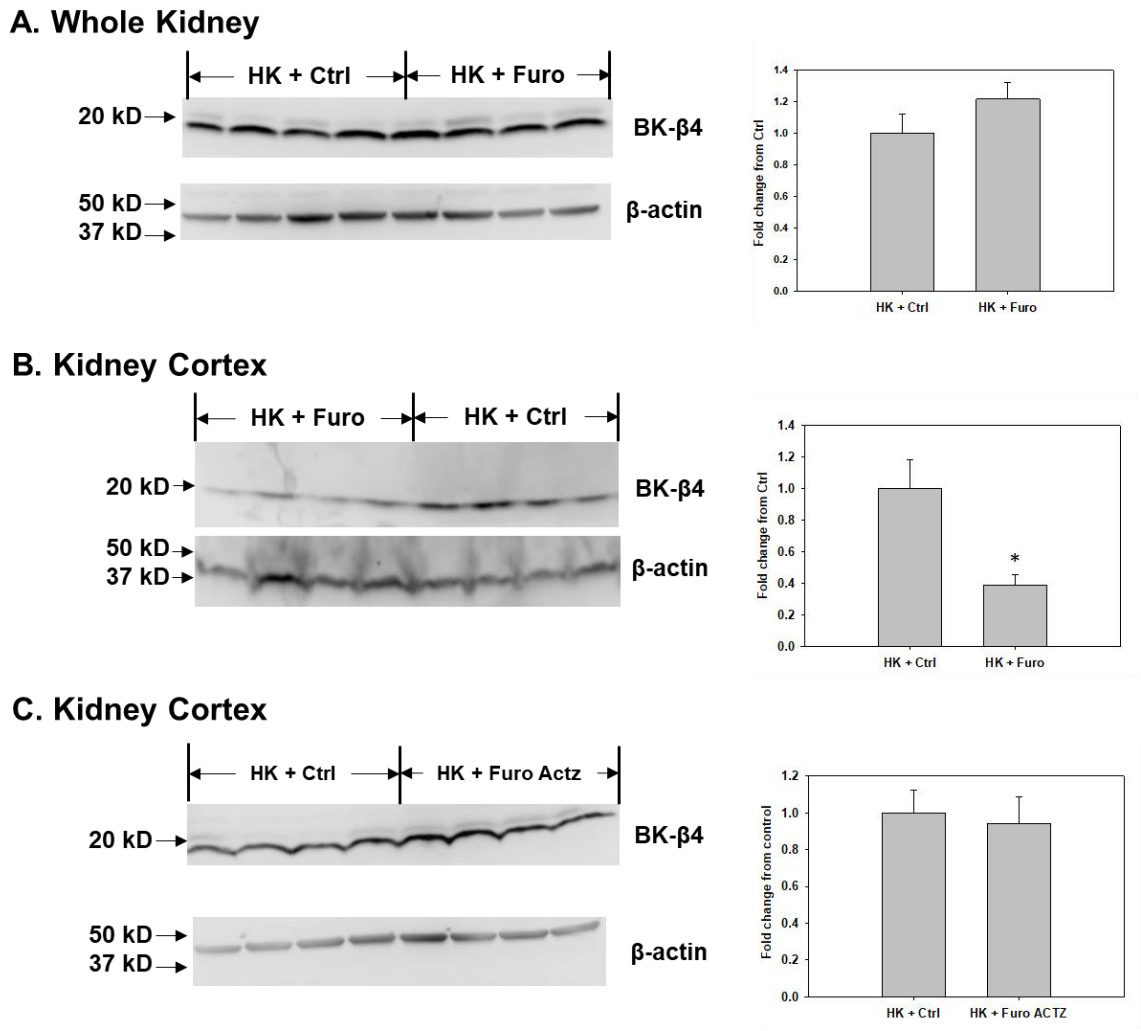

Figure 23. Furosemide effect on BK-β4 expression in the kidney.

BK-β4 expression normalized to β-actin in the whole kidney **(A)** and kidney cortex **(B)** of WT on HK treated with Ctrl vs Furo water. **C.** BK-β4 expression normalized to β-actin in the kidney cortex of WT on HK treated with Ctrl vs Furo Actz water *$p < 0.05$ vs. HK + Ctrl analyzed with a student's t-test.

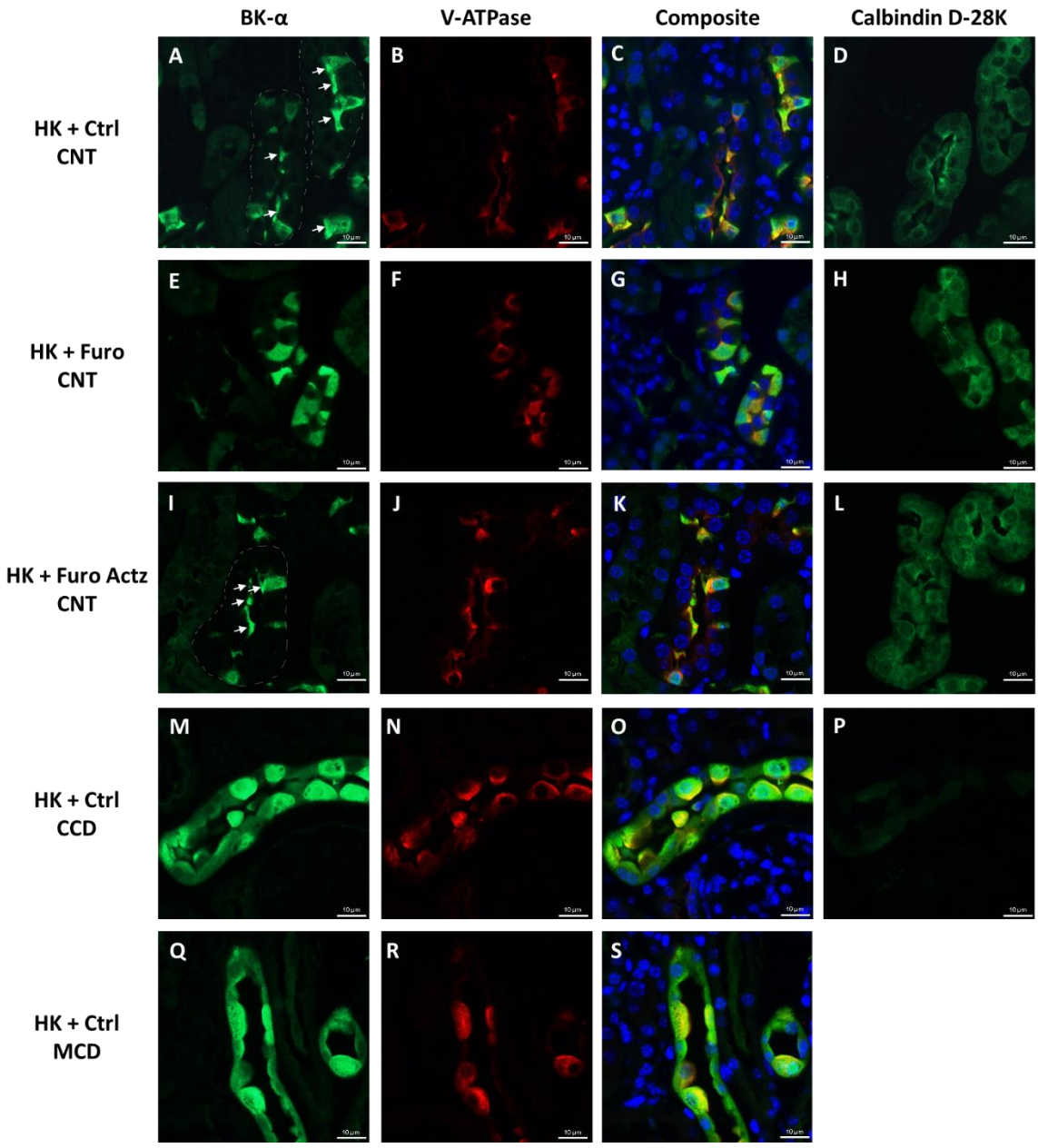

Figure 24. BK-α localization in kidney sections of WT on HK treated with Ctrl or Furo water.

A-D: Representative images from the CNT of HK + Ctrl group. **E-H:** Representative images from the CNT of HK + Furo group. **I-L:** Representative images from the CNT of HK + Furo Actz group. **M-P:** Representative images from the CCD of HK + Ctrl group. **Q-S:** Representative images from the MCD of HK + Ctrl group. A, E, I, M, Q were stained with anti-BK-α; B, F, J, N, R were stained with anti-V-ATPase; D, H, L, P were serial sections of their respective row and stained with anti-Calbidin-D28K. Scale bars are 10 µm.

Discussion

The results of the present study demonstrate the following: 1) chronic furosemide treatment acidified the urine partly by upregulating V-ATPase expression; 2) chronic furosemide treatment reduced renal K^+ clearance and increased plasma [K^+] in WT but not BK-β4 KO on HK; 3) chronic furosemide treatment downregulated BK-β4 expression in the cortex and decreased BK-α apical localization in the CNT of WT on HK; 4) the effect of furosemide on K^+ handling and BK-αβ4 was prevented by alkalinizing the urine with acetazolamide.

Urine Acidification by Furosemide

Furosemide causes marked urine acidification and is used to diagnose distal renal tubular acidosis (166, 172, 173). The classical explanation was similar to the K-wasting effect of furosemide. The increased distal Na^+ delivery to ENaC generates a more negative lumen potential in the ASDN for both K^+ and H^+ secretion (160). The study by Kovacikova J *et. al.* (161) also showed that the acute urine acidification effect was dependent on ENaC in the CNT. However, the recent study by de Bruijin *et. al.* (163) showed that acutely, furosemide-induced urine acidification was caused by increased H^+ secretion from NHE3 in the TAL. Another study showed that chronic furosemide treatment in mice on a regular diet acidified urine in an ENaC-independent manner and increased V-ATPase expression without changes in plasma aldosterone (162).

Consistent with previous studies, our data showed that chronically, furosemide reduced the urine pH starting from the 1st day of treatment and caused a gradual decrease until day 7. After 11 days of treatment, the V-ATPase expression in the whole kidney was doubled. However, unlike the previous study (162), our data showed increased plasma aldosterone levels in the HK + Furo group, which is consistent with their elevated plasma [K^+]. Furthermore, by inhibiting Na^+ reabsorption in TAL, furosemide inhibits Ca^{2+} reabsorption in the TAL and sends more Na^+ to be

reabsorbed by NCC and ENaC, which reduces the driving force for Na^+-Ca^{2+} exchange by Na^+-Ca^{2+} exchanger 1 (NCX1), inhibiting Ca^{2+} reabsorption in DCT and CNT (174, 175). In addition to aldosterone, the activity of V-ATPase may be stimulated by the increased urinary [Ca^{2+}] via the action of Ca-sensing receptor (CaSR) (176). Although the NHE3 expression remained unchanged by furosemide, the synergistic effect of furosemide + acetazolamide suggests that NHE3 activity may be upregulated during furosemide treatment and contribute to the urine acidification by furosemide. Further investigations are required to determine the activity of NHE3 in the TAL during chronic furosemide treatment.

Furosemide, Urine pH and BK-αβ4-mediated K^+ Secretion

The link between pH and BK-αβ4 has been previously demonstrated by our lab. As the diet becomes more acidic, BK-β4 expression is decreased, reducing apical membrane localization of BK-α (58, 90, 99). In the current study, chronic furosemide treatment reduced urine pH, BK-β4 expression, and apical membrane localization of BK-α in WT on HK. This effect astoundingly overrides the K-wasting effect from increased distal Na^+ delivery, resulting in an overall decrease in renal K^+ clearance and an elevation of plasma [K^+]. In fact, furosemide did not cause a significant increase in urine flow ($\dot{V}$) or $U_{Na}\dot{V}$ in mice on HK, despite the fact that the urinary concentration of furosemide measured with HPLC was 683 ± 97 μM, about 50 folds higher than its IC50 (7.2 – 15.1 μM) (177) (**Table 8**, **Figure 25**). This could be because NKCC2 activity is partly inhibited in mice on HK (122, 159). However, the effectiveness of furosemide was still demonstrated by the further decreased urine osmolality, increased hematocrit, increased plasma aldosterone levels, and reduced urine pH in HK + Furo group. Moreover, the less profound diuretic and natriuretic effect of furosemide under HK conditions did not stimulate ROMK and BK-αβ1-mediated K^+ secretion as much as regular dietary conditions. This might have caused the

reduction in BK-αβ4-mediated K^+ secretion to be the predominant effect and resulted in a net decrease in K^+ excretion.

Table 8. Furosemide concentrations in urine and plasma of WT and BK-β4 KO.

	WT HK + Furo	BK-β4 KO HK + Furo
[Furo] in urine (μM)	683 ± 97	610 ± 123
[Furo] in plasma (μM)	6.5 ± 3.2	21.7 ± 17.4

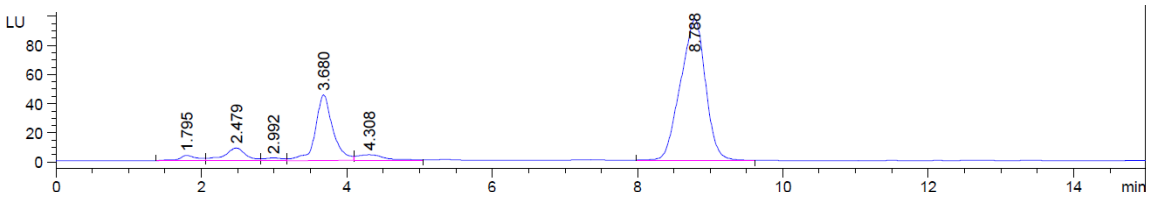

Figure 25. A sample HPLC trace for a urine sample.

It shows a distinct peak at 3.680 min, corresponding to the elution of furosemide.

Interestingly, in BK-β4 KO on HK, furosemide acidified the urine without affecting renal K^+ clearance or plasma [K^+], which were comparable to those of WT HK + furo group. These results suggest that the K-sparing effect of furosemide in WT on HK is due to the inhibition of K^+ secretion via BK-αβ4 channels. The K-sparing effect was abolished when the urine is alkalinized with acetazolamide. This could also be due to the further increase in distal Na^+ delivery stimulating K^+ secretion. However, the fact that BK-β4 expression and BK-α localization were similar between HK + Furo and HK + Furo Actz groups indicates that the furosemide effect on BK-αβ4 was due to urine acidification. This synergistic effect was previously reported (169, 178) and suggested as a potential combination therapy for the treatment of congestive heart failure refractory to high doses of loop diuretics (168). Such patients have increased Na^+ reabsorption in the proximal tubules, rendering loop diuretics ineffective (179).

The apical localization of BK-α is regulated by BK-β4 via its protection from lysosomal degradation (58). However, the mechanism of how luminal pH regulates BK-β4 expression remains unclear. The pH needs to be sensed from the luminal side of intercalated cells. One possible pH sensor is the CaSR located in the apical membrane of both principal cells and intercalated cells of the DCT and CD (180). Studies showed that extracellular alkalinization above pH 6 increased CaSR activity due to a sensitization towards extracellular Ca^{2+} (181, 182). The activation of CaSR would release Ca^{2+} from intracellular storage and increase Ca^{2+} entry via TRPV5 channels (183) to further activate BK channels (44). The TRPV4 channel plays a critical role in upregulating BK-mediated K^+ secretion during adaptation to HK diets (98). The coupling of CaSR and TRPV4 was recently demonstrated in gastric cancer cells (184); however, such a relationship remains to be investigated in the kidney.

Another interesting finding in this study is that pH regulation of BK-αβ4 only occurs in the CNT but not CCD or MCD. This was supported by both IF staining, where BK-α was localized in the apical membrane of CNT only, and the western blot, where BK-β4 expression

was only reduced in the kidney cortex. CNT has been identified as the major site of K^+ secretion [180] and furosemide-induced H^+ secretion (161, 185). According to our IF staining, in the CNT, BK-α was almost exclusively expressed in the intercalated cells. This agrees with the notion that intercalated cells play the major role in BK-mediated flow-induced K^+ secretion (83, 97).

The association between luminal pH and K^+ secretion has been known for decades (170, 171, 186). Luminal acidification from pH 7.4 to 6.8 impairs K^+ secretion in rabbit CCD without changing Na^+ reabsorption (187). Although ROMK channels are regulated by cytosolic pH (171, 188), they are insensitive to extracellular pH (41, 188). The intracellular pH of principal cells is unlikely to be affected by luminal pH due to lack of acid-base transporter in the apical membrane (189). The link between luminal pH and K^+ secretion has been attributed to several possibilities including a pH-sensitive apical K-Cl cotransporter in principal cells (186), a TASK2 K^+ channel that is regulated by extracellular pH (186), and ENaC modulation by luminal HCO_3^- [(190)]. Our current study provides another explanation that luminal pH regulates BK-αβ4-mediated K^+ secretion, as evidenced by our finding that BK-β4 is required for the positive correlation between urine pH and renal K^+ clearance.

Limitations and conclusions

One limitation of our study is the use of drinking water for drug treatment. This method is non-invasive and minimizes stress but also makes drug dosage different in each animal. According to **Table 7**, although the water intake is not statistically different among the different groups on HK, it may vary among individuals, leading to larger standard errors. Another limitation of our study is that at high doses, furosemide may inhibit NCC in the DCT. However, NCC activity is highly inhibited on HK due to elevated plasma $[K^+]$. Since the plasma $[K^+]$ was even higher in HK + Furo group, NCC activity should also be inhibited. Another explanation for the K-sparing effect of furosemide is that it may inhibit NKCC1 in the basolateral membrane of

intercalated cells to limit K^+ secretion through BK (191). However, the plasma concentration of furosemide in the HK + Furo group (6.5 ± 3.2 μM) was much lower than its IC50 (23 ± 12 μM) (192) (**Table 8**). Additionally, the restoration of BK-β4 expression and BK-α localization by co-administration of acetazolamide strongly suggests that furosemide exerts its effect on BK-αβ4 via urinary acidification.

Furosemide is a commonly used K-wasting diuretic, and patients taking furosemide often require K^+ supplements to prevent hypokalemia. However, our current study found that furosemide became a K-sparing diuretic in mice adapted to HK. Instead of the risk for hypokalemia, furosemide increased the plasma [K^+] in these mice. As shown by our proposed model in **Figure 26**, on a regular diet, ROMK is the main K^+ channel responsible for K^+ secretion in the ASDN. Furosemide increases Na^+ delivery to the ASDN, generating a more negative lumen potential, increasing K^+ secretion via ROMK channels. The increased flow will also activate the BK-αβ1 channels in principal cells. The net result is an increase in urinary K^+ excretion. On an alkaline high K^+ diet, furosemide acidifies the urine by increasing H^+ secretion from NHE3 and V-ATPase. Lower pH downregulates BK-β4 expression, decreasing apical localization of BK-α, reducing BK-αβ4-mediated K^+ secretion. Because of the less profound natriuretic and diuretic effect of furosemide under HK, the increase in ROMK and BK-αβ1-mediated K^+ secretion is less than the decrease in BK-αβ4-mediated K^+ secretion. The net result is a decrease in total K^+ excretion.

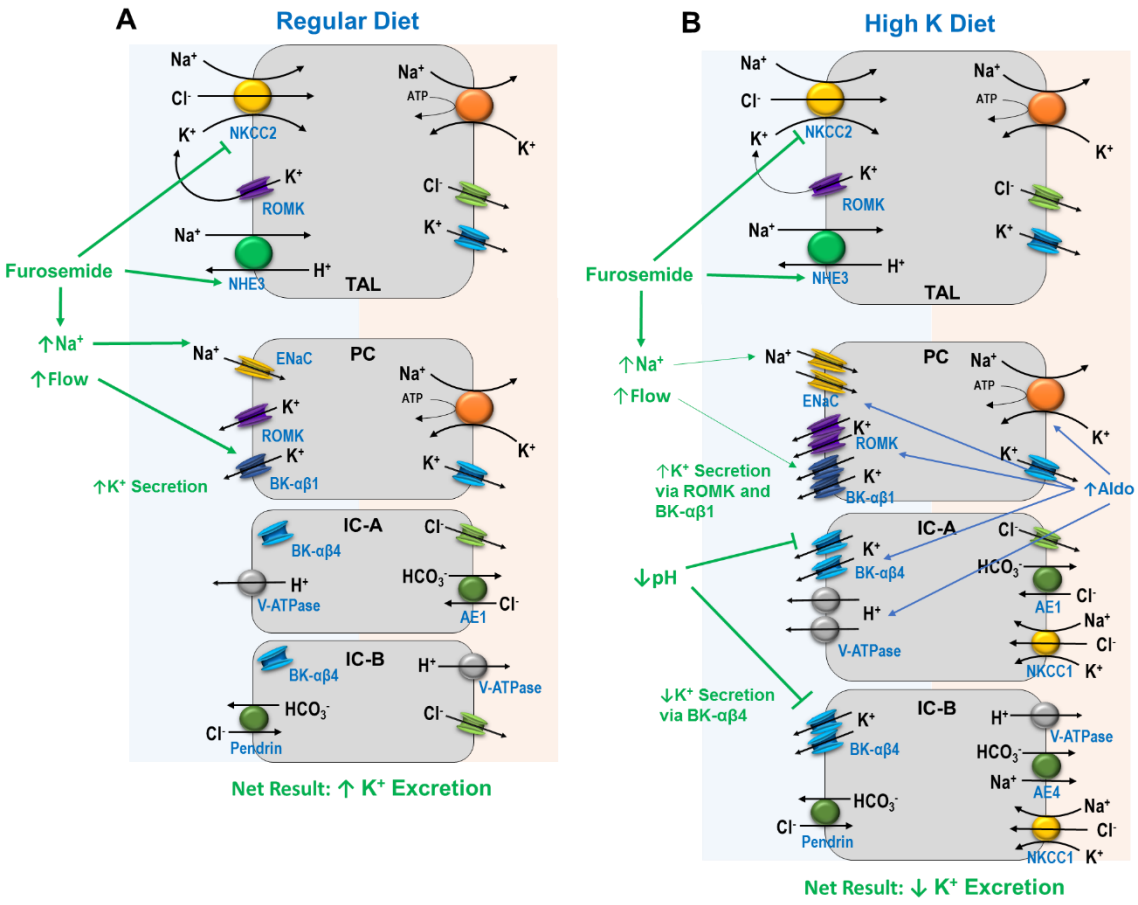

Figure 26. Differential effects of furosemide on K^+ clearance in mice on regular diet vs an alkaline high K^+ diet.

A. On a regular diet, BK-α stays in the cytoplasm, and K^+ is mainly secreted via the ROMK channel. Furosemide blocks Na^+ reabsorption by NKCC2, increasing Na^+ delivery to distal nephron, increasing K^+ secretion via ROMK, leading to increased K^+ clearance. **B.** On an alkaline high K^+ diet, K^+ is secreted by both ROMK and BK channels. Furosemide blocks Na^+ reabsorption by NKCC2, increasing Na^+ delivery and flow to distal nephron, increasing K^+ secretion via ROMK and BK-αβ1. On the other hand, furosemide increases acid secretion from NHE3 and V-ATPase, acidifying the urine, which decreases BK-β4 expression and reduces apical localization of BK-α. The net result is a decrease in K^+ clearance, making furosemide a K-sparing diuretic.

In one rat study by Rodicio JL and Hernando L, furosemide and acetazolamide each caused increased K^+ excretion separately; however, when furosemide was added during acetazolamide administration, K^+ excretion was reduced despite profoundly increased Na^+ excretion (178). This phenomenon can be potentially explained by our findings that urine pH regulates BK-αβ4-mediated K^+ secretion. During acetazolamide administration, urine was alkalinized, increasing BK-αβ4-mediated K^+ secretion, contributing to the kaliuretic effect of acetazolamide. When furosemide was added, urine was acidified, reducing BK-αβ4-mediated K^+ secretion, leading to decreased kaliuresis despite increased natriuresis. Furthermore, in a clinical study, when furosemide and thiazide were administered in doses with equal natriuretic effects, the kaliuresis induced by furosemide was lower than that of hydrochlorothiazide (193). This phenomenon has been explained by the fact that during furosemide treatment, the Na^+ not reabsorbed by TAL was picked up by NCC in early DCT, reducing the delivery of Na^+ to distal K^+ secretion sites (193, 194). However, our study provides an alternative explanation that furosemide may inhibit BK-mediated K^+ secretion, leading to a lower kaliuretic effect than thiazide.

In conclusion, our study indicates that furosemide decreases BK-αβ4-mediated K^+ secretion by acidifying the urine, making furosemide a K-sparing diuretic in mice adapted to an alkaline high K^+ diet.

GENERAL DISCUSSION

Major findings of the dissertation

In summary, the major findings of this dissertation are:

1. There is a ROMK-mediated net K^+ secretion in the TAL of mice adapted to LNaHK but not HK (Chapter 1).
2. Furosemide decreases renal K^+ clearance in mice on LNaHK by inhibiting the net K^+ secretion in the TAL (Chapter 1).
3. BK-αβ4 channels are regulated by luminal pH in the intercalated cells of CNT (Chapter 2).
4. Furosemide reduces BK-β4 expression and BK-α apical localization in the CNT by acidifying the urine, thereby decreasing renal K^+ clearance in mice on HK (Chapter 2).

Taken together, these findings demonstrate how dietary Na^+ and K^+ intake affect furosemide actions on renal K^+ handling. On a regular Western diet, furosemide is a K-wasting diuretic; while on an alkaline low/normal Na^+ high K^+ diet, furosemide is a K-sparing diuretic.

Mechanisms for the net K^+ secretion in the TAL

As discussed in Chapter 1, Ang II is possibly a critical upstream regulator of the net K^+ secretion in the TAL by regulating both ROMK and NKCC2 activities. In addition to ROMK and NKCC2, the basolateral K^+ exit should also play an important role in the net K^+ secretion. In order for a net K^+ secretion, K^+ must preferentially exit the apical side. The elevated plasma [K^+] of mice on LNaHK may have inhibited the basolateral K^+ channels. However, the luminal [K^+] was also elevated to a similar extent. Since ROMK became more active on LNaHK, there must be other factors that inhibit the basolateral K^+ channels but not the apical ROMK channel.

Both a 50-pS (195-197) and an 80-pS (198) K^+ channels have been identified in the basolateral membrane of both cortical and medullary TAL (cTAL and mTAL). The 80-pS K^+ channel is activated by vasopressin (199). The 50-pS K^+ channel is activated by adenosine (196) and Ang II (200) and inhibited by arachidonic acid (195), PGE_2 (197), and CaSR activation (201) . Although the inhibition of the 50-pS K^+ channel by Ang II via AT1 receptor seems contradictory to the net K^+ secretion in TAL, Ang II may exert the opposite effect via AT2 receptor on LNaHK, similar to its action on ROMK (157). One study claimed that KCNJ10, the major basolateral Kir channel in DCT and CD (202-204), formed the basolateral 40~50-pS K^+ channel in TAL (205). However, this seems unlikely because this particular study found the 40-pS KCNJ10 channel only in the distal half of cTAL; while the 50-pS channel has been found in both mTAL and cTAL. In addition to K^+ channels, one study found a K^+-Cl^- cotransporter 4 (KCC4) in the basolateral membrane of TAL (206). Although the KCC4 expression is not affected by a high K^+ diet (207), the effect of LNaHK remains unclear.

Components involved in the K-sparing effect of furosemide in mice on LNaHK

Studies from Chapter 1 and Chapter 2 show that furosemide decreases renal K^+ clearance in mice on both LNaHK and HK through different mechanisms. Comparing the experiments between LNaHK + Furo and HK + Furo, a few things are worth noting. 1) Micropuncture experiments show a furosemide-sensitive net K^+ secretion in the TAL of mice on LNaHK but not HK. 2) Furosemide evokes a much greater natriuresis and diuresis in mice on LNaHK than HK. 3) Furosemide reduces urine pH in mice on both LNaHK and HK. This indicates that there are at least three components involved in the furosemide effect on renal K^+ handling on LNaHK. In mice on LNaHK, furosemide inhibits the net K^+ secretion in TAL but increases the K^+ secretion through ROMK by delivering more Na^+ to ASDN. By acidifying the urine, furosemide probably

reduces BK-αβ4-mediated K^+ secretion as well. The combined effect on the TAL, ROMK and BK makes furosemide a K-sparing diuretic in mice on LNaHK.

Mechanisms for furosemide-induced urine acidification

The mechanism for furosemide-induced urine acidification seems to be multifactorial. The study by Na *et. al.* (162) showed that chronic furosemide treatment increased the V-ATPase expression but did not affect serum aldosterone levels. However, we found an increase in the V-ATPase expression with elevated aldosterone. The discrepancy may be caused by elevated plasma $[K^+]$ in furosemide-treated mice on HK. Other studies also showed that furosemide increased plasma aldosterone levels probably by activation of RAAS (116, 208, 209). Aside from furosemide, elevated plasma AVP could also upregulate V-ATPase activity. Although some studies showed that furosemide increased plasma AVP acutely (210, 211), others showed no effect during chronic furosemide treatments (211). Another possibility is that furosemide elevated plasma Ang II levels (116-118), which has been shown to increase V-ATPase expression in unilaterally nephrectomized rats (212). However, aldosterone, AVP, and Ang II are unlikely to account for all factors involved in the furosemide-induced urine acidification. According to previous studies done by our lab, mice on LNaHK exhibited even higher plasma aldosterone levels (around 3600 pg/mL) (99). They should also have elevated AVP and Ang II levels due to the low Na^+ content of the diet. However, these mice were still able to maintain alkaline urine pH above 8.8. One possible explanation is that by inhibiting Na^+ reabsorption in TAL, furosemide inhibits Ca^{2+} reabsorption in the TAL as well as DCT and CNT (174, 175). The increased luminal $[Ca^{2+}]$ activates CaSR and stimulates V-ATPase activity (176). Additionally, chronic furosemide treatment induces hypertrophy of DCT, CNT and CCD (213). The increased V-ATPase expression could also be due to the hypertrophy of CNT and increased number of type A intercalated cells in response to furosemide treatment (162).

Mechanisms for luminal pH regulation of BK-αβ4 channels

The linear relationship between renal K^+ clearance and urine pH agrees with the pH sensitivity of CaSR activity (181, 182). This supports our proposed mechanism of BK-αβ4 regulation by CaSR shown in **Figure 27**. In mice on HK + Ctrl, the luminal pH in CNT is very alkaline, greatly enhancing CaSR activity in the apical membrane. It can increase intracellular [Ca^{2+}] to activate BK channels by releasing Ca^{2+} from ER and increasing Ca^{2+} reabsorption via TRPV5 channels (44). It may also upregulate BK-β4 expression via unknown pathways, possibly involving cAMP (214, 215). As a feedback inhibition mechanism, CaSR stimulates V-ATPase activity to acidify the lumen (176). In mice on HK + Furo, the lumen in CNT is acidified by increased activity of NHE3 and V-ATPase, reducing CaSR activity, which decreases BK channel activity and BK-β4 expression. The only known study demonstrating a direct link between CaSR and BK channels was in rat bronchopulmonary sensory neurons (216), where CaSR activation increased BK currents in cells with low baseline BK activity but slightly inhibited BK currents in cells with high baseline BK activity. The relationship between CaSR and BK activation remains to be investigated in the kidney.

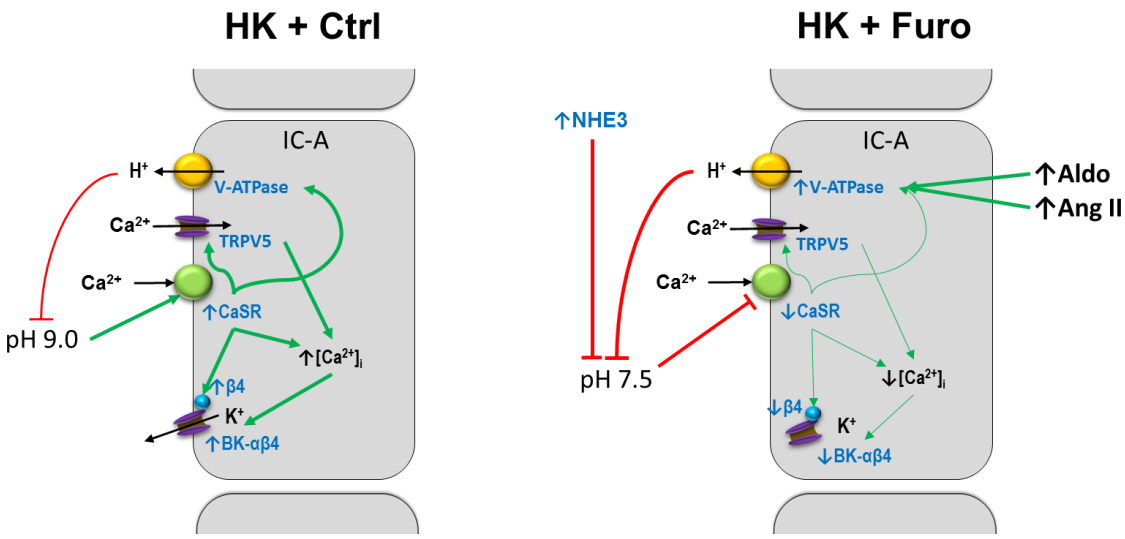

Figure 27. Proposed Mechanism of BK-αβ4 regulation by CaSR.

One potential flaw of our hypothesis is that urinary Ca^{2+} excretion is reduced on high K^+ diets (217-219), for which the mechanism is unclear. Ca^{2+} are passively reabsorbed by PT and TAL via paracellular route but actively reabsorbed in the DCT and CNT transcellularly via TRPV5 channels (180, 220, 221). Since Na^+ reabsorption in PT and TAL are inhibited on high K^+ diets (105, 119, 123), it is likely that Ca^{2+} reabsorption in the DCT and CNT are upregulated by high K^+ diets. Similar to the thiazide effect on Ca^{2+} reabsorption, by inhibiting NCC, high K^+ diets increase Ca^{2+} reabsorption in DCT by increasing Na^+ transport through NCX. However, another study showed that CNT played the predominant role for Ca^{2+} reabsorption (222). In any case, with increased Ca^{2+} sensitivity, the luminal [Ca^{2+}] in DCT2/CNT may be just enough to stimulate CaSR to regulate BK-αβ4 channels there. In fact, this provides an explanation why the regulation of BK-α localization by pH was only observed in DCT2/CNT but not CD. It may be because after increased Ca^{2+} reabsorption by TRPV5 in DCT2/CNT, the luminal [Ca^{2+}] in CD was not high enough to stimulate CaSR to regulate BK-αβ4, leaving BK-α inside the cytoplasm of CD cells. Additionally, the relationship between BK and TRPV4 channels has been demonstrated (104). High K^+ diets increases the expression and apical localization of TRPV4 in the ASDN in an aldosterone-dependent manner, which augments the flow-induced TRPV4-mediated Ca^{2+} entry, activating BK channels. TRPV5 channels may also be upregulated by high K^+ diets and activate BK channels in a similar manner. On the other hand, CaSR may be upstream of the TRPV4-dependent BK activation since CaSR can activate both TRPV4 and TRPV5 (183, 184).

Other than CaSR, another potential regulator of BK-αβ4 is the G-protein coupled receptor 4 (GPR4), which was recently shown to be a pH sensor in the kidney (223, 224). However, GPR4 is mainly expressed in the endothelial cells of the peritubular capillaries with rather low expressions in the epithelial cells (225). One abstract reported GPR4 expression in the basolateral membrane of intercalated cells (226). Therefore, GPR4 is unlikely to sense pH from the luminal side. Sensitive to extracellular pH, klotho is another possible regulator of BK-αβ4. Studies

showed that klotho can increase the activity of TRPV5 in the DCT (227), increasing Ca^{2+} reabsorption, which may lead to BK channel activation. However, klotho shows enhanced TRPV5 activity at a lower pH (228), opposite to our finding of the BK-αβ4 channel regulation. Other pH sensors in the CNT, such as soluble adenylyl cyclase and the insulin receptor–related receptor also sense the pH from the basolateral side and are unlikely to regulate BK-αβ4.

Diets and Diuretics

Overall, results in this dissertation reflect just a small part of the complicated interactions between diets and diuretics. Healthy diets, especially those low in Na^+ and high in K, are often recommended along with diuretics for hypertensive patients. As shown by the data on furosemide and LNaHK, the combination of the two elicited a marked diuretic and natriuretic effect. However, extra precautions should be taken to monitor plasma $[K^+]$ to avoid devastating consequences of hyperkalemia.

BIBLIOGRAPHY

1. Frassetto, L., Morris, R. C., Jr., Sellmeyer, D. E., Todd, K., and Sebastian, A. (2001) Diet, evolution and aging--the pathophysiologic effects of the post-agricultural inversion of the potassium-to-sodium and base-to-chloride ratios in the human diet. *Eur J Nutr* **40**, 200-213

2. Meneely, G. R., and Ball, C. O. (1958) Experimental epidemiology of chronic sodium chloride toxicity and the protective effect of potassium chloride. *Am J Med* **25**, 713-725

3. Meneely, G. R., and Battarbee, H. D. (1976) High sodium-low potassium environment and hypertension. *Am J Cardiol* **38**, 768-785

4. Jackson, S. L., King, S. M., Zhao, L., and Cogswell, M. E. (2016) Prevalence of Excess Sodium Intake in the United States - NHANES, 2009-2012. *MMWR Morb Mortal Wkly Rep* **64**, 1393-1397

5. Bailey, R. L., Parker, E. A., Rhodes, D. G., Goldman, J. D., Clemens, J. C., Moshfegh, A. J., Thuppal, S. V., and Weaver, C. M. (2016) Estimating Sodium and Potassium Intakes and Their Ratio in the American Diet: Data from the 2011-2012 NHANES. *J Nutr*

6. Sacks, F. M., Svetkey, L. P., Vollmer, W. M., Appel, L. J., Bray, G. A., Harsha, D., Obarzanek, E., Conlin, P. R., Miller, E. R., 3rd, Simons-Morton, D. G., Karanja, N., Lin, P. H., and Group, D. A.-S. C. R. (2001) Effects on blood pressure of reduced dietary sodium and the Dietary Approaches to Stop Hypertension (DASH) diet. DASH-Sodium Collaborative Research Group. *N Engl J Med* **344**, 3-10

7. Jonsson, T., Granfeldt, Y., Ahren, B., Branell, U. C., Palsson, G., Hansson, A., Soderstrom, M., and Lindeberg, S. (2009) Beneficial effects of a Paleolithic diet on cardiovascular risk factors in type 2 diabetes: a randomized cross-over pilot study. *Cardiovasc.Diabetol.* **8**, 35

8. Whalen, K. A., Judd, S., McCullough, M. L., Flanders, W. D., Hartman, T. J., and Bostick, R. M. (2017) Paleolithic and Mediterranean Diet Pattern Scores Are Inversely Associated with All-Cause and Cause-Specific Mortality in Adults. *J Nutr* **147**, 612-620

9. Babio, N., Toledo, E., Estruch, R., Ros, E., Martinez-Gonzalez, M. A., Castaner, O., Bullo, M., Corella, D., Aros, F., Gomez-Gracia, E., Ruiz-Gutierrez, V., Fiol, M., Lapetra, J., Lamuela-Raventos, R. M., Serra-Majem, L., Pinto, X., Basora, J., Sorli, J. V., and Salas-Salvado, J. (2014) Mediterranean diets and metabolic syndrome status in the PREDIMED randomized trial. *CMAJ.*

10. Lau, K. K., Wong, Y. K., Chan, Y. H., Li, O. Y., Sing Lee, P. Y., Yuen, G. G., Wong, Y. K., Tong, S., Wong, D., Chan, K. H., Cheung, R. T., Siu, C. W., Ho, S. L., and Tse, H. F. (2014) Mediterranean-Style Diet Is Associated With Reduced Blood Pressure Variability and Subsequent Stroke Risk in Patients With Coronary Artery Disease. *Am.J.Hypertens.*

11. Rouse, I. L., Beilin, L. J., Armstrong, B. K., and Vandongen, R. (1984) Vegetarian diet, blood pressure and cardiovascular risk. *Aust N Z J Med* **14**, 439-443

12. Printz, C. (2015) Vegetarian diet associated with lower risk of colorectal cancer. *Cancer* **121**, 2667

13. Eaton, S. B., and Konner, M. (1985) Paleolithic nutrition. A consideration of its nature and current implications. *N Engl J Med* **312**, 283-289

14. Oliver, W. J., Cohen, E. L., and Neel, J. V. (1975) Blood pressure, sodium intake, and sodium related hormones in the Yanomamo Indians, a "no-salt" culture. *Circulation* **52**, 146-151

15. Tanaka, M., Schmidlin, O., Yi, S. L., Bollen, A. W., and Morris, R. C., Jr. (1997) Genetically determined chloride-sensitive hypertension and stroke. *Proc Natl Acad Sci U S A* **94**, 14748-14752

16. Tanaka, M., Schmidlin, O., Olson, J. L., Yi, S. L., and Morris, R. C. (2001) Chloride-sensitive renal microangiopathy in the stroke-prone spontaneously hypertensive rat. *Kidney Int* **59**, 1066-1076

17. He, F. J., Marciniak, M., Carney, C., Markandu, N. D., Anand, V., Fraser, W. D., Dalton, R. N., Kaski, J. C., and MacGregor, G. A. (2010) Effects of potassium chloride and potassium bicarbonate on endothelial function, cardiovascular risk factors, and bone turnover in mild hypertensives. *Hypertension* **55**, 681-688

18. Vongpatanasin, W., Peri-Okonny, P., Velasco, A., Arbique, D., Wang, Z., Ravikumar, P., Adams-Huet, B., Moe, O. W., and Pak, C. Y. C. (2016) Effects of Potassium Magnesium Citrate Supplementation on 24-Hour Ambulatory Blood Pressure and Oxidative Stress Marker in Prehypertensive and Hypertensive Subjects. *Am J Cardiol* **118**, 849-853

19. Braschi, A., and Naismith, D. J. (2008) The effect of a dietary supplement of potassium chloride or potassium citrate on blood pressure in predominantly normotensive volunteers. *Br J Nutr* **99**, 1284-1292

20. Wingo, C. S., and Weiner, I. D. (2000) Disorders of potassium balance. In *Brenner and Rector's the Kidney* (Brenner, B. M., ed) pp. 998-1035, Saunders, Philadelphia

21. Koeppen, B. M., and Stanton, B. A. (2008) In *Berne & Levy Physiology* (Koeppen, B. M., and Stanton, B. A., eds), Mosby, Elsevier, Philadelphia

22. Ho, K., Nichols, C. G., Lederer, W. J., Lytton, J., Vassilev, P. M., Kanazirska, M. V., and Hebert, S. C. (1993) Cloning and expression of an inwardly rectifying ATP-regulated potassium channel. *Nature* **362**, 31-38

23. Palmer, L. G., Choe, H., and Frindt, G. (1997) Is the secretory K channel in the rat CCT ROMK? *Am J Physiol* **273**, F404-410

24. Woda, C. B., Bragin, A., Kleyman, T. R., and Satlin, L. M. (2001) Flow-dependent K+ secretion in the cortical collecting duct is mediated by a maxi-K channel. *Am.J.Physiol Renal Physiol* **280**, F786-F793

25. Sansom, S. C., and Welling, P. A. (2007) Two channels for one job. *Kidney Int.* **72**, 529-530

26. Bailey, M. A., Cantone, A., Yan, Q., MacGregor, G. G., Leng, Q., Amorim, J. B., Wang, T., Hebert, S. C., Giebisch, G., and Malnic, G. (2006) Maxi-K channels contribute to urinary potassium excretion in the ROMK-deficient mouse model of Type II Bartter's syndrome and in adaptation to a high-K diet. *Kidney Int.* **70**, 51-59

27. Rieg, T., Vallon, V., Sausbier, M., Sausbier, U., Kaissling, B., Ruth, P., and Osswald, H. (2007) The role of the BK channel in potassium homeostasis and flow-induced renal potassium excretion. *Kidney Int.* **72**, 566-573

28. Welling, P. A., and Ho, K. (2009) A comprehensive guide to the ROMK potassium channel: form and function in health and disease. *Am.J.Physiol Renal Physiol* **297**, F849-F863

29. Frindt, G., and Palmer, L. G. (1989) Low-conductance K channels in apical membrane of rat cortical collecting tubule. *Am J Physiol* **256**, F143-151

30. Wang, W. H., Schwab, A., and Giebisch, G. (1990) Regulation of small-conductance K+ channel in apical membrane of rat cortical collecting tubule. *Am J Physiol* **259**, F494-502

31. Wang, W. H., White, S., Geibel, J., and Giebisch, G. (1990) A potassium channel in the apical membrane of rabbit thick ascending limb of Henle's loop. *Am J Physiol* **258**, F244-253

32. Wang, W. H. (1994) Two types of K+ channel in thick ascending limb of rat kidney. *Am J Physiol* **267**, F599-605

33. Kohda, Y., Ding, W., Phan, E., Housini, I., Wang, J., Star, R. A., and Huang, C. L. (1998) Localization of the ROMK potassium channel to the apical membrane of distal nephron in rat kidney. *Kidney Int* **54**, 1214-1223

34. Mennitt, P. A., Wade, J. B., Ecelbarger, C. A., Palmer, L. G., and Frindt, G. (1997) Localization of ROMK channels in the rat kidney. *J Am Soc Nephrol* **8**, 1823-1830

35. Xu, J. Z., Hall, A. E., Peterson, L. N., Bienkowski, M. J., Eessalu, T. E., and Hebert, S. C. (1997) Localization of the ROMK protein on apical membranes of rat kidney nephron segments. *Am J Physiol* **273**, F739-748

36. Nichols, C. G., Ho, K., and Hebert, S. (1994) Mg(2+)-dependent inward rectification of ROMK1 potassium channels expressed in Xenopus oocytes. *J Physiol* **476**, 399-409

37. Lu, M., Wang, T., Yan, Q., Yang, X., Dong, K., Knepper, M. A., Wang, W., Giebisch, G., Shull, G. E., and Hebert, S. C. (2002) Absence of small conductance K+ channel (SK)

activity in apical membranes of thick ascending limb and cortical collecting duct in ROMK (Bartter's) knockout mice. *J.Biol.Chem.* **277**, 37881-37887

38. Fremont, O. T., and Chan, J. C. (2012) Understanding Bartter syndrome and Gitelman syndrome. *World J Pediatr* **8**, 25-30

39. Sundar, U., Lakkas, Y., Asole, D., and Vaidya, M. (2010) Gitelman's syndrome presenting as recurrent paralytic ileus due to chronic renal tubular K+ wasting. *J Assoc Physicians India* **58**, 322-324

40. Lorenz, J. N., Baird, N. R., Judd, L. M., Noonan, W. T., Andringa, A., Doetschman, T., Manning, P. A., Liu, L. H., Miller, M. L., and Shull, G. E. (2002) Impaired renal NaCl absorption in mice lacking the ROMK potassium channel, a model for type II Bartter's syndrome. *J.Biol.Chem.* **277**, 37871-37880

41. Giebisch, G. (1998) Renal potassium transport: mechanisms and regulation. *Am.J.Physiol* **274**, F817-F833

42. Welling, P. A. (2013) Regulation of renal potassium secretion: molecular mechanisms. *Semin.Nephrol.* **33**, 215-228

43. Dong, K., Yan, Q., Lu, M., Wan, L., Hu, H., Guo, J., Boulpaep, E., Wang, W., Giebisch, G., Hebert, S. C., and Wang, T. (2016) Romk1 Knockout Mice Do Not Produce Bartter Phenotype but Exhibit Impaired K Excretion. *J Biol Chem* **291**, 5259-5269

44. Grimm, P. R., and Sansom, S. C. (2007) BK channels in the kidney. *Curr.Opin.Nephrol.Hypertens.* **16**, 430-436

45. Zhang, J., and Yan, J. (2014) Regulation of BK channels by auxiliary gamma subunits. *Front Physiol* **5**, 401

46. Meera, P., Wallner, M., Song, M., and Toro, L. (1997) Large conductance voltage- and calcium-dependent K+ channel, a distinct member of voltage-dependent ion channels with seven N-terminal transmembrane segments (S0-S6), an extracellular N terminus, and an intracellular (S9-S10) C terminus. *Proc Natl Acad Sci U S A* **94**, 14066-14071

47. Wallner, M., Meera, P., and Toro, L. (1996) Determinant for beta-subunit regulation in high-conductance voltage-activated and Ca(2+)-sensitive K+ channels: an additional transmembrane region at the N terminus. *Proc Natl Acad Sci U S A* **93**, 14922-14927

48. Morrow, J. P., Zakharov, S. I., Liu, G., Yang, L., Sok, A. J., and Marx, S. O. (2006) Defining the BK channel domains required for beta1-subunit modulation. *Proc Natl Acad Sci U S A* **103**, 5096-5101

49. Lee, U. S., and Cui, J. (2010) BK channel activation: structural and functional insights. *Trends Neurosci.* **33**, 415-423

50. Golowasch, J., Kirkwood, A., and Miller, C. (1986) Allosteric effects of Mg2+ on the gating of Ca2+-activated K+ channels from mammalian skeletal muscle. *J Exp Biol* **124**, 5-13

51. Latorre, R., and Miller, C. (1983) Conduction and selectivity in potassium channels. *J Membr Biol* **71**, 11-30

52. Behrens, R., Nolting, A., Reimann, F., Schwarz, M., Waldschutz, R., and Pongs, O. (2000) hKCNMB3 and hKCNMB4, cloning and characterization of two members of the

large-conductance calcium-activated potassium channel beta subunit family. *FEBS Lett* **474**, 99-106

53. Brenner, R., Jegla, T. J., Wickenden, A., Liu, Y., and Aldrich, R. W. (2000) Cloning and functional characterization of novel large conductance calcium-activated potassium channel beta subunits, hKCNMB3 and hKCNMB4. *J Biol Chem* **275**, 6453-6461

54. Savalli, N., Kondratiev, A., de Quintana, S. B., Toro, L., and Olcese, R. (2007) Modes of operation of the BKCa channel beta2 subunit. *J Gen Physiol* **130**, 117-131

55. Contreras, G. F., Neely, A., Alvarez, O., Gonzalez, C., and Latorre, R. (2012) Modulation of BK channel voltage gating by different auxiliary beta subunits. *Proc Natl Acad Sci U S A* **109**, 18991-18996

56. Xia, X. M., Ding, J. P., and Lingle, C. J. (1999) Molecular basis for the inactivation of Ca2+- and voltage-dependent BK channels in adrenal chromaffin cells and rat insulinoma tumor cells. *J Neurosci* **19**, 5255-5264

57. Uebele, V. N., Lagrutta, A., Wade, T., Figueroa, D. J., Liu, Y., McKenna, E., Austin, C. P., Bennett, P. B., and Swanson, R. (2000) Cloning and functional expression of two families of beta-subunits of the large conductance calcium-activated K+ channel. *J Biol Chem* **275**, 23211-23218

58. Wen, D., Cornelius, R. J., Yuan, Y., and Sansom, S. C. (2013) Regulation of BK-alpha expression in the distal nephron by aldosterone and urine pH. *Am.J.Physiol Renal Physiol* **305**, F463-F476

59. Yan, J., and Aldrich, R. W. (2010) LRRC26 auxiliary protein allows BK channel activation at resting voltage without calcium. *Nature* **466**, 513-516

60. Yan, J., and Aldrich, R. W. (2012) BK potassium channel modulation by leucine-rich repeat-containing proteins. *Proc Natl Acad Sci U S A* **109**, 7917-7922

61. Li, Q., Fan, F., Kwak, H. R., and Yan, J. (2015) Molecular basis for differential modulation of BK channel voltage-dependent gating by auxiliary gamma subunits. *J Gen Physiol* **145**, 543-554

62. Yuan, P., Leonetti, M. D., Pico, A. R., Hsiung, Y., and MacKinnon, R. (2010) Structure of the human BK channel Ca2+-activation apparatus at 3.0 A resolution. *Science* **329**, 182-186

63. Robitaille, R., Garcia, M. L., Kaczorowski, G. J., and Charlton, M. P. (1993) Functional colocalization of calcium and calcium-gated potassium channels in control of transmitter release. *Neuron* **11**, 645-655

64. Fettiplace, R., and Fuchs, P. A. (1999) Mechanisms of hair cell tuning. *Annu Rev Physiol* **61**, 809-834

65. Nelson, M. T., Cheng, H., Rubart, M., Santana, L. F., Bonev, A. D., Knot, H. J., and Lederer, W. J. (1995) Relaxation of arterial smooth muscle by calcium sparks. *Science* **270**, 633-637

66. Brenner, R., Perez, G. J., Bonev, A. D., Eckman, D. M., Kosek, J. C., Wiler, S. W., Patterson, A. J., Nelson, M. T., and Aldrich, R. W. (2000) Vasoregulation by the beta1 subunit of the calcium-activated potassium channel. *Nature* **407**, 870-876

67. Petkov, G. V., Bonev, A. D., Heppner, T. J., Brenner, R., Aldrich, R. W., and Nelson, M. T. (2001) Beta1-subunit of the Ca2+-activated K+ channel regulates contractile activity of mouse urinary bladder smooth muscle. *J Physiol* **537**, 443-452

68. Kaczorowski, G. J., Knaus, H. G., Leonard, R. J., McManus, O. B., and Garcia, M. L. (1996) High-conductance calcium-activated potassium channels; structure, pharmacology, and function. *J Bioenerg Biomembr* **28**, 255-267

69. Navaratnam, D. S., Bell, T. J., Tu, T. D., Cohen, E. L., and Oberholtzer, J. C. (1997) Differential distribution of Ca2+-activated K+ channel splice variants among hair cells along the tonotopic axis of the chick cochlea. *Neuron* **19**, 1077-1085

70. Rosenblatt, K. P., Sun, Z. P., Heller, S., and Hudspeth, A. J. (1997) Distribution of Ca2+-activated K+ channel isoforms along the tonotopic gradient of the chicken's cochlea. *Neuron* **19**, 1061-1075

71. Tseng-Crank, J., Foster, C. D., Krause, J. D., Mertz, R., Godinot, N., DiChiara, T. J., and Reinhart, P. H. (1994) Cloning, expression, and distribution of functionally distinct Ca(2+)-activated K+ channel isoforms from human brain. *Neuron* **13**, 1315-1330

72. Fallet, R. W., Bast, J. P., Fujiwara, K., Ishii, N., Sansom, S. C., and Carmines, P. K. (2001) Influence of Ca(2+)-activated K(+) channels on rat renal arteriolar responses to depolarizing agonists. *Am J Physiol Renal Physiol* **280**, F583-591

73. Stockand, J. D., and Sansom, S. C. (1994) Large Ca(2+)-activated K+ channels responsive to angiotensin II in cultured human mesangial cells. *Am J Physiol* **267**, C1080-1086

74. Morton, M. J., Hutchinson, K., Mathieson, P. W., Witherden, I. R., Saleem, M. A., and Hunter, M. (2004) Human podocytes possess a stretch-sensitive, Ca2+-activated K+ channel: potential implications for the control of glomerular filtration. *J Am Soc Nephrol* **15**, 2981-2987

75. Guggino, S. E., Guggino, W. B., Green, N., and Sacktor, B. (1987) Ca2+-activated K+ channels in cultured medullary thick ascending limb cells. *Am J Physiol* **252**, C121-127

76. Taniguchi J, G. W. (1989) Membrane stretch: a physiological stimulator of Ca2+-activated K+ channels in thick ascending limb. *Am J Physiol.* **408**, 600-608

77. Belfodil, R., Barriere, H., Rubera, I., Tauc, M., Poujeol, C., Bidet, M., and Poujeol, P. (2003) CFTR-dependent and -independent swelling-activated K+ currents in primary cultures of mouse nephron. *Am J Physiol Renal Physiol* **284**, F812-828

78. Frindt, G., and Palmer, L. G. (2004) Apical potassium channels in the rat connecting tubule. *Am J Physiol Renal Physiol* **287**, F1030-1037

79. Pluznick, J. L., Wei, P., Grimm, P. R., and Sansom, S. C. (2005) BK-{beta}1 subunit: immunolocalization in the mammalian connecting tubule and its role in the kaliuretic response to volume expansion. *Am J Physiol Renal Physiol* **288**, F846-854

80. Taniguchi, J., and Imai, M. (1998) Flow-dependent activation of maxi K+ channels in apical membrane of rabbit connecting tubule. *J Membr Biol* **164**, 35-45

81. Hunter, M., Lopes, A. G., Boulpaep, E. L., and Giebisch, G. H. (1984) Single channel recordings of calcium-activated potassium channels in the apical membrane of rabbit cortical collecting tubules. *Proc Natl Acad Sci U S A* **81**, 4237-4239

82. Morita, T., Hanaoka, K., Morales, M. M., Montrose-Rafizadeh, C., and Guggino, W. B. (1997) Cloning and characterization of maxi K+ channel alpha-subunit in rabbit kidney. *Am J Physiol* **273**, F615-624

83. Pacha, J., Frindt, G., Sackin, H., and Palmer, L. G. (1991) Apical maxi K channels in intercalated cells of CCT. *Am J Physiol* **261**, F696-705

84. Good, D. W., and Wright, F. S. (1979) Luminal influences on potassium secretion: sodium concentration and fluid flow rate. *Am.J.Physiol* **236**, F192-F205

85. Grimm, P. R., Foutz, R. M., Brenner, R., and Sansom, S. C. (2007) Identification and localization of BK-beta subunits in the distal nephron of the mouse kidney. *Am.J.Physiol Renal Physiol* **293**, F350-F359

86. Najjar, F., Zhou, H., Morimoto, T., Bruns, J. B., Li, H. S., Liu, W., Kleyman, T. R., and Satlin, L. M. (2005) Dietary K+ regulates apical membrane expression of maxi-K channels in rabbit cortical collecting duct. *Am J Physiol Renal Physiol* **289**, F922-932

87. Pluznick, J. L., Wei, P., Carmines, P. K., and Sansom, S. C. (2003) Renal fluid and electrolyte handling in BKCa-beta1-/- mice. *Am J Physiol Renal Physiol* **284**, F1274-1279

88. Grimm, P. R., Irsik, D. L., Settles, D. C., Holtzclaw, J. D., and Sansom, S. C. (2009) Hypertension of Kcnmb1-/- is linked to deficient K secretion and aldosteronism. *Proc.Natl.Acad.Sci.U.S.A* **106**, 11800-11805

89. Holtzclaw, J. D., Grimm, P. R., and Sansom, S. C. (2010) Intercalated cell BK-alpha/beta4 channels modulate sodium and potassium handling during potassium adaptation. *Journal of the American Society of Nephrology* **21**, 634-645

90. Cornelius, R. J., Wen, D., Hatcher, L. I., and Sansom, S. C. (2012) Bicarbonate promotes BK-alpha/beta4-mediated K excretion in the renal distal nephron. *Am.J.Physiol Renal Physiol* **303**, F1563-F1571

91. Larsen, C. K., Jensen, I. S., Sorensen, M. V., de Bruijn, P. I., Bleich, M., Praetorius, H. A., and Leipziger, J. (2016) Hyperaldosteronism after decreased renal K+ excretion in KCNMB2 knockout mice. *Am J Physiol Renal Physiol* **310**, F1035-1046

92. Liu, W., Morimoto, T., Woda, C., Kleyman, T. R., and Satlin, L. M. (2007) Ca2+ dependence of flow-stimulated K secretion in the mammalian cortical collecting duct. *Am J Physiol Renal Physiol* **293**, F227-235

93. Holtzclaw, J. D., Cornelius, R. J., Hatcher, L. I., and Sansom, S. C. (2011) Coupled ATP and potassium efflux from intercalated cells. *Am.J.Physiol Renal Physiol* **300**, F1319-F1326

94. Flores, D., Liu, Y., Liu, W., Satlin, L. M., and Rohatgi, R. (2012) Flow-induced prostaglandin E2 release regulates Na and K transport in the collecting duct. *Am J Physiol Renal Physiol* **303**, F632-638

95. Liu, Y., Flores, D., Carrisoza-Gaytan, R., and Rohatgi, R. (2014) Biomechanical regulation of cyclooxygenase-2 in the renal collecting duct. *Am J Physiol Renal Physiol* **306**, F214-223

96. Carrisoza-Gaytan, R., Wang, L., Schreck, C., Kleyman, T. R., Wang, W. H., and Satlin, L. M. (2017) The mechanosensitive BKalpha/beta1 channel localizes to cilia of principal cells in rabbit cortical collecting duct (CCD). *Am J Physiol Renal Physiol* **312**, F143-F156

97. Welling, P. A. (2016) Roles and Regulation of Renal K Channels. *Annu Rev Physiol* **78**, 415-435

98. Berrout, J., Jin, M., Mamenko, M., Zaika, O., Pochynyuk, O., and O'Neil, R. G. (2012) Function of transient receptor potential cation channel subfamily V member 4 (TRPV4) as a mechanical transducer in flow-sensitive segments of renal collecting duct system. *J Biol Chem* **287**, 8782-8791

99. Cornelius, R. J., Wen, D., Li, H., Yuan, Y., Wang-France, J., Warner, P. C., and Sansom, S. C. (2015) Low Na, high K diet and the role of aldosterone in BK-mediated K excretion. *PLoS.One.* **10**, e0115515

100. Frindt, G., and Palmer, L. G. (2010) Effects of dietary K on cell-surface expression of renal ion channels and transporters. *Am.J.Physiol Renal Physiol* **299**, F890-F897

101. Hamm, L. L., Feng, Z., and Hering-Smith, K. S. (2010) Regulation of sodium transport by ENaC in the kidney. *Curr Opin Nephrol Hypertens* **19**, 98-105

102. Vinciguerra, M., Mordasini, D., Vandewalle, A., and Feraille, E. (2005) Hormonal and nonhormonal mechanisms of regulation of the NA,K-pump in collecting duct principal cells. *Semin Nephrol* **25**, 312-321

103. Yoo, D., Kim, B. Y., Campo, C., Nance, L., King, A., Maouyo, D., and Welling, P. A. (2003) Cell surface expression of the ROMK (Kir 1.1) channel is regulated by the aldosterone-induced kinase, SGK-1, and protein kinase A. *J Biol Chem* **278**, 23066-23075

104. Mamenko, M. V., Boukelmoune, N., Tomilin, V. N., Zaika, O. L., Jensen, V. B., O'Neil, R. G., and Pochynyuk, O. M. (2017) The renal TRPV4 channel is essential for adaptation to increased dietary potassium. *Kidney Int* **91**, 1398-1409

105. Terker, A. S., Zhang, C., Erspamer, K. J., Gamba, G., Yang, C. L., and Ellison, D. H. (2016) Unique chloride-sensing properties of WNK4 permit the distal nephron to modulate potassium homeostasis. *Kidney Int* **89**, 127-134

106. United States. Department of Health and Human Services., Center for Disease Control., and National Center for Health Statistics (U.S.). (2016) *Health, United States, 2015 : with special feature on racial and ethnic health disparities*, National Center for Health Statistics, Hyattsville, MD

107. Chaudhry, S. (2013) DIURETICS AND RENAL HORMONES.

108. Wen, D., Cornelius, R. J., and Sansom, S. C. (2014) Interacting influence of diuretics and diet on BK channel-regulated K homeostasis. *Curr.Opin.Pharmacol.* **15**, 28-32

109. Wen, D., Cornelius, R. J., Rivero-Hernandez, D., Yuan, Y., Li, H., Weinstein, A. M., and Sansom, S. C. (2014) Relation between BK-alpha/beta4-mediated potassium secretion and ENaC-mediated sodium reabsorption. *Kidney Int.* **86**, 139-145

110. Rose, B. D. P., T. (1994) *Clinical Physiology of Acid-Base and Electrolyte Disorders* McGraw–Hill, New York

111. Wright, F. S., and Schnermann, J. (1974) Interference with feedback control of glomerular filtration rate by furosemide, triflocin, and cyanide. *The Journal of clinical investigation* **53**, 1695-1708

112. Gutsche, H. U., Brunkhorst, R., Muller-Ott, K., Franke, H., and Niedermayer, W. (1984) Effect of diuretics on the tubuloglomerular feedback response. *Can J Physiol Pharmacol* **62**, 412-417

113. Johnston, P. A., and Kau, S. T. (1992) The effect of loop of Henle diuretics on the tubuloglomerular feedback mechanism. *Methods Find Exp Clin Pharmacol* **14**, 523-529

114. Colussi, G., Rombola, G., Surian, M., De Ferrari, M. E., Airaghi, C., Benazzi, E., Malberti, F., and Minetti, L. (1989) Effects of acute administration of acetazolamide and frusemide on lithium clearance in humans. *Nephrol Dial Transplant* **4**, 707-712

115. Guidi, E., Colussi, G., Rombola, G., Airaghi, C., Minetti, E., and Malberti, F. (1995) Evaluation of the tubuloglomerular feedback system in human subjects. *Exp Nephrol* **3**, 61-64

116. Cenac, A., London, A., Menard, J., and Corvol, P. (1975) [Effect of furosemide and ACTH on plasma renin, aldosterone and cortisol levels in normal man]. *Ann Endocrinol (Paris)* **36**, 153-162

117. Chobanian, A. V., Garvras, H., Gavras, I., Bresnahan, M., Sullivan, P., and Melby, J. C. (1978) Studies on the activity of the sympathetic nervous system in essential hypertension. *J Human Stress* **4**, 22-28

118. Petersen, J. S., and DiBona, G. F. (1995) Furosemide elicits immediate sympathoexcitation via a renal mechanism independent of angiotensin II. *Pharmacol Toxicol* **77**, 106-113

119. Ellison, D. H., Terker, A. S., and Gamba, G. (2016) Potassium and Its Discontents: New Insight, New Treatments. *J Am Soc Nephrol* **27**, 981-989

120. Adrogue, H. J., and Madias, N. E. (2007) Sodium and potassium in the pathogenesis of hypertension. *N Engl J Med* **356**, 1966-1978

121. Battilana, C. A., Dobyan, D. C., Lacy, F. B., Bhattacharya, J., Johnston, P. A., and Jamison, R. L. (1978) Effect of chronic potassium loading on potassium secretion by the pars recta or descending limb of the juxtamedullary nephron in the rat. *J.Clin.Invest* **62**, 1093-1103

122. Stokes, J. B. (1982) Consequences of potassium recycling in the renal medulla. Effects of ion transport by the medullary thick ascending limb of Henle's loop. *J.Clin.Invest* **70**, 219-229

123. Brandis, M., Keyes, J., and Windhager, E. E. (1972) Potassium-induced inhibition of proximal tubular fluid reabsorption in rats. *Am J Physiol* **222**, 421-427

124. Martinez-Gonzalez, M. A., and Bes-Rastrollo, M. (2014) Dietary patterns, Mediterranean diet, and cardiovascular disease. *Curr.Opin.Lipidol.* **25**, 20-26

125. Huo, R., Du, T., Xu, Y., Xu, W., Chen, X., Sun, K., and Yu, X. (2014) Effects of Mediterranean-style diet on glycemic control, weight loss and cardiovascular risk factors among type 2 diabetes individuals: a meta-analysis. *Eur.J.Clin.Nutr.*

126. Widmer, R. J., Flammer, A. J., Lerman, L. O., and Lerman, A. (2015) The Mediterranean diet, its components, and cardiovascular disease. *Am J Med* **128**, 229-238

127. Cornelius, R. J., Wang, B., Wang-France, J., and Sansom, S. C. (2016) Maintaining K balance on the low Na, high K diet. *Am J Physiol Renal Physiol*, ajprenal 00330 02015

128. Pluznick, J. L., and Sansom, S. C. (2006) BK channels in the kidney: role in K(+) secretion and localization of molecular components. *Am.J.Physiol Renal Physiol* **291**, F517-F529

129. Jamison, R. L., Work, J., and Schafer, J. A. (1982) New pathways for potassium transport in the kidney. *Am J Physiol* **242**, F297-312

130. Schiessl, I. M., Rosenauer, A., Kattler, V., Minuth, W. W., Oppermann, M., and Castrop, H. (2013) Dietary salt intake modulates differential splicing of the Na-K-2Cl cotransporter NKCC2. *Am.J.Physiol Renal Physiol* **305**, F1139-F1148

131. Fraser, S. A., Choy, S. W., Pastor-Soler, N. M., Li, H., Davies, M. R., Cook, N., Katerelos, M., Mount, P. F., Gleich, K., McRae, J. L., Dwyer, K. M., van Denderen, B. J., Hallows, K. R., Kemp, B. E., and Power, D. A. (2013) AMPK couples plasma renin to cellular metabolism by phosphorylation of ACC1. *Am J Physiol Renal Physiol* **305**, F679-690

132. Tsuruoka, S., Koseki, C., Muto, S., Tabei, K., and Imai, M. (1994) Axial heterogeneity of potassium transport across hamster thick ascending limb of Henle's loop. *Am J Physiol* **267**, F121-129

133. Bailly, C., Imbert-Teboul, M., Roinel, N., and Amiel, C. (1990) Isoproterenol increases Ca, Mg, and NaCl reabsorption in mouse thick ascending limb. *Am J Physiol* **258**, F1224-1231

134. Wen, D., Yuan, Y., Warner, P. C., Wang, B., Cornelius, R. J., Wang-France, J., Li, H., Boettger, T., and Sansom, S. C. (2015) Increased Epithelial Sodium Channel Activity Contributes to Hypertension Caused by Na+-HCO3- Cotransporter Electrogenic 2 Deficiency. *Hypertension* **66**, 68-74

135. Foutz, R. M., Grimm, P. R., and Sansom, S. C. (2008) Insulin increases the activity of mesangial BK channels through MAPK signaling. *Am.J.Physiol Renal Physiol* **294**, F1465-F1472

136. Stockand, J. D., Silverman, M., Hall, D., Derr, T., Kubacak, B., and Sansom, S. C. (1998) Arachidonic acid potentiates the feedback response of mesangial BKCa channels to angiotensin II. *Am J Physiol* **274**, F658-664

137. Knochel, J. P. (1984) Diuretic-induced hypokalemia. *Am J Med* **77**, 18-27

138. Hropot, M., Fowler, N., Karlmark, B., and Giebisch, G. (1985) Tubular action of diuretics: distal effects on electrolyte transport and acidification. *Kidney Int* **28**, 477-489

139. Stokes, J. B. (1981) Potassium secretion by cortical collecting tubule: relation to sodium absorption, luminal sodium concentration, and transepithelial voltage. *Am.J.Physiol* **241**, F395-F402

140. Lu, M., Wang, T., Yan, Q., Wang, W., Giebisch, G., and Hebert, S. C. (2004) ROMK is required for expression of the 70-pS K channel in the thick ascending limb. *Am.J.Physiol Renal Physiol* **286**, F490-F495

141. Mandon, B., Siga, E., Roinel, N., and de Rouffignac, C. (1993) Ca2+, Mg2+ and K+ transport in the cortical and medullary thick ascending limb of the rat nephron: influence of transepithelial voltage. *Pflugers Arch* **424**, 558-560

142. Di Stefano, A., Wittner, M., Nitschke, R., Braitsch, R., Greger, R., Bailly, C., Amiel, C., Elalouf, J. M., Roinel, N., and de Rouffignac, C. (1989) Effects of glucagon on Na+, Cl-, K+, Mg2+ and Ca2+ transports in cortical and medullary thick ascending limbs of mouse kidney. *Pflugers Arch* **414**, 640-646

143. Ponto, L. L., and Schoenwald, R. D. (1990) Furosemide (frusemide). A pharmacokinetic/pharmacodynamic review (Part I). *Clin Pharmacokinet* **18**, 381-408

144. Sica, D. A., Carter, B., Cushman, W., and Hamm, L. (2011) Thiazide and loop diuretics. *J Clin Hypertens (Greenwich)* **13**, 639-643

145. Cohn, J. N., Kowey, P. R., Whelton, P. K., and Prisant, L. M. (2000) New guidelines for potassium replacement in clinical practice: a contemporary review by the National Council on Potassium in Clinical Practice. *Arch Intern Med* **160**, 2429-2436

146. Bia, M. J., and DeFronzo, R. A. (1981) Extrarenal potassium homeostasis. *Am J Physiol* **240**, F257-268

147. Unwin, R. J., Walter, S. J., Giebisch, G., Capasso, G., and Shirley, D. G. (2000) Localization of diuretic effects along the loop of Henle: an in vivo microperfusion study in rats. *Clin Sci (Lond)* **98**, 481-488

148. Kortenoeven, M. L., Pedersen, N. B., Rosenbaek, L. L., and Fenton, R. A. (2015) Vasopressin regulation of sodium transport in the distal nephron and collecting duct. *Am J Physiol Renal Physiol* **309**, F280-299

149. Roos, K. P., Bugaj, V., Mironova, E., Stockand, J. D., Ramkumar, N., Rees, S., and Kohan, D. E. (2013) Adenylyl cyclase VI mediates vasopressin-stimulated ENaC activity. *J Am Soc Nephrol* **24**, 218-227

150. Cristia, E., Amat, C., Naftalin, R. J., and Moreto, M. (2007) Role of vasopressin in rat distal colon function. *J Physiol* **578**, 413-424

151. Matsuguchi, H., Schmid, P. G., Van Orden, D., and Mark, A. L. (1981) Does vasopressin contribute to salt-induced hypertension in the Dahl strain? *Hypertension* **3**, 174-181

152. Kovacs, G., Peti-Peterdi, J., Rosivall, L., and Bell, P. D. (2002) Angiotensin II directly stimulates macula densa Na-2Cl-K cotransport via apical AT(1) receptors. *Am J Physiol Renal Physiol* **282**, F301-306

153. van der Lubbe, N., Moes, A. D., Rosenbaek, L. L., Schoep, S., Meima, M. E., Danser, A. H., Fenton, R. A., Zietse, R., and Hoorn, E. J. (2013) K+-induced natriuresis is preserved during Na+ depletion and accompanied by inhibition of the Na+-Cl- cotransporter. *Am J Physiol Renal Physiol* **305**, F1177-1188

154. Palmer, L. G., and Frindt, G. (1999) Regulation of apical K channels in rat cortical collecting tubule during changes in dietary K intake. *Am J Physiol* **277**, F805-812

155. Hebert, S. C., Desir, G., Giebisch, G., and Wang, W. (2005) Molecular diversity and regulation of renal potassium channels. *Physiol Rev.* **85**, 319-371

156. Bostanjoglo, M., Reeves, W. B., Reilly, R. F., Velazquez, H., Robertson, N., Litwack, G., Morsing, P., Dorup, J., Bachmann, S., and Ellison, D. H. (1998) 11Beta-hydroxysteroid dehydrogenase, mineralocorticoid receptor, and thiazide-sensitive Na-Cl cotransporter expression by distal tubules. *J Am Soc Nephrol* **9**, 1347-1358

157. Lu, M., Zhu, Y., Balazy, M., Reddy, K. M., Falck, J. R., and Wang, W. (1996) Effect of angiotensin II on the apical K+ channel in the thick ascending limb of the rat kidney. *J.Gen.Physiol* **108**, 537-547

158. Shirley, D. G., Skinner, J., and Walter, S. J. (1987) The influence of dietary potassium on the renal tubular effect of hydrochlorothiazide in the rat. *Br.J.Pharmacol.* **91**, 693-699

159. Wang, B., Wen, D., Li, H., Wang-France, J., and Sansom, S. C. (2017) Net K(+) secretion in the thick ascending limb of mice on a low-Na, high-K diet. *Kidney Int* **92**, 864-875

160. Giebisch, G. (1986) Mechanisms of renal tubular acidification. *Klin Wochenschr* **64**, 853-861

161. Kovacikova, J., Winter, C., Loffing-Cueni, D., Loffing, J., Finberg, K. E., Lifton, R. P., Hummler, E., Rossier, B., and Wagner, C. A. (2006) The connecting tubule is the main site of the furosemide-induced urinary acidification by the vacuolar H+-ATPase. *Kidney Int* **70**, 1706-1716

162. Na, K. Y., Kim, G. H., Joo, K. W., Lee, J. W., Jang, H. R., Oh, Y. K., Jeon, U. S., Chae, S. W., Knepper, M. A., and Han, J. S. (2007) Chronic furosemide or hydrochlorothiazide administration increases H+-ATPase B1 subunit abundance in rat kidney. *Am J Physiol Renal Physiol* **292**, F1701-1709

163. de Bruijn, P. I., Larsen, C. K., Frische, S., Himmerkus, N., Praetorius, H. A., Bleich, M., and Leipziger, J. (2015) Furosemide-induced urinary acidification is caused by pronounced H+ secretion in the thick ascending limb. *Am J Physiol Renal Physiol* **309**, F146-153

164. Grimm, P. R., Lazo-Fernandez, Y., Delpire, E., Wall, S. M., Dorsey, S. G., Weinman, E. J., Coleman, R., Wade, J. B., and Welling, P. A. (2015) Integrated compensatory network is activated in the absence of NCC phosphorylation. *The Journal of clinical investigation* **125**, 2136-2150

165. Reeuwijk, H. J., Tjaden, U. R., and van der Greef, J. (1992) Simultaneous determination of furosemide and amiloride in plasma using high-performance liquid chromatography with fluorescence detection. *J Chromatogr* **575**, 269-274

166. Batlle, D. C. (1986) Segmental characterization of defects in collecting tubule acidification. *Kidney Int* **30**, 546-554

167. Walsh, S. B., Shirley, D. G., Wrong, O. M., and Unwin, R. J. (2007) Urinary acidification assessed by simultaneous furosemide and fludrocortisone treatment: an alternative to ammonium chloride. *Kidney Int* **71**, 1310-1316

168. Brater, D. C. (1998) Diuretic therapy. *N Engl J Med* **339**, 387-395

169. Brater, D. C., Kaojarern, S., and Chennavasin, P. (1983) Pharmacodynamics of the diuretic effects of aminophylline and acetazolamide alone and combined with furosemide in normal subjects. *J Pharmacol Exp Ther* **227**, 92-97

170. Malnic, G., De Mello Aires, M., and Giebisch, G. (1971) Potassium transport across renal distal tubules during acid-base disturbances. *Am J Physiol* **221**, 1192-1208

171. McNicholas, C. M., MacGregor, G. G., Islas, L. D., Yang, Y., Hebert, S. C., and Giebisch, G. (1998) pH-dependent modulation of the cloned renal K+ channel, ROMK. *Am J Physiol* **275**, F972-981

172. Shavit, L., Chen, L., Ahmed, F., Ferraro, P. M., Moochhala, S., Walsh, S. B., and Unwin, R. (2016) Selective screening for distal renal tubular acidosis in recurrent kidney stone formers: initial experience and comparison of the simultaneous furosemide and fludrocortisone test with the short ammonium chloride test. *Nephrol Dial Transplant* **31**, 1870-1876

173. Rastogi, S. P., Crawford, C., Wheeler, R., Flanigan, W., and Arruda, J. A. (1984) Effect of furosemide on urinary acidification in distal renal tubular acidosis. *J Lab Clin Med* **104**, 271-282

174. Lee, C. T., Chen, H. C., Lai, L. W., Yong, K. C., and Lien, Y. H. (2007) Effects of furosemide on renal calcium handling. *Am J Physiol Renal Physiol* **293**, F1231-1237

175. Friedman, P. A., and Bushinsky, D. A. (1999) Diuretic effects on calcium metabolism. *Semin Nephrol* **19**, 551-556

176. Renkema, K. Y., Velic, A., Dijkman, H. B., Verkaart, S., van der Kemp, A. W., Nowik, M., Timmermans, K., Doucet, A., Wagner, C. A., Bindels, R. J., and Hoenderop, J. G. (2009) The calcium-sensing receptor promotes urinary acidification to prevent nephrolithiasis. *J Am Soc Nephrol* **20**, 1705-1713

177. Carota, I., Theilig, F., Oppermann, M., Kongsuphol, P., Rosenauer, A., Schreiber, R., Jensen, B. L., Walter, S., Kunzelmann, K., and Castrop, H. (2010) Localization and functional characterization of the human NKCC2 isoforms. *Acta Physiol (Oxf)* **199**, 327-338

178. Rodicio, J. L., and Hernando, L. (1977) Effects and interactions of furosemide and acetazolamide on tubular function in rat kidney. *Rev Esp Fisiol* **33**, 113-118

179. Gibson, D. G., Marshall, J. C., and Lockey, E. (1970) Assessment of proximal tubular sodium reabsorption during water diuresis in patients with heart disease. *Br Heart J* **32**, 399-405

180. Riccardi, D., and Valenti, G. (2016) Localization and function of the renal calcium-sensing receptor. *Nat Rev Nephrol* **12**, 414-425

181. Quinn, S. J., Bai, M., and Brown, E. M. (2004) pH Sensing by the calcium-sensing receptor. *J Biol Chem* **279**, 37241-37249

182. Doroszewicz, J., Waldegger, P., Jeck, N., Seyberth, H., and Waldegger, S. (2005) pH dependence of extracellular calcium sensing receptor activity determined by a novel technique. *Kidney Int* **67**, 187-192

183. Topala, C. N., Schoeber, J. P., Searchfield, L. E., Riccardi, D., Hoenderop, J. G., and Bindels, R. J. (2009) Activation of the Ca2+-sensing receptor stimulates the activity of the epithelial Ca2+ channel TRPV5. *Cell Calcium* **45**, 331-339

184. Xie, R., Xu, J., Xiao, Y., Wu, J., Wan, H., Tang, B., Liu, J., Fan, Y., Wang, S., Wu, Y., Dong, T. X., Zhu, M. X., Carethers, J. M., Dong, H., and Yang, S. (2017) Calcium Promotes Human Gastric Cancer via a Novel Coupling of Calcium-Sensing Receptor and TRPV4 Channel. *Cancer Res* **77**, 6499-6512

185. Rubera, I., Loffing, J., Palmer, L. G., Frindt, G., Fowler-Jaeger, N., Sauter, D., Carroll, T., McMahon, A., Hummler, E., and Rossier, B. C. (2003) Collecting duct-specific gene inactivation of alphaENaC in the mouse kidney does not impair sodium and potassium balance. *J.Clin.Invest* **112**, 554-565

186. Amorim, J. B., Bailey, M. A., Musa-Aziz, R., Giebisch, G., and Malnic, G. (2003) Role of luminal anion and pH in distal tubule potassium secretion. *Am.J.Physiol Renal Physiol* **284**, F381-F388

187. Boudry, J. F., Stoner, L. C., and Burg, M. B. (1976) Effect of acid lumen pH on potassium transport in renal cortical collecting tubules. *Am J Physiol* **230**, 239-244

188. Fakler, B., Schultz, J. H., Yang, J., Schulte, U., Brandle, U., Zenner, H. P., Jan, L. Y., and Ruppersberg, J. P. (1996) Identification of a titratable lysine residue that determines sensitivity of kidney potassium channels (ROMK) to intracellular pH. *EMBO J* **15**, 4093-4099

189. Weiner, I. D., and Hamm, L. L. (1991) Regulation of Cl-/HCO3- exchange in the rabbit cortical collecting tubule. *The Journal of clinical investigation* **87**, 1553-1558

190. Pech, V., Pham, T. D., Hong, S., Weinstein, A. M., Spencer, K. B., Duke, B. J., Walp, E., Kim, Y. H., Sutliff, R. L., Bao, H. F., Eaton, D. C., and Wall, S. M. (2010) Pendrin modulates ENaC function by changing luminal HCO3. *J Am Soc Nephrol* **21**, 1928-1941

191. Liu, W., Schreck, C., Coleman, R. A., Wade, J. B., Hernandez, Y., Zavilowitz, B., Warth, R., Kleyman, T. R., and Satlin, L. M. (2011) Role of NKCC in BK channel-mediated net K(+) secretion in the CCD. *Am.J.Physiol Renal Physiol* **301**, F1088-F1097

192. Glanville, M., Kingscote, S., Thwaites, D. T., and Simmons, N. L. (2001) Expression and role of sodium, potassium, chloride cotransport (NKCC1) in mouse inner medullary collecting duct (mIMCD-K2) epithelial cells. *Pflugers Arch* **443**, 123-131

193. Reyes, A. J. (1991) Effects of diuretics on outputs and flows of urine and urinary solutes in healthy subjects. *Drugs* **41 Suppl 3**, 35-59

194. Reyes, A. J., and Taylor, S. H. (1999) Diuretics in cardiovascular therapy: the new clinicopharmacological bases that matter. *Cardiovasc Drugs Ther* **13**, 371-398

195. Gu, R. M., and Wang, W. H. (2002) Arachidonic acid inhibits K channels in basolateral membrane of the thick ascending limb. *Am J Physiol Renal Physiol* **283**, F407-414

196. Gu, R., Wang, J., Zhang, Y., Li, W., Xu, Y., Shan, H., Wang, W. H., and Yang, B. (2007) Adenosine stimulates the basolateral 50 pS K channels in the thick ascending limb of the rat kidney. *Am J Physiol Renal Physiol* **293**, F299-305

197. Gu, R., Jin, Y., Zhai, Y., Yang, L., Zhang, C., Li, W., Wang, L., Kong, S., Zhang, Y., Yang, B., and Wang, W. H. (2008) PGE2 inhibits basolateral 50 pS potassium channels in the thick ascending limb of the rat kidney. *Kidney Int* **74**, 478-485

198. Paulais, M., Lachheb, S., and Teulon, J. (2006) A Na+- and Cl- -activated K+ channel in the thick ascending limb of mouse kidney. *J.Gen.Physiol* **127**, 205-215

199. Fan, L., Wang, X., Zhang, D., Duan, X., Zhao, C., Zu, M., Meng, X., Zhang, C., Su, X. T., Wang, M. X., Wang, W. H., and Gu, R. (2015) Vasopressin-induced stimulation of the Na(+)-activated K(+) channels is responsible for maintaining the basolateral K(+) conductance of the thick ascending limb (TAL) in EAST/SeSAME syndrome. *Biochim Biophys Acta* **1852**, 2554-2562

200. Wang, M., Luan, H., Wu, P., Fan, L., Wang, L., Duan, X., Zhang, D., Wang, W. H., and Gu, R. (2014) Angiotensin II stimulates basolateral 50-pS K channels in the thick ascending limb. *Am.J.Physiol Renal Physiol* **306**, F509-F516

201. Kong, S., Zhang, C., Li, W., Wang, L., Luan, H., Wang, W. H., and Gu, R. (2012) Stimulation of Ca2+-sensing receptor inhibits the basolateral 50-pS K channels in the thick ascending limb of rat kidney. *Biochim Biophys Acta* **1823**, 273-281

202. Lachheb, S., Cluzeaud, F., Bens, M., Genete, M., Hibino, H., Lourdel, S., Kurachi, Y., Vandewalle, A., Teulon, J., and Paulais, M. (2008) Kir4.1/Kir5.1 channel forms the

major K+ channel in the basolateral membrane of mouse renal collecting duct principal cells. *Am J Physiol Renal Physiol* **294**, F1398-1407

203. Zhang, C., Wang, L., Thomas, S., Wang, K., Lin, D. H., Rinehart, J., and Wang, W. H. (2013) Src family protein tyrosine kinase regulates the basolateral K channel in the distal convoluted tubule (DCT) by phosphorylation of KCNJ10 protein. *J Biol Chem* **288**, 26135-26146

204. Pessia, M., Tucker, S. J., Lee, K., Bond, C. T., and Adelman, J. P. (1996) Subunit positional effects revealed by novel heteromeric inwardly rectifying K+ channels. *EMBO J* **15**, 2980-2987

205. Zhang, C., Wang, L., Su, X. T., Lin, D. H., and Wang, W. H. (2015) KCNJ10 (Kir4.1) is expressed in the basolateral membrane of the cortical thick ascending limb. *Am J Physiol Renal Physiol* **308**, F1288-1296

206. Velazquez, H., and Silva, T. (2003) Cloning and localization of KCC4 in rabbit kidney: expression in distal convoluted tubule. *Am.J.Physiol Renal Physiol* **285**, F49-F58

207. Melo, Z., Cruz-Rangel, S., Bautista, R., Vazquez, N., Castaneda-Bueno, M., Mount, D. B., Pasantes-Morales, H., Mercado, A., and Gamba, G. (2013) Molecular evidence for a role for K(+)-Cl(-) cotransporters in the kidney. *Am.J.Physiol Renal Physiol* **305**, F1402-F1411

208. Wilcox, C. S., Mitch, W. E., Kelly, R. A., Skorecki, K., Meyer, T. W., Friedman, P. A., and Souney, P. F. (1983) Response of the kidney to furosemide. I. Effects of salt intake and renal compensation. *J Lab Clin Med* **102**, 450-458

209. Hori, Y., Takusagawa, F., Ikadai, H., Uechi, M., Hoshi, F., and Higuchi, S. (2007) Effects of oral administration of furosemide and torsemide in healthy dogs. *Am J Vet Res* **68**, 1058-1063

210. Chun, T. Y., Bankir, L., Eckert, G. J., Bichet, D. G., Saha, C., Zaidi, S. A., Wagner, M. A., and Pratt, J. H. (2008) Ethnic differences in renal responses to furosemide. *Hypertension* **52**, 241-248

211. Iwasaki, Y., Gaskill, M. B., and Robertson, G. L. (1995) Adaptive resetting of the volume control of vasopressin secretion during sustained hypovolemia. *Am J Physiol* **268**, R349-357

212. Levine, D. Z., Iacovitti, M., Buckman, S., Hincke, M. T., Luck, B., and Fryer, J. N. (1997) ANG II-dependent HCO3- reabsorption in surviving rat distal tubules: expression/activation of H(+)-ATPase. *Am J Physiol* **272**, F799-808

213. Krauson, A. W., E.; Iyer, S.; Velarde, N.; Nizar, J.; Bhalla, V. (2017) Chronic Loop Diuretic Treatment Mediates Segment-Specific Hypertrophy in the Nephron (Abstract).

214. Gamba, G., and Friedman, P. A. (2009) Thick ascending limb: the Na(+):K (+):2Cl (-) co-transporter, NKCC2, and the calcium-sensing receptor, CaSR. *Pflugers Arch* **458**, 61-76

215. Conigrave, A. D., and Ward, D. T. (2013) Calcium-sensing receptor (CaSR): pharmacological properties and signaling pathways. *Best Pract Res Clin Endocrinol Metab* **27**, 315-331

216. Vysotskaya, Z. V., Moss, C. R., 2nd, Gilbert, C. A., Gabriel, S. A., and Gu, Q. (2014) Modulation of BK channel activities by calcium-sensing receptor in rat bronchopulmonary sensory neurons. *Respir Physiol Neurobiol* **203**, 35-44

217. Osorio, A. V., and Alon, U. S. (1997) The relationship between urinary calcium, sodium, and potassium excretion and the role of potassium in treating idiopathic hypercalciuria. *Pediatrics* **100**, 675-681

218. He, F. J., and MacGregor, G. A. (2008) Beneficial effects of potassium on human health. *Physiol Plant* **133**, 725-735

219. Sellmeyer, D. E., Schloetter, M., and Sebastian, A. (2002) Potassium citrate prevents increased urine calcium excretion and bone resorption induced by a high sodium chloride diet. *J Clin Endocrinol Metab* **87**, 2008-2012

220. de Groot, T., Bindels, R. J., and Hoenderop, J. G. (2008) TRPV5: an ingeniously controlled calcium channel. *Kidney Int* **74**, 1241-1246

221. Costanzo, L. S., Windhager, E. E., and Ellison, D. H. (2000) Calcium and sodium transport by the distal convoluted tubule of the rat. 1978. *J Am Soc Nephrol* **11**, 1562-1580

222. Greger, R., Lang, F., and Oberleithner, H. (1978) Distal site of calcium reabsorption in the rat nephron. *Pflugers Arch* **374**, 153-157

223. Sun, X., Yang, L. V., Tiegs, B. C., Arend, L. J., McGraw, D. W., Penn, R. B., and Petrovic, S. (2010) Deletion of the pH sensor GPR4 decreases renal acid excretion. *J Am Soc Nephrol* **21**, 1745-1755

224. Brown, D., and Wagner, C. A. (2012) Molecular mechanisms of acid-base sensing by the kidney. *J Am Soc Nephrol* **23**, 774-780

225. Sun, X., Tommasi, E., Molina, D., Sah, R., Brosnihan, K. B., Diz, D., and Petrovic, S. (2016) Deletion of proton-sensing receptor GPR4 associates with lower blood pressure and lower binding of angiotensin II receptor in SFO. *Am J Physiol Renal Physiol* **311**, F1260-F1266

226. Codina, J. D., W.; Willingham, M. C.; Penn, R. B.; DuBose, T. D. Jr. (2008) GPR4 may serve as a pH sensor to regulate the colonic H+,K+-ATPase (HKalpha2) in the renal medulla [Abstract]. *J Am Soc Nephrol* **19**

227. Lu, P., Boros, S., Chang, Q., Bindels, R. J., and Hoenderop, J. G. (2008) The beta-glucuronidase klotho exclusively activates the epithelial Ca2+ channels TRPV5 and TRPV6. *Nephrol Dial Transplant* **23**, 3397-3402

228. Cha, S. K., Ortega, B., Kurosu, H., Rosenblatt, K. P., Kuro, O. M., and Huang, C. L. (2008) Removal of sialic acid involving Klotho causes cell-surface retention of TRPV5 channel via binding to galectin-1. *Proc Natl Acad Sci U S A* **105**, 9805-9810

APPENDIX

Table 9. Na^+ and K^+ Contents of the diets used.

Diet	Na^+	K^+	Anion
RD	0.3%	0.6%	Cl^-
HK	0.3%	5.0%	Citrate, Carbonate, Cl^- (equal molar)
HKCl	0.3%	5.0%	Cl^-
LNaHK	0.01%	5.0%	Citrate, Carbonate, Cl^- (equal molar)
LNaHKCl	0.01%	5.0%	Cl^-